

**SOME STUDIES ON THE PRODUCTION AND USE OF
BIO-DIESEL AS CI ENGINE FUEL**

**THESIS SUBMITTED BY
SUDIPTA CHOUDHURY**

DOCTOR OF PHILOSOPHY (ENGINEERING)

**SCHOOL OF AUTOMOTIVE ENGINEERING,
FACULTY COUNCIL OF ENGINEERING & TECHNOLOGY
JADAVPUR UNIVERSITY
KOLKATA – 700032
INDIA**

2015

Dedicated to my mother

Certificate from the Supervisors

*This is to certify that the thesis entitled “**SOME STUDIES ON THE PRODUCTION AND USE OF BIODIESEL AS CI ENGINE FUEL**” submitted by Sudipta Choudhury who got his name registered on 14th September, 2011 (Ref No.D-7/E/610/2011) for the award of Ph.D (Engineering) Degree of Jadavpur University, is absolutely based upon his own work under the supervision of Dr. Probir Kumar Bose, Ex-Professor, Mechanical Engineering Department, Jadavpur University, Ex Director, NIT, Agartala and Dr. Soupayan Mitra, Associate Professor, Mechanical Engineering Department, Jalpaiguri Government Engineering College, Jalpaiguri, West Bengal, India and that neither his thesis nor any part of the thesis has been submitted for any degree/diploma or any other academic award anywhere before.*

1.

(Signature of sole Supervisor and date with Official seal)

2.

(Signature of joint Supervisor and date with Official seal)

ACKNOWLEDGEMENTS

I would like to express my sincere gratitude to Ex Prof. (Dr.) Probir Kumar Bose, Department of Mechanical Engineering, Jadavpur University and Dr. Soupayan Mitra, Associate Professor, Department of Mechanical Engineering, Jalpaiguri Government Engineering College for providing me with the opportunity to work on such an important and relevant subject. Prof. Probir Kumar Bose with his vast knowledge in the field of renewable energy guided me with the different aspects of biodiesel as an alternative fuel in CI engine, while Dr. Mitra guided me to exercise thoughtful and scientific approach to the problem.

I would like to thank Mr. Ranajit Kumar Chakrabarti, Asst. Professor, Department of Mechanical Engineering, Jadavpur University for extending the hands of cooperation many a time during the course of my work.

I would also like to mention the assistance provided me by Miss. Rakhi Bhattacharjee, Mr. Ranjit Kumar Das and Mr. Shoumick Sengupta.

I am again grateful to my project guides Ex-Prof (Dr.) Probir Kumar Bose and Dr. Soupayan Mitra who were amazing at keeping me on track with deadlines and paperwork. Special thanks to them as they not only shared many illuminating deliberations with me through the hours of revisions done on this thesis but also helped me out many a time by rendering various facts & figures related to my study.

Finally, to my family, without whom I could not have been accomplished all I have to this day, thank you with all my heart.

Date:

Sudipta Choudhury

ABOUT THE AUTHOR

Name: Sudipta Choudhury

Date of birth: 01.01.1972

Permanent address:

kethardanga, P.O & Dist: Bankura, West Bengal – 722101.

Communication address:

Lecturer in Mechanical Engineering
Murshidabad Institute of Technology
Cossimbazar Raj, Berhampore
Murshidabad – 742102, West Bengal
E-mail: [sudiptacin@yahoo.co.in/](mailto:sudiptacin@yahoo.co.in)
sudipta.choudhury@gmail.com

Education:

BE (Mechanical) 1996: PESIT, B.U, Karnataka, India

PGDC (Thermal Power Plant Engg.) 1998, NPTI, Durgapur, West Bengal, India

M Tech (Design & Production Engg.) 2000, N.I.T, Durgapur, West Bengal, India

Professional Experience:

- 2003-2009: Lecturer, Dr. B.C. Roy Engineering College, Durgapur.
- 2009 onwards: Lecturer, Murshidabad Institute of Technology, Murshidabad, Govt. Of West Bengal.

Journal publications [International – 5 and National – 1]: 6 (published)

Conference publication: (International -2): 2(published)

Details of Scientific publications:

International Conference:

- i. Choudhury S., Bose P.K., 'Karanja or Jatropha – a better option for an Alternative Fuel in CI Engine', Proceedings of the INTERNATIONAL CONFERENCE & XX

NATIONAL CONFERENCE On I.C. ENGINES AND COMBUSTION (ICONICE – 2007), pp 321 – 326.

- ii. Choudhury S., Bose P.K., 'Jatropha Derived Biodiesel – its suitability as CI engine fuel', Proceedings of the SAE INDIA International Mobility Conference **SIIM C 2008** (SAE Number 2008 – 28 – 0040).

International Journal:

- i. Mitra S., Bose P.K., Choudhury S., 'Production of bio-diesel from jatropha curcas and performance along with emission characteristics of an agricultural diesel engine using bio-diesel', 2ND International Conference On Energy and Sustainability, Energy 2009, Italy, Energy and Sustainability II, Vol. – 121, pp. 367 – 376.
- ii. Choudhury S, Bose P.K., 'Empirical approach for the prediction of cetane number from the FAME composition', Int. J. Renewable Energy Technology, Vol. – 2, No. – 2, 2011, pp 143 – 154.
- iii. Mitra S., Bose P.K., Choudhury S., 'Mathematical Modeling for the prediction of Fuel Properties of Biodiesel from their FAME Composition', Key Engineering Materials Vol. 450 (2011) pp 157-160
- iv. Choudhury S., Mitra S., Bose P.K., 'Mathematical Modeling of Brake Thermal Efficiency of Vegetable Oils by Using Buckingham's π (Pi) Theorem', International Journal of Emerging Technology and Advanced Engineering, Vol. – 5, Issue – 10(October 2015) pp 124 – 131.

- v. Choudhury S., Mitra S., Bose P.K., 'Effect of Temperature and Unsaturation of Fatty Acid Methyl Ester) on Viscosity Prediction for Biodiesel', International Journal of Emerging Technology and Advanced Engineering, Vol. – 5, Issue – 10(October 2015) pp 174 – 178.

National Journal:

- i. Choudhury S., Bose P.K., 'Karanja oil – its potential and suitability as biodiesel', The Bulletin of Engineering and Science, Vol. – 3, No. – 2, BES/3/2/2008, pp20 – 27.

Membership of professional bodies:

- Associate member of Institutions of Engineers [AM/092213/5]
- Life member of "The Combustion Institute(Indian Section) [LMC 972]
- Life member of "Indian Society for Technical Education (LM 52791)

Abstract

During the last decade, India has maintained a high growth rate, which has also led to increasing energy demand / consumption. The share of hydrocarbons in the primary energy consumption of the country has been increasingly over the years and presently estimated as 44.9% (36% for oil & 8.9% for Natural Gas). Drive for alternative fuels gathered momentum with the introduction of CNG and LPG and setting up of an ethanol-petrol blending projects in selected states in India. Alternative sources for diesel has been also explored.

To cope up with the highly skewed situation of the demand for fossil fuel, vegetable oil is found to be the most promising solution. Biodiesel is an alternative fuel made from renewable biological resources such as vegetable oil and animal fat. It can both act as a substitute and an additive to diesel fuel.

The study of non-edible vegetable oil compared to edible oil is very significant in developing countries like India. It is also reported by few researchers that, there are many tree species that been seeds rich in non-edible vegetable oils on which much attention is not made so far. The present study is initiated to investigate the potential of vegetable oil as a source of bio-diesel and feasibility of vegetable oil for the production of biodiesel by optimizing different parameters. For finding a solution to these problems it has been decided to study the two non-edible vegetable oils, e.g. jatropha curcas and karanja (pongamia pinnata) which is converted into biodiesel. The baseline data has been set up from the measured physiochemical properties of the diesel. Certain

equations have been developed for predicting different physiochemical properties and that are compared and validated with the existing values.

The research activity is started with the conversion of raw jatropha and karanja oil, collected from local market into Jatropha Oil Methyl Ester (biodiesel, known as JOME) and Karanja Oil Methyl Ester (biodiesel, known as KOMÉ) respectively by transesterification process. In next phase a test rig has been developed for a detailed investigation on straight diesel operation as well as with diesel biodiesel blend and pure biodiesel. The engine chosen for this experiment is a single cylinder, air cooled, direct injection engine in which additional fuel and air measuring systems are incorporated for measuring the amount of fuel burnt for a particular time period against a fixed load and also for measuring their respective air-fuel ratios. Then Physiochemical properties of the biodiesel prepared are measured and compared with the standard values of fossil diesel fuel. Next, a mathematical model has been developed to find the cetane number which is highly essential for determining the performance of CI engine and the cetane number obtained through the developed model is quite comparable with the published experimentally obtained cetane number. Separate mathematical models have also been developed to predict some of the fundamental fuel properties like viscosity, density and High Heat Value (HHV) and the values obtained from the model are validated with the published experimentally obtained values.

The next step is the experimental phase where the necessary data's are generated for analyzing the engine performance over a wide range of load variation. The comprehensive experimental activities are carried out for baseline diesel, diesel-biodiesel blend and pure biodiesel. The engine performance, combustion and exhaust

emission characteristics at various diesel-biodiesel proportions are also analyzed at different loads for finding the optimum performance of fuel blends.

The results of this research work showed that both the biodiesel (jatropha oil methyl ester and Karanja oil methyl ester) are the comparable substitute for replacing the diesel oil in terms of performance and emission characters. In a long duration running situation, blending of biodiesel (JOME and KOME) are the preferred choice for the replacement of diesel in CI engines as it shows a stable mixture. For blended biodiesel, KB25 and JB50 are found to be the optimum choices for the diesel fuel replacement. The brake thermal efficiency of diesel is found to be 34.41% whereas for the KB 25 and JB50 the values are 31.31% and 31.28 respectively which are quite comparable. The CO emission of diesel at full load is 0.024% whereas that of optimum karanja derived biodiesel is 0.016% i.e. there is a reduction in 34% CO emission in case of KB 25 than diesel fuel. For optimum jatropha derived biodiesel (JB 50), the reduction is found around 50% less than the diesel fuel. The HC emission of diesel at maximum load is 32 ppm whereas that of JB100 is 16 ppm i.e. 50% reduction in HC emission for pure biodiesel in comparison to diesel fuel. For karanja derived biodiesel the HC emission at full load is found 23 ppm i.e. around 35% less than diesel fuel.

The effect of delay period could be considered as another selection criteria for diesel, diesel biodiesel blend and pure biodiesel which is not the scope of our present study. The metallurgical effects of the engine during long run by using biodiesel have also not been included in the present work. The further research may be carried out considering those parameters.

CONTENTS

	Page No.
Certificate	iii
Acknowledgements	iv
About the author	v
Abstract	viii
Contents	xi
List of Figures	xvi
List of Plates	xx
List of Tables	xxi
Nomenclature	xxiii
Chapter 1: INTRODUCTION	
1.1 GENERAL	01
1.2 ALTERNATIVE ENGINE FUELS	02
1.3 BIODIESEL	03
1.4 BIODIESEL – INDIAN SCENARIO	05
1.5 BIODIESEL – GLOBAL SCENARIO	06
Chapter 2: REVIEW OF LITERATURE	
2.1 FUNDAMENTALS OF DIESEL ENGINE	08
2.2 POLLUTANTS FORMATION IN DIESEL ENGINE	10
2.2.1 Particulate matter emissions	11

2.2.2	NO _x emissions	14
2.2.3	Unburned hydrocarbon emissions	15
2.2.4	CO emissions	17
2.3	LITERATURE SURVEY OF BIODIESEL REPLACEMENT IN DIESEL ENGINE	
2.3.1	Historical perspective	18
2.3.2	Biodiesel as diesel engine replacement	19
2.4	BIODIESEL – AN OVERVIEW	28
2.4.1	Direct use/Blending	28
2.4.2	Micro-emulsification	29
2.4.3	Pyrolysis	29
2.4.4	Transesterification	30
2.5	ADVANTAGES OF BIODIESEL	31
2.6	DISADVANTAGES OF BIODIESEL	32
2.7	CONCLUSIONS FROM LITERATURE REVIEW	33
2.8	NEED FOR PRESENT WORK	34
2.9	STATEMENT OF THE PROBLEM	35
Chapter 3: PRODUCTION METHODOLOGY OF BIODIESEL		
3.1	PRODUCTION OF BIODIESEL	37
3.1.1	Procedural steps for the production of biodiesel	
	i. Transesterification	39
	ii. Separation	40
	iii. Washing	41
	iv. Vacuum distillation	41
3.2	BIODIESEL SPECIFICATIONS AND PROPERTIES	42
3.3	PROPERTY REQUIREMENTS AND SPECIFIED METHODS	

FOR B100	43
3.3.1 ASTM D 93- Flash point, closed cup	43
3.3.2 ASTM D 2709 – Water and sediment	44
3.3.3 ASTM D 445 – Kinematic viscosity, 40 ° C	45
3.3.4 ASTM D 874 – Sulfated Ash	45
3.3.5 ASTM D 5453 – Total sulphur	45
3.3.6 ASTM D 130 – Copper strip corrosion	46
3.3.7 ASTM D 613 – Cetane number	46
3.3.8 ASTM D 2500 – Cloud point	47
3.3.9 ASTM D 4530 – Carbon residue	47
3.3.10 ASTM D 664 – Acid number	48
3.3.11 ASTM D 6584 – Free glycerine	48
3.3.12 ASTM D 6584 – Total glycerine	49
3.3.13 ASTM D 4951 – Phosphorus	49
3.3.14 ASTM D 1160 – Vacuum distillation end point	49
3.4 MEASURED FUEL PROPERTIES	
3.4.1 Kinematic viscosity (centistokes, cSt)	50
3.4.2 Calorific value (kj/kg)	53
3.4.3 Specific gravity	56
3.4.4 Cloud point and pour point (°C)	57
3.4.5 Flash point and fire point (°C)	58
3.4.6 Cetane number	60

3.5	ANALYSIS OF FUEL PROPERTIES	62
3.6	PRODUCTION OF BIODIESEL FROM JATROPHA	63
Chapter 4: MATHEMATICAL MODELING FOR PREDICTING FUEL PROPERTIES		
4.1	INTRODUCTION	66
4.2	PREDICTION OF CETANE NUMBER	67
	4.2.1 CN prediction by ASTM D 976 and ASTM D 4737	68
	4.2.2 CN prediction from the physical properties of FAME	69
	4.2.3 CN prediction from the average percentage composition of FAME	74
	4.2.4 Results and Discussion	76
4.3	PREDICTION OF VISCOSITY, DENSITY, AND HHV	78
	4.3.1 Correlation analysis	80
	4.3.2 Pearson product moment of correlation coefficient(r)	81
	4.3.3 Regression model	85
	4.3.4 Results and Discussion	85
	4.3.5 Evaluation and comparison of HHV of biodiesels from their predicted equation and available published models	89
Chapter 5: EXPERIMENTAL TEST RIG DEVELOPMENT & METHODOLOGY		
5.1	ENGINE DETAILS	91
5.2	INSTRUMENTATION	
	5.2.1 Eddy current dynamometer	92
	5.2.2 Engine speed	92
	5.2.3 Air flow measurement	93
	5.2.4 Temperature measurement	94
	5.2.5 Fuel supply measurement	95

5.2.6 Exhaust emissions analyzer	96
----------------------------------	----

Chapter 6: EXPERIMENTAL RESULTS AND DISCUSSIONS

6.1	INTRODUCTION	97
6.2	EXPERIMENTAL APPROACH	97
	6.2.1 Experiments on diesel:	98
	6.2.2 Experiments on karanja derived biodiesel	99
	6.2.3 Experiments on jatropha derived biodiesel	112
6.3	COMPARISON AMONG DIESEL, KARANJA DERIVED BIODIESEL & JATROPHA DERIVED BIODIESEL	125
6.4	COMPARISON AMONG DIESEL, OPTIMUM KOME BLEND AND OPTIMUM JOME BLEND	131
6.5	SALIENT POINTS OF EXPERIMENTS	136

Chapter 7: CONCLUSIONS AND RECOMMENDATIONS

REFERENCES	144
------------	-----

LIST OF PUBLICATIONS	153
----------------------	-----

APPENDICES

APPENDIX 1: Specifications and accuracy of the instrument
used for measuring fuel properties

APPENDIX 2: Engine specifications

APPENDIX 3: Dynamometer specifications

APPENDIX 4: AVL Digas 444 analyzer specification

APPENDIX 5: Performance and emission data for diesel

APPENDIX 6: Performance and emission data for KOME blend
with diesel

APPENDIX 7: Performance and emission data for JOME blend with
diesel

LIST OF FIGURES

Sl. No.	Title	Page No.
Figure 2.1	Combustion phenomenon of diesel engine	09
Figure 2.2	Formation of first aromatic ring	12
Figure 2.3	Growth of aromatic ring (H – abstraction)	12
Figure 2.4	PAH growth initiated by aromatics condensation	13
Figure 3.1	Process cycle of biodiesel	42
Figure 3.2	Comparative study of viscosities at different temperature	52
Figure 4.1	Plot of CN vs. Viscosity for saturated fame	71
Figure 4.2	Plot of CN vs. Heat of combustion for saturated FAME	72
Figure 4.3	Plot of CN vs. Carbon number for saturated FAME	72
Figure 4.4	Plot of CN vs. Boiling point for saturated FAME	73
Figure 4.5	Plot of CN vs. Melting point for saturated FAME	73
Figure 4.6	Plot of CN vs. Density for saturated FAME	74
Figure 4.7	Comparison between measured and predicted values of CN	77
Figure 4.8	Scatter plot of viscosity vs. FAME's with fitted regression line	82
Figure 4.9	Scatter plot of density vs. FAME's with fitted regression line	83
Figure 4.10	Scatter plot of HHV vs. FAME's with fitted regression line.	84
Figure 4.11	Determined and predicted viscosity value of biodiesels	87
Figure 4.12	Determined and predicted density value of biodiesels	88
Figure 4.13	Determined and predicted HHV of biodiesels	89
Figure 6.1	Variation of BSFC with varied torque for diesel KOME blend	100
Figure 6.2	Variation of BSFC with percentage of KOME in the blend for different load conditions	101
Figure 6.3	Variation of BSEC with varied torque for diesel KOME blend	102

Figure 6.4	Variation of BSEC with percentage of KOME in the blend for different load conditions	103
Figure 6.5	Variation of B.Th. Efficiency with varied torque for diesel KOME blend	104
Figure 6.6	Variation of B.Th. Efficiency with percentage of KOME in the blend for different load conditions	105
Figure 6.7	Variation of exhaust temperature with varied torque for diesel KOME blend	106
Figure 6.8	Variation of exhaust temperature with percentage of KOME in the blend for different load conditions	106
Figure 6.9	Variation of CO with varied torque for diesel KOME blend	107
Figure 6.10	Variation of CO with percentage of KOME in the blend for different load conditions	108
Figure 6.11	Variation of HC with varied torque for diesel KOME blend	109
Figure 6.12	Variation of HC with percentage of KOME in the blend for different load conditions	110
Figure 6.13	Variation of NO _x with varied torque for diesel KOME blend	111
Figure 6.14	Variation of NO _x with percentage of KOME in the blend for different load conditions	112
Figure 6.15	Variation of BSFC with varied torque for diesel JOME blend	113
Figure 6.16	Variation of BSFC with percentage of JOME in the blend for different load conditions	114
Figure 6.17	Variation of BSEC with varied torque for diesel JOME blend	115
Figure 6.18	Variation of BSEC with percentage of JOME in the blend for different load conditions	116
Figure 6.19	Variation of B.Th. Efficiency with varied torque for diesel JOME blend	117

Figure 6.20	Variation of B.Th. Efficiency with percentage of JOME in the blend for different load conditions	118
Figure 6.21	Variation of exhaust temperature with varied torque for diesel JOME blend	119
Figure 6.22	Variation of exhaust temperature with percentage of JOME in the blend for different load conditions	119
Figure 6.23	Variation of CO with varied torque for diesel JOME blend	120
Figure 6.24	Variation of CO with percentage of JOME in the blend for different load conditions	121
Figure 6.25	Variation of HC with varied torque for diesel JOME blend	122
Figure 6.26	Variation of HC with percentage of JOME in the blend for different load conditions	123
Figure 6.27	Variation of NO _x with varied torque for diesel JOME blend	124
Figure 6.28	Variation of NO _x with percentage of JOME in the blend for different load conditions	125
Figure 6.29	Variations of BSFC at different load for diesel karanja derived biodiesel & jatropha derived biodiesel	126
Figure 6.30	Variations of B.Th. Efficiency at different load for diesel karanja derived biodiesel & jatropha derived biodiesel	127
Figure 6.31	Variations of exhaust temperature at different load for diesel karanja derived biodiesel & jatropha derived biodiesel	128
Figure 6.32	Variations of CO at different load for diesel karanja derived biodiesel & jatropha derived biodiesel	129
Figure 6.33	Variations of HC at different load for diesel karanja derived biodiesel & jatropha derived biodiesel	130
Figure 6.34	Variations of NO _x at different load for diesel karanja derived biodiesel & jatropha derived biodiesel	131
Figure 6.35	Variations of BSFC at different load for diesel, KB25 & JB50	132

Figure 6.36	Variations of B.Th. Efficiency at different load for diesel, KB25 & JB50	133
Figure 6.37	Variations of exhaust temperature at different load for diesel, KB25 & JB50	134
Figure 6.38	Variations of HC at different load for diesel, KB25 & JB50	135
Figure 6.39	Variations of CO at different load for diesel, KB25 & JB50	135
Figure 6.40	Variations of NO _x at different load for diesel, KB25 & JB50	136

LIST OF PLATES

Sl. No.	Title	Page No.
Plate 3.1	7 litre capacity reactor with oil bath	37
Plate 3.2	Reactor from top	38
Plate 3.3	Reactor with internal view	38
Plate 3.4	Biodiesel reactor plant of 200 litre capacity	41
Plate 3.5	Red wood viscometer	52
Plate 3.6	Bomb calorimeter	53
Plate 3.7	Cloud and pour point apparatus	57
Plate 3.8	Flash and fire point apparatus	59
Plate 3.9	Aniline point apparatus	61
Plate 5.1	Experimental test rig	91
Plate 5.2	Eddy current dynamometer	92
Plate 5.3	Speed sensor	93
Plate 5.4	Surge tank fitted with orifice	94
Plate 5.5	Thermocouple used for temperature measurement	94
Plate 5.6	Fuel supply measurement	95
Plate 5.7	Gas analyzer	96

LIST OF TABLES

Sl. No.	Title	Page No.
Table 1.1	Properties of alternative fuels	02
Table 3.1	ASTM D – 6751 specifications	43
Table 3.2	Viscosity dependency on temperature variation of biodiesel and karanja	51
Table 3.3	Observation table for bomb calorimeter	54
Table 3.4	Specific gravity of raw karanja and biodiesel	57
Table 3.5	Cloud and pour points of raw karanja and biodiesel	58
Table 3.6	Flash point and fire points	59
Table 3.7	Comparative study of fuel properties	62
Table 3.8	Properties of the fuels selected for engine experiment (KOME)	63
Table 3.9	Viscosity dependency on temperature variation of biodiesel and jatropha	64
Table 3.10	Specific gravity of raw jatropha and biodiesel	64
Table 3.11	Cloud and pour points of raw jatropha and biodiesel	64
Table 3.12	Flash point and fire points	64
Table 3.13	Comparative study of fuel properties of diesel and biodiesel	65
Table 3.14	Properties of the fuels selected for engine experiment (JOME)	65
Table 4.1	Distillation temperature, density and viscosity of reference fuels	68
Table 4.2	Comparative studies of cetane number	69
Table 4.3	Physical properties of pure FAME	70

Table 4.4	Regression equations based on physical properties of FAME	70
Table 4.5	Predicted CN values from the regression equation	74
Table 4.6	Fatty acid compositions and the experimental cetane numbers of esters	75
Table 4.7	Experimental and predicted cetane numbers of some biodiesels	76
Table 4.8	FAME compositions in different biodiesels	79
Table 4.9	Properties of different biodiesels	79
Table 4.10	Pearson product moment correlation coefficient (r) between viscosity, density, HHV vs. FAME's composition	80
Table 4.11	Comparison between determined and predicted viscosity of biodiesel	86
Table 4.12	Comparison between determined and predicted density of biodiesel.	87
Table 4.13	Comparison between determined and predicted HHV of biodiesel.	88
Table 4.14	Comparison between predicted and published models of HHV	90
Table 5.1	Engine performance and emission results of diesel	72

NOMENCLATURE

%	Percentage
°C	Centigrade
A/F	Air-Fuel Ratio
API	American Petroleum Institute
ASTM	American Society for Testing and Materials
B Th E	Brake Thermal Efficiency
b.m.e.p	Brake mean effective pressure
B100	neat biodiesel
B20	20% biodiesel + 80% diesel
BDC	Bottom Dead Centre
BIS	Bureau of Indian Standard
BP	Brake power
BSEC	Brake Specific Energy Consumption
BSFC	Brake Specific Fuel Consumption
C.P	Centipoise
CI	Compressed Ignition
CN	Cetane number
CNG	Compressed Natural Gas
CO	Carbon Monoxide
CO ₂	Carbon Dioxide
Cst	Centistoke
CV	Calorific Value
DF	Diesel fuel
DI	Direct Ignition
FAME	Fatty Acid Methyl Ester

FFA	Free Fatty Acids
g	gram
HC	Hydrocarbons
HHV	High Heat Value
HMN	Hepta Methyl Nonane
HP	Horse Power
hr	hour
JOME	Jatropha Oil Methyl Ester
K	Kelvin
kJ	Kilo joules
KOME	Karanja Oil Methyl Ester
KW	Kilowatt
KW _{hr}	Kilowatt hour
LPG	Liquified Petroleum Gas
MJ	Mega Joule
NO	Nitric Oxide
NO _x	Oxides of Nitrogen
P	Pressure
PAH	Polycyclic Aromatic Hydrocarbon
PAN	Peroxyacyl Nitrate
PM	Particulate matter
r.p.m	Revolution per minute
RME	Rapeseed Methyl Ester
s	second
SI	Spark Ignition
t	Time

CHAPTER 1

INTRODUCTION

1.1 GENERAL

Increasing industrialization and enhanced new technology have led to a steep rise in the demand for petroleum products. The indiscriminate extraction and consumption of fossil fuels have led to a depletion of petroleum reserves. As a result, the major challenges of today's world are energy crisis i.e. fossil fuel exhaustion and its associative as environmental degradation.

One probable solution is to improve thermal efficiency and reduce exhaust emissions. The excellent thermal efficiency of diesel engines certainly has advantages for conserving energy and solving greenhouse problems. However, a diesel engine has a problem with the trade-off, that is to say, a difficulty to reduce both smoke and NO_x simultaneously [1].

Over the last decade, several research studies worldwide have been undertaken to determine the best solution against the increasing stringent emissions regulation. Energy conversion alone is inadequate to satisfy long-term energy demands and replace petroleum-based fuels. Since 1990, great strides have been made to reduce harmful effects of vehicle emissions. Especially oxides of Nitrogen (NO_x), unburned hydrocarbon (HC) and particulate matter (PM) emission have been emphasized due to their contributions to smog formation and associated health

hazards. In spite of significant improvement in diesel engine design, fuel exhaust regulation norms still continue to tighten.

In such critical situation, the only possible solution is the search for an alternative fuel that can work without much engine modification and also cope up with the emission regulation norms.

1.2 ALTERNATIVE ENGINE FUELS

The increasing uncertainties concerning fossil fuel reserves and growing vehicular exhaust emission have focused the attention on the task of finding alternate clean burning fuel for use in internal combustion engines.

Table 1.1 Properties of alternative fuels

Properties	Diesel	(LPG)	(CNG)	Methanol	Ethanol	Hydrogen
Chemical structure	C ₁₀ – C ₂₀	C ₃ H ₈	CH ₄	CH ₃ OH	C ₂ H ₅ OH	H ₂
Density (kg/m ³)	835 – 860 815	536	160 (at 150kg/cm ²)	791	785 – 789	70 liq. 0.09 gas
Specific gravity @15°C	0.86	-	-	0.796	0.794	
Viscosity at 20°C (C.P)	40	-	-	0.59	1.19	
Auto ignition point (°C)	250	450 – 510	540 620	450	420	585
Boiling point (°C)	180 – 360	-42	-162	65		
Low Heat Value (MJ/kg)	42	46.05 (/dm ³)	50 4.8(/dm ³)	19.5	27	121
Stoichiometric ratio	14 – 14.7	15.7	17.1	6.52	9.06	34.5
Cetane number	40 – 55	N/A	N/A	5	8	N/A
Octane Number	8 – 15	104	120+	111	108	130+
Oxygen content (by % Wt.	0			50	34.7	0

Hosts of alternative fuels that are available include Ethanol, Methanol, CNG, LPG, Hydrogen, and Biodiesel. It is, therefore, of great importance that all potential fuel alternatives are being recognized and examined.

1.3 BIODIESEL

The consumption of diesel oil is several times higher than that of petrol [2]. Due to the depletion of petroleum products along with its increasing cost, efforts have been made to develop alternative fuels for partial or full replacement of diesel.

It has been observed that the biomass-based fuel is an attractive approach for diesel replacement. Oxygenated diesel fuels can be obtained either by blending oxygenates to diesel or using biofuels. The fuels of bio-origin may be alcohol, vegetable oil, biomass, animal fat, and biogas. Some of these can be directly used in the engine while others need to be formulated to bring the relevant properties close to diesel fuel.

Vegetable oils are one of the most promising fuels because their properties are similar to that of diesel and are produced easily and renewably from the crops. Vegetable oils have a comparable energy density, cetane number, the heat of combustion and stoichiometric air-fuel ratio with that of diesel fuel [3].

Rudolph Diesel, the father of diesel engine demonstrated the first use of vegetable oil in a diesel engine. He used peanut oil as fuel for his experimental engine.

However, straight vegetable oils cannot be used directly in the engine due to their high viscosity, low volatility, and polyunsaturated character, as it affects the flow properties of the fuel, like piston ring sticking, fuel injector choking, fuel pumps failure, lubricating oil dilution, etc.

Several techniques are adopted to reduce the viscosity of vegetable oil such as blending, pyrolysis, micro-emulsification, thermal cracking, transesterification, etc. Among these processes, transesterification has been reported as an effective process to overcome the problems associated with vegetable oils [4].

Biodiesel is the name of a chemically modified clean burning alternative fuel derived from vegetable oils or animal fats. Biodiesel contains no petroleum, but can be blended at any level with petroleum diesel to create stable mixture named as biodiesel blend. Biodiesel is simple to use, nontoxic, biodegradable and essentially free from sulphur and aromatics. Moreover, it can be used in CI engine with little or no modification.

Biodiesel is produced commercially by the transesterification of vegetable oils with alcohol. Methanol (CH_3OH) and ethanol ($\text{C}_2\text{H}_5\text{OH}$) are the commonly used alcohols for this process. The process leaves behind two products – methyl ester (biodiesel) and glycerin, a valuable byproduct for the soap industry.

The carbon cycle of vegetable oils consists of release and absorption of carbon dioxide. Combustion and respiration process release carbon dioxide, and crops, for their photosynthesis process, absorb the carbon dioxide. Thus, the accumulation of carbon dioxide in the atmosphere reduces. Therefore, biodiesel is a better option for the environment as it is made from renewable sources. It is also advantageous for their lower emission profile in comparison to diesel.

1.4 BIODIESEL – INDIAN SCENARIO

Since biodiesel is made from renewable sources such as edible or nonedible oils, fats, waste cooking oils etc. Its use decreases our dependence on foreign oil and contributes to our national economy. At present, India produces around 30% of the total demand of petroleum diesel and the remaining 70% is being imported that costs about Rs. 80,000 crore every year [2]. It is quite surprising that even 5% mixing of biodiesel with present diesel fuel can save about 4000 crores every year. Even Planning Commission, Government of India recommends the use of biodiesel from 5% blend to 20% in the next five years. It is essential that India will be able to produce 288 metric tonnes of biodiesel by the end of 2012, which will supplement 41.14% of the total demand of diesel fuel consumption in India [5].

Most of the esterified oils used in diesel engines are soybean, sunflower, peanut, palm, safflower, rapeseed, etc. These oils are essentially edible oils in the Indian context. In a developing country like India where scarcity of edible oils is already present, the use of edible oil as biodiesel is not feasible. There are many tree species bearing seeds rich in nonedible vegetable oils available in India. But most surprisingly, as per their potential, a very minimum percentage of utilization is done. Hosts of nonedible oils available are karanja, jatropha, mahua, polonga etc.

Therefore, in India, the feasibility of producing biodiesel as diesel substitute can be significantly thought as, along with the un-utilization of the available potential of the nonedible oil sources, there are large junks of degraded forest land, un-utilized public land and fallow lands of farmers, even rural areas that will be beneficial.

The Planning Commission of India has launched a biodiesel project in 200 districts from 18 states in India. It has recommended two plant species, viz. jatropha (*Jatropha Curcas*) and karanja (*Pongamia Pinnata*) for biodiesel production. *Jatropha Curcas* has been identified for India as the most suitable Tree Borne Oil seed (TBO) for the production of biodiesel in view of nonedible oil available from it and its presence throughout the country [6]. Karanja is an oil seed bearing tree, which is also nonedible and does not find any suitable application with only 6% being utilized of 200 million tonnes per annum [7].

1.5 BIODIESEL – GLOBAL SCENARIO

Use of biodiesel is catching up all over the world especially in developed countries. In the present scenario, biodiesel has been accepted as a clean alternative fuel by most of the developed and developing countries. Countries like USA, France, Germany, Italy, Malaysia, Czechoslovakia, Austria and other European and Asian countries have put a major thrust on the production of biodiesel from vegetable oil through extensive research and development. Rapeseed methyl ester (biodiesel), has been in commercial use as a primary alternative fuel since 1988 in many European countries, including France, Austria, Germany, Sweden, Italy, Belgium, Hungary and Czech Republic. Rapeseed oil is the primary sources of biodiesel in Europe while in the United States both rapeseed and soybean oils are used. Canola oil, a cultivated version of Rapeseed oil is now widely used in Western Canada [8]. In Malaysia, the tropical climate encourages production of biodiesel from Palm oil [9]. At present, USA uses 50 million gallons and European countries use 350 million gallons

of biodiesel annually. It is mixed with 20% of biodiesel in fossil fuel. France uses 50% of biodiesel mixed with diesel oil. Brazil uses ethanol as 100% fuel in about 20% of vehicles & 25% blend with gasoline in the rest of the vehicles.

CHAPTER 2

REVIEW OF LITERATURE

2.1 FUNDAMENTALS OF DIESEL ENGINE

The operation of diesel (CI) engine, found in most light duty application is fundamentally different from the spark ignition (SI) engine. In a diesel engine, only air is induced into the combustion chamber through the intake valve. The fuel is injected directly at high pressure in the form of fine droplets and it is primarily the injection timing that governs the combustion phenomena. Most diesel engines used in vehicles operate on a four stroke cycle. The process contains suction, compression, combustion, and expansion. The behavior of combustion is illustrated in figure 2.1. As shown in figure, start of fuel injection typically occurs $10^{\circ} - 26^{\circ}$ before Top Dead Center (TDC) where each minute droplet of fuel as it enters the highly heated air of engine cylinder is quickly surrounded by an envelope of its own vapour and this, in turn, and an appreciable interval is inflamed at the surface of the envelope. After a short delay auto ignition of the portion of fuel –air mixture that is within flammability limits occurs, termed as pre-mixed combustion phase and may occur over a few crank angle degrees. The phase is characterized by high heat release rate. Combustion continues in the mixing controlled

phase, where the rate of fuel-air mixture fixes the rate of combustion. It is during this phase where most of the soot formation occurs [10].

In cylinder mixing of fuel and air, air swirl is extremely important for diesel engine combustion process. It means an orderly movement of the whole body of the air, with or without some eddying or turbulence, so as to bring a continuous supply of fresh air to each burning droplet and sweep away the products of combustion. The mixing process can be strongly affected by the design of certain engine components. In addition, high fuel injection pressure (usually 200 bars) is used to increase the fuel penetration, better fuel atomization, and air entrainment.

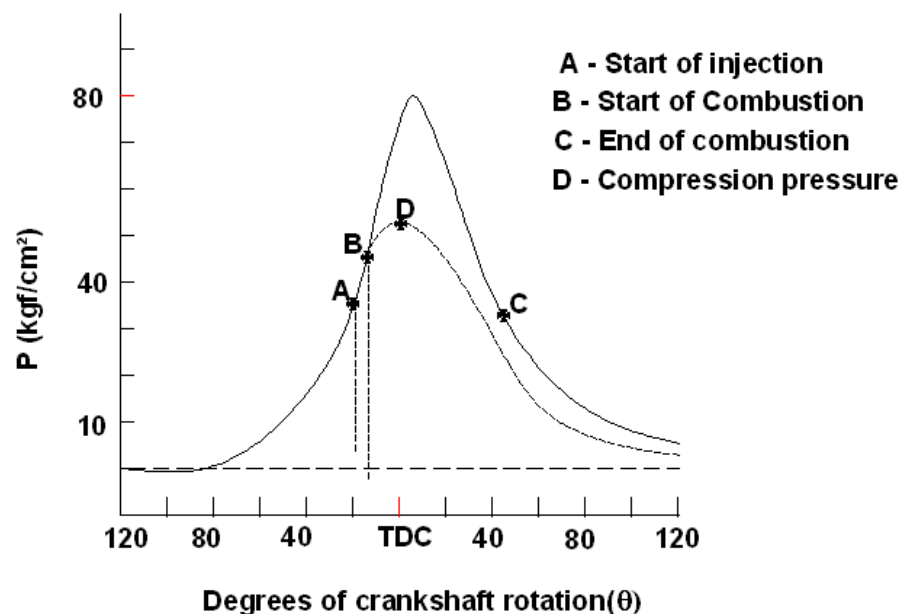


Figure 2.1 Combustion phenomenon of diesel engine

2.2 POLLUTANTS FORMATION IN DIESEL ENGINE

Since the present work is based on a diesel engine, it is important to study some significant aspects of emission characteristics. For diesel engine, two major pollutants of concern are particulate matter (PM) and NO_x . These two emissions are closely related to public health concern along with environmental hazards as the emitted particles containing hundreds of toxic chemicals, easily respirable to the human body, and oxides of nitrogen are ozone precursors. Other pollutants such as carbon monoxide (CO), carbon dioxide (CO_2) and unburned hydrocarbon (HC) are comparatively low because of lean air-fuel stoichiometric ratio. The primary source of PM and NO_x in urban areas from diesel combustion are automobiles and, with smaller levels, stationary engines. It is well established that NO_x plays an important role as a primary precursor to tropospheric ozone formation [11]. Ozone is a known lung irritant which can cause respiratory problems among the young and the old, especially asthmatics. Also, relatively stable nitrogen containing species such as peroxyacyl nitrate (PAN), nitric and nitrous acid, and nitrate particulates are formed from NO_x in the atmosphere. It is estimated to cause about 25%– 30% of acidity in rain, which is thought to be responsible for the damage of forests and other plant life. Effects to reduce the impact of diesel engine emissions have resulted in legislative action to impose emission limits on both NO_x and PM. Currently, technologies exist which prevent Diesel Engines from meeting these standards.

2.2.1. Particulate matter emissions:

PM is the general term for a variety of condensed phase compounds that are found in diesel exhaust. Most of the PM mass occurs due to the formation of carbonaceous soot in a diesel engine. The beginning of soot formation starts during fuel pyrolysis when the parent fuel is broken down into smaller hydrocarbon fragments. It is well accepted that acetylene (C_2H_2) and propargyl (C_3H_3) play a major role in the formation of aromatics. Aromatics species generated in the flame subsequently combine to form polycyclic aromatic hydrocarbons (PAHs). The continued growth of these PAHs ultimately leads to the formation of smallest soot spherules ^[12], which are in the order of 1 – 2nm in diameter. The overall model of soot formation can be thought of as consisting of four major processes: **initial PAH formation**, which includes the formation of the first aromatic ring in an aliphatic system; **planar PAH growth**, comprised of replicating-type growth; **particle nucleation**, consisting of coalescence of PAHs into three-dimensional clusters; and **particle growth** by coagulation and surface reactions of the formed clusters and particles. The formation of the first aromatic ring in flames of non-aromatic fuels usually begins with the vinyl addition to acetylene as shown in figure 2.2. Once formed, aromatic rings grow by a sequential two-step process: H-abstraction which activates the aromatic molecules and acetylene addition which propagates molecular growth and cyclization of PAHs shown in figure 2.3. Starting with an aromatic fuel, a “direct” condensation of intact aromatic rings becomes important. For example, in the case of

high-temperature pyrolysis of benzene, the reactions shown in figure 2.4 are found to dominate the initial stages of PAH growth [13].

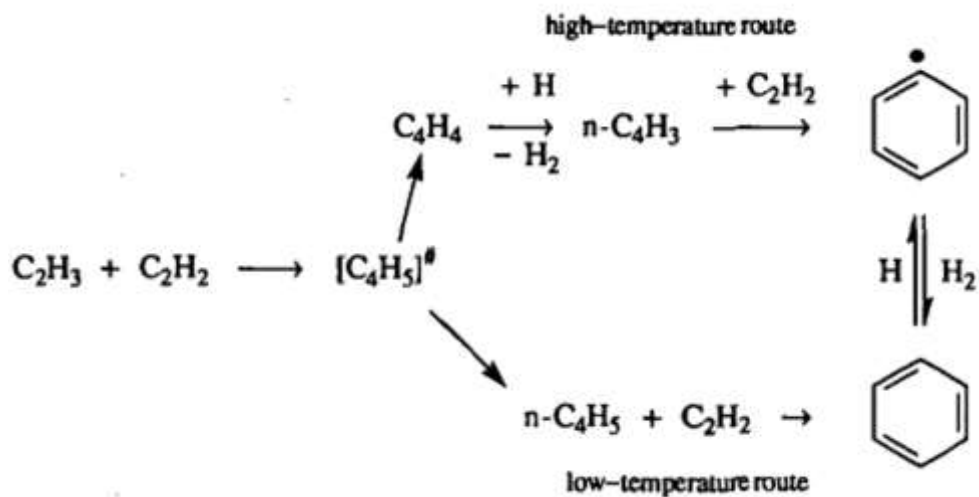


Figure 2.2 Formation of first aromatic ring

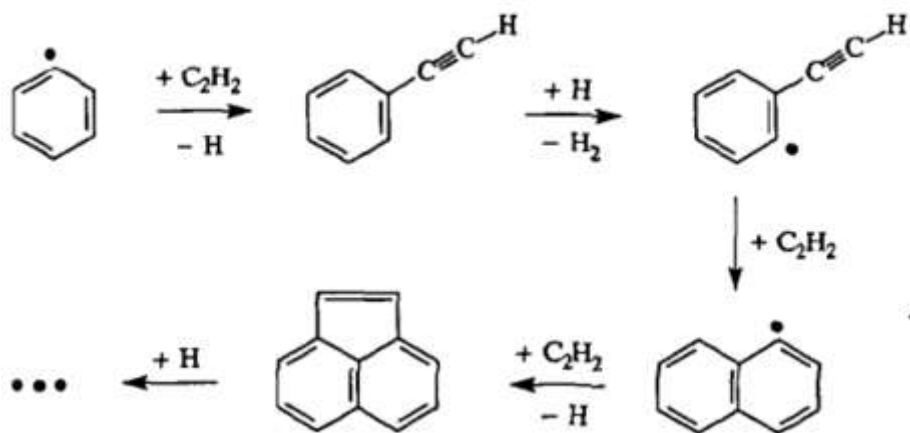


Figure 2.3 Growth of aromatic ring (H – abstraction)

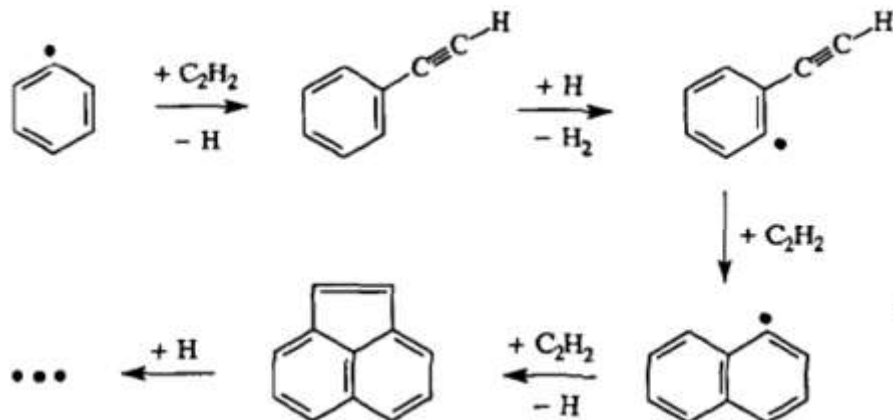


Figure 2.4 PAH growth initiated by aromatics condensation

The condensation mechanism leads to the surface growth of the particles and increases soot mass. Particles collide with one another and agglomerate. When still small (< 10 nm), the particles tend to retain a spherical shape due to the effect of surface condensation ^[14]. As the soot particles grow larger, however, they typically aggregate into chainlike structures and ultimately are in the order of 100 nm in size. Throughout the soot formation process, carbon content repeatedly increases due to the addition of large, hydrogenised polymers and through the removal of hydrogen from the soot particles themselves ^[15]. Soot oxidation also takes place and has a major impact on soot concentrations. In cylinder sampling techniques, for example, a vast majority of the soot produced during soot produced during diesel combustion is oxidized to CO and CO₂ before the exhaust process ^[16].

2.2.2 NO_x emissions:

Most of the NO_x emitted from diesel engines is in the form of nitric oxide (NO).

Production of NO_x in IC engines is primarily due to the high temperature extended Zeldovich reaction mechanism [17]:



The strongest bond is the triple bond in the N≡N molecule, resulting in the activation energy of about 75kcal/mol for reaction 2.1, which is the principal cause of the large temperature dependence of the extended Zeldovich NO_x mechanism. This large temperature dependency is characterized by breaking of high activation energy that tightly bonds oxygen and nitrogen molecules. In most engines, NO_x is therefore produced primarily in the high temperature combustion product gasses. Reaction 2.1 is the rate limiting step and has a strong dependence on peak combustion temperature. A significant amount of NO formation occurs in the diffusion flame of the mixing controlled phase of combustion.

The cause of this increase is not fully known, but it has largely been attributed to differences in the physical properties of biodiesel and petrodiesel fuels. Although biodiesel does have a higher cetane number than petrodiesel and therefore should

improve combustion and lower NO_x, other physical properties such as viscosity and bulk modulus impact the injection and combustion behavior of the fuels as well. Biodiesel has a higher bulk modulus than conventional petrodiesel, which has been shown to contribute to higher NO_x production [18].

An overview of the most common reasons for the NO_x emissions given in the literature is presented. These explanations are closely related to effects due to premixed combustion, injection timing, soot radiation, and fuel chemistry. None of these effects should be considered to be uniquely responsible for the NO_x emission characteristics of biodiesel; rather, they should be viewed as contributing factors to NO_x emissions in various fuel and combustion situations.

2.2.3 Unburned hydrocarbon emissions:

Exhaust gasses leaving the combustion chamber of a CI engine contains unburned fuel components and some reacted components that were not present in the original fuel is known as an unburned hydrocarbon. These consist of small non-equilibrium molecules which are formed when large fuel molecules break up (thermal cracking) during the combustion reaction. When hydrocarbon emissions get into the atmosphere, they act as irritants and odorants; some are carcinogenic. All components except CH₄ react with atmospheric gasses to form photochemical smog.

Diesel particulates consist of an elemental carbon core with several organic compounds (soluble and insoluble in organic solvents), sulfates, nitrogen oxides, heavy metals,

trace elements and irritants (such as acrolein, ammonia, acids, fuel vapors, unburned lubricating oils, moisture) adsorbed to its surface. The organic or hydrocarbon compounds are made up of a continuous gradation of carbon-containing compounds that change from a hydrogen to carbon ratio of 2:1 to eventually a ratio of 0:1 [19]. They include various classes of compounds such as aldehydes, alkanes, and alkenes, (both straight and branched chain), and aromatic compounds (single rings, substituted, and poly-nuclear). Any of these species may also contain functional groups such as carbonyl (C=O), hydroxyl (OH) and nitro (NO₂).

About 90% of diesel particulates encompass a size range from 7.5 nm to 1.0 μm [20] and are therefore important in terms of potential health impacts due to the ability of tiny particles to be inhaled and eventually get trapped in the bronchial passages and alveoli of the lungs.

Most of the particulates emitted by engines lie in the nanoparticulate range (<50 nm), while most of the particulate mass lies in the accumulation mode range that is 50 nm < D < 1000 nm range [21]. Particle size influences the environmental impact of engine exhaust particles in several ways: it influences the atmospheric residence time of the particles, the optical properties of the particles, the particle surface area and their ability to participate in atmospheric chemistry, and finally, the health effects of the particulates.

The main source of HC in engines is incomplete combustion due to bulk quenching of flames in a fraction of the engine cycles where combustion is especially slower. The

composition of an organic fraction can be divided into two distinct sub-groups: compounds that are already present in the fuel and compounds that are synthesized from original compounds.

The emission mechanism for synthesized organic compounds links to the mechanism of formation of soot. In soot formation, fuel molecules are first cracked or pyrolysed into simpler and smaller molecules and then these simpler molecules build into new structures of ever higher molecular mass which act as soot precursor.

The first step is irrefutable since light hydrocarbons, e.g. methane appear in exhaust gas even when wholly absent from the fuel ^[22] and hence hydrocarbon emission is composed of native and new born compounds ^[23]. In the second step, soot formation is interrupted such as by insufficient temperatures or flame quenching or too high or too lean fuel zones, soot precursors are then emitted instead of organic particulates. For these reasons, hydrocarbons, organic particulates, and carbonaceous particulates are all interlinked by a web of chemical reactions that take place inside the combustion chamber.

2.2.4 CO emissions:

Carbon monoxide (CO) is an odorless, colorless gas that is very dangerous to human health. Even at low levels of exposure, carbon monoxide can cause serious health problems. It is produced by a number of different fuels. Sources of carbon monoxide are numerous and prevalent in everyday life. In its natural state, CO will

usually dissipate quickly over a large area without posing any significant threat to human health. However, non-natural carbon monoxide emissions produced as a result of incomplete burning of carbon-containing fuels, including coal, wood, charcoal, natural gas, and fuel oil, are harmful to the body. Carbon monoxide results from incomplete combustion of fuel and is emitted directly from vehicle tailpipes. Incomplete combustion is most likely to occur at low air-to-fuel ratios in the engine. These conditions are common during vehicle starting when the air supply is restricted (“choked”) when cars are not tuned properly, and at altitudes, where “thin” air effectively reduces the amount of oxygen available for combustion. Nationwide, two-thirds of the carbon monoxide emissions come from transportation sources, with the largest contribution coming from highway motor vehicles. In urban areas, the motor vehicle contribution to carbon monoxide pollution can exceed 90 percent.

2.3 LITERATURE SURVEY OF BIODIESEL REPLACEMENT IN DIESEL ENGINE

2.3.1 Historical perspective:

The concept of using vegetal oil as an engine fuel likely dates when **Rudolf Diesel** (1858-1913) developed the first engine to run on groundnut oil ^[24], as he demonstrated at the World Exhibition in Paris in 1900. Rudolf Diesel firmly believed the utilization of a biomass fuel to be the real future of his engine. He wanted to provide farmers the opportunity to produce their own fuel. In 1911, he said, "The diesel engine can be fed with vegetable oils and would help considerably in the development of

agriculture of the countries which use it". In the year 1912, he said "The use of vegetable oils for engine fuels may seem insignificant today. But such oils may become in the course of time as important as the petroleum and coal tar products of the present time" [25]. Unfortunately, R. Diesel died 1913 before his vision of a vegetable oil powered engine was fully realized. Later, in the 1940's, vegetable oils were used again as fuel in emergency situations, during the period of World War II. Because of the increase in crude oil prices, limited resources of fossil fuel concern, there has been renewed focus on vegetable oils and animal fats for the production of biodiesel fuel. Hence, after eight decades the awareness for environmental concern rose among the people to search for an alternative fuel that could burn with less pollution. Rudolf Diesel's prediction is becoming true today with more and more biodiesel being used all over the world.

2.3.2 Biodiesel as diesel engine replacement:

Fast depletion of fossil fuels is demanding an urgent need to carry out research work to find out the variable alternative fuels. A large number of experiments were carried out with vegetable oils' replacement of I.C. engine fuel by researchers from various parts of the world. Most of these experiments were reported from US, Europe, India, Malaysia, and Germany.

Christopher et al. [26] conducted tests in Chicago using biodiesel as an alternative fuel for in-service motor coaches. This was an exploratory investigation to determine the

effect of fuel on engine performance characteristics and infrastructure needed to use this fuel. The test proved that biodiesel could be used as a feasible alternative fuel.

Montague ^[27] conducted experiments by using rapeseed oil in a diesel engine. The introduction of 5% of rapeseed methyl ester (RME) led to a reduction in the volumetric efficiency around 0.4%. It has been reported that even after a 71, 50,000 km run by vehicles no abnormal aging was observed. Senator ^[28] analyzed the performance and emission of a turbocharged direct injection (DI) diesel engine fueled with a mixture of RME and diesel fuel. It has been reported that performance is substantially unaffected if the comparison is made in terms of equivalence ratio. With a fall in equivalence ratio (i.e. as the load is increased), CO and PM emission are sharply increased. The concentration of NO_x showed a significant increase up to 20% in part load condition, compared to that of diesel.

Tadashi et al. ^[29] evaluated the feasibility of rapeseed oil and palm oil for diesel fuel in a naturally aspirated DI diesel engine. It was found that vegetable oil fuels gave an acceptable engine performance and exhaust emission levels for short-term operation. However, they caused carbon deposit buildups and sticking of piston rings with extended operations.

Chio ^[30] conducted tests on biodiesel-diesel blend in the concentration of 20 and 40% by volume on a single cylinder caterpillar engine with single and multiple injection

systems. It was reported that at high loads with single injection particular matter, CO emissions were reduced and a slight increase of NO_x was noticed with the increase in biodiesel concentration. But a decrease in particulate matter emission with little or no effect on NO_x was observed while using multiple injection systems. At low loads, the addition of biodiesel and multiple injection schemes were found to be detrimental to particulate matter and CO emission.

Ghormade et al. [31] used soyabean oil as fuel to run a compression ignition engine. He reported that there were only slight variations in part load efficiency but no improvement in brake specific fuel consumption.

Pangavhane et al. [32] conducted experiments by using soyabean oil in CI engine. It was reported the CO emissions and HC emissions reduced by 21 and 47% respectively, but NO_x was found to increase with load.

Salvatore et al. [33] conducted experiments on a DI turbo charged diesel engine using methyl ester of rapeseed oil. It has been reported that at the same injection timing, a rise in NO_x emissions and decrease of HC and CO with a large reduction of smoke take place.

Basic and Humke [34] studied the effect of mixing peanut oil and sunflower oil with diesel fuel in a single cylinder engine. They observed that with the increase of vegetable oil in the blend the amount of carbon deposits on the injector tip was increased when

compared with 100% diesel fuel. They found that the vegetable oil fuel blends gave a lower mass-based heating value than that of diesel fuel. It was also reported that when the diesel engine was run with vegetable oil as fuel, it produced power equivalent to that of diesel fuel because fuel mass flow energy delivery increased due to higher density and viscosity of the vegetable oil. It also increased due to higher density and viscosity of the vegetable oil. It also increased fuel flow by reducing internal pump leakage. The lower mass-based heating values of vegetable oils required larger mass fuel flow to maintain constant energy input to the engine.

Zhang and Van Gerpen ^[35] investigated the use of blends of methyl esters of soybean oil and diesel in a turbo-charged, four cylinder, direct injection diesel engine modified with a bowl in the piston and medium swirl type. They found that the blends gave a shorter ignition delay and similar combustion characteristics as diesel.

Labeckas and Slavinskas et al. ^[36] analyzed the emission characteristics of four stroke, four-cylinder, direct injection, unmodified, naturally aspirated diesel engine when operating on neat rapeseed methyl ester (RME) and its 5%, 10%, 20% and 35% blends with diesel fuel. They found that carbon monoxide, hydrocarbon, and visible emissions had decreased while an oxide of nitrogen emissions increased for methyl ester compared to diesel.

Recep et al.^[37] conducted a test on a single cylinder four strokes direct injected diesel engine with diesel fuel and nine different vegetable oil fuels including their methyl esters. The engine was operated at 1300 rpm. A comparison was reported assuming diesel fuel as reference fuel. The observed maximum torque differences between the reference value and peak values of the vegetable oil fuels were about 10% obtained with that of raw sunflower oil, raw soyabean oil, and opium poppy oil fuels. The maximum power differences between the reference value and peak values of the vegetable oil fuels were about 18% obtained with raw cottonseed oil and raw soyabean oil fuels. The minimum torque and power difference was about 3% between reference value and oils. These results may be due to the higher viscosity and lower heating values of vegetable oils. The specific fuel consumption of diesel was very low in comparison with all vegetable oils and their esters. Specific fuel consumption values of methyl esters were generally less than those of the raw oil fuels. The higher specific fuel consumption values of vegetable oils are due to their lower energy content, generally less than those of the raw oil fuels. The higher specific fuel consumption values of vegetable oils are due to their lower energy content. Relatively low CO emissions were obtained with the esters in comparison with raw vegetable oils. Maximum CO₂ emissions were about 10.5% with diesel fuel and slightly lower with vegetable oil. It was due to better spraying qualities and more uniform mixture preparation of these esters. NO_x emissions with vegetable oil fuels were lower than those with diesel fuel and NO_x

values of methyl esters were higher than those of raw fuels. NO_x formation was due to maximum combustion temperatures. Since the injected particle size of the vegetable oils was greater than those of diesel fuel, the combustion efficiency, and maximum combustion temperatures with each of the vegetable oils were lower and NO_x emissions were less.

Raheman and Phadatare ^[38] investigated the fuel properties of raw karanja oil, its methyl ester and its blends with varying proportion of high-speed diesel from 20% to 80% by volume (B20, B40, B60, and B80). The kinematic viscosity of karanja oil was found to be 10.7 times more than that of diesel at 40°C and after transesterification, it reduced to 2.9 times. The calorific value of karanja oil was increased from 34 MJ/kg to 36.12MJ/kg when transesterification was done. The flash points of karanja and biodiesel were reported to be greater than 100°C. A single cylinder four strokes, DI, water cooled diesel engine having a rated output of 7.5 KW at 3000 rpm was used for the test.

The emissions were studied at different engine loads (10%, 25%, 50%, 75%, 85% and 100% of the load corresponding to the load at maximum power) at an average engine speed of 2525 (62%) rpm. It was reported that the minimum and maximum CO produced were 0.004, 0.0016% resulting in a reduction of 94% and 73% as compared to diesel. For smoke density, it was 1% and 3% with a maximum and minimum reduction of 80% and 20 % as compared to diesel. On an average 26% reduction in NO_x was obtained for biodiesel and its blend as compared to diesel.

For engine performance, it was reported that the torque produced in case of B20 and B40 were 0.1% – 13% higher than that of diesel whereas for B60 to B100 it was reduced by 4% -23% from that of diesel. Brake specific fuel consumption for B20 and B40 was 0.8% – 7.4% lower than diesel, while for B60 – B100 it was 11% – 48% higher than that of diesel. The maximum brake thermal efficiency was reported to be 26.79% for B20 and 26.19% for B40 higher than diesel (24.62%). Finally, it was concluded that B40 blend could replace diesel for running the diesel engine without sacrificing power output and having less emissions.

Chitra et al. ^[39] optimized transesterification of jatropha oil using a NaOH alkaline catalyst. Under the optimum reaction conditions, the conversion of jatropha oil to methyl esters was 98% in 90 min. It is significant that the FFA content in crude jatropha oil was reduced to 0.25% from 3.1% using NaOH. It is indubitable that NaOH will induce soap formation but at the same time, NaOH will also neutralize free fatty acids to an acceptable level to meet biodiesel specifications. However, an extra step is needed to remove the sodium soap after the reaction. The catalyst amount, the molar ratio of methanol and reaction time were not only investigated but also optimized using completely randomized design (CRD). Large-scale production of biodiesel from 25 kg of jatropha oil has resulted in 24 kg of biodiesel (96% of yield), which is only reduced by 2% as compared to lab scale. The properties of biodiesel produced from jatropha oil also fall within the limits of Bureau of Indians Standards (BIS) specification.

Agarwal et al. [2] investigated on a single cylinder diesel engine with Karanja oil and its blends with or without preheating the fuel and suggested no modification in engine hardware. However, while using preheated fuel, engine efficiency was improved slightly compared to the normal fuel blend. Performance and emission characteristics of Karanja oil and its blends were found to be comparable to that of mineral diesel. The thermal efficiency of the engine with preheated oil blends is nearly 30% and for lower blends (unheated) such as K10, K20, and K50, it was 24%–27%. The brake specific fuel consumption and brake specific energy consumption of the engine with preheated lower blends showed an improved trend. The unheated oil blends up to K50 also showed an improved trend compared to mineral diesel. The smoke density from the exhaust gas of preheated lower blends as well as unheated lower blends was almost similar to that of diesel fuel. The HC emissions from unheated and preheated lower blends (K10 and K20) are lower than that of mineral diesel. The emissions of NO from all blends with and without preheating are lower than mineral diesel at all load conditions that shows a significant advantage over mineral diesel while using vegetable oil and their blends. He concluded that the Karanja oil blends with diesel up to 50% (v/v) without preheating as well as with preheating would replace diesel for running the CI engine for lower emissions and improved performance.

Bari et al. [40] performed short-term performance tests using crude palm oil as a fuel for diesel engine and found crude palm oil to be a suitable substitute, with a peak

pressure about 5% higher and ignition delay about 3^o shorter compared with diesel. Emissions of NO_x and CO (carbon monoxide) were about 29% and 9% higher respectively for crude palm oil. He also suggested that prolonged use of crude palm oil as fuel may cause the engine performance to deteriorate.

Silvio ^[41] used heated palm oil as fuel in a diesel generator. Studies reveal that exhaust gas temperature and specific fuel consumption were increased with an increase in charge percentage. The CO emission was increased with the increase of load. Unburned HC emissions were lower at higher loads but tended to increase at higher loads. This was due to a lack of oxygen resulting from the operation at higher equivalence ratios. Palm oil NO_x emissions were lower as compared to the diesel fuel. They also reported that a diesel generator can be adapted to run with heated palm oil and would give better performance.

Chauhan et al. ^[42] used preheated jatropha oil as fuel in dual fuel test rig. Results showed that brake thermal efficiency of the engine was lower and brake specific energy consumption was higher as compared to diesel fuel. The increase in fuel inlet temperature resulted in an increase of brake thermal efficiency and reduction in brake specific energy consumption and they also optimized fuel inlet temperature at 80^oC. Emissions of NO_x from Jatropha oil during the experimental range were lower than diesel fuel and it increases with increase in fuel inlet temperature. CO (carbon monoxide), HC (hydrocarbon), CO₂ (carbon dioxide) emissions from Jatropha oil were

found higher than diesel fuel. However, with an increase in fuel inlet temperature, a downward trend was observed. Finally, they have suggested by using heat exchanger preheated Jatropha oil can be a good substitute fuel for a diesel engine in the near future.

2.4 BIODIESEL – AN OVERVIEW

Biodiesel is a fuel consisting of the mono-alkyl esters of fatty acids from vegetable oils or animal fats. Biodiesel is receiving attention as an alternative, non-toxic, biodegradable and renewable diesel fuel. Many standardized procedures are available for the production of biodiesel fuel oil [43]. The commonly used methods for biodiesel production are explained below.

2.4.1 Direct use/Blending

Vegetable oil can be directly used as diesel fuel without any changes to the engine. The blending of vegetable oil with diesel fuel was experimented successfully by various researchers. In 1980, Caterpillar Brazil Company used pre-combustion chamber engines with a mixture of 10% vegetable oil to maintain total power without any modification to the engine. A blend of 20% oil and 80% diesel was found to be successful [44]. It has been proved that the use of 100% vegetable oil was also possible with some minor modifications in the fuel system. The primary concern with vegetable oil as fuel is its high viscosity, which leads to problems in long run.

2.4.2 Micro-emulsification

Micro-emulsion is defined as a colloidal dispersion of fluid microstructures (1 – 150 nm) in a solvent forming two immiscible phases. The common solvents used are methanol and ethanol. Micro-emulsions are the probable solution to a high viscosity of the vegetable oil. Their atomisation is relatively easy because of lower viscosity. These can improve spray characteristics by explosive vaporization of the low boiling constituents in the micelles. Czerwinski ^[45] prepared an emulsion of sunflower oil, ethanol and butanol having a viscosity 6.3 Cst at 40°C compatible with diesel fuel and the lower viscosities were observed with the increase in butanol.

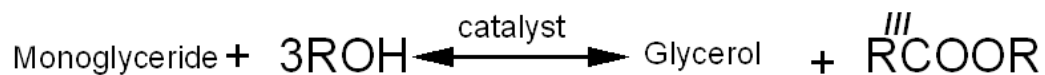
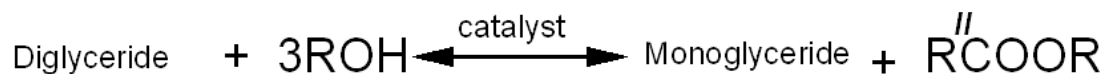
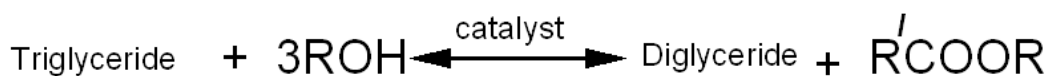
2.4.3 Pyrolysis

Pyrolysis means conversion of one substance to other by application of heat. The catalyst is used to speed up the process. Different products can be obtained from the same material depending on the different path of reaction and this makes pyrolytic chemistry difficult. It involves heating in the absence of air or oxygen and cleavage of chemical bonds to yield small molecules. During World War I, many investigators had studied the pyrolysis of vegetable oil to obtain products suitable for engine fuel application. The pyrolyzed material can be vegetable oils, animal fats, natural fatty acids and methyl esters of fatty acids.

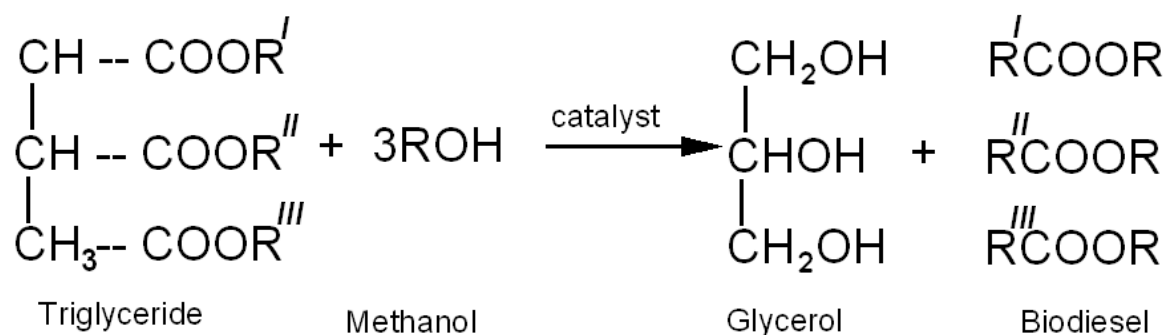
2.4.4 Transesterification

Transesterification is otherwise known as alcoholysis. It is the reaction of fat or oil with an alcohol to form esters and glycerin. The monoesters produced by transesterification of vegetable oil or animal fats are known as biodiesel. A catalyst is used to improve the reaction rate and yield. Among the alcohols, methanol and ethanol are used commercially because of their low cost and their physical and chemical advantages. They quickly react with tri-glycerides and NaOH and are easily dissolved in them. Transesterification significantly reduces the viscosity of the vegetable oil. The variables that have the greatest influence on the transesterification chemical reaction time and conversion efficiency are concentration, purity of the reactants, ratio of the alcohol to oil, temperature, catalyst type, and the stirring rate.

The overall transesterification reaction is given by three consecutive and reversible equations as follows:



The first step is the conversion of triglyceride to diglycerides, followed by the conversion of diglycerides to monoglycerides, and monoglycerides to glycerol, yielding one methyl ester molecule per mole of glyceride at each step.



The overall chemical reaction of transesterification process is shown above. Where R^I, R^{II} and R^{III} are long chain hydrocarbons which may be the same or different with R = – CH₃/C₂H₅.

2.5 ADVANTAGES OF BIODIESEL

There are a few advantages that encourage the use of biodiesel as an alternative fuel.

- ✓ Petroleum import cost can be reduced by producing domestically.
- ✓ It contains low aromatics.
- ✓ Biodiesel can be produced directly in CI engine with no major modification of the engine.

- ✓ It is nontoxic and degradation rate is faster than diesel.
- ✓ Biodiesel contains very low/no sulphur, hence eco-friendly and suitable for future Euro-norms.
- ✓ The higher flash point makes the storage safer and improved personal safety.
- ✓ Biodiesel does not produce greenhouse effects, because of the balance between the CO₂ emission and the amount of CO₂ absorbed by the plants producing vegetable oil.
- ✓ The exhaust emissions from biodiesel are much lower than diesel fuel. It provides a significant reduction in HC, CO, PM emissions. But most emission tests have shown a slighter increase in NO_x in biodiesel.

2.6 DISADVANTAGES OF BIODIESEL

- ✗ Higher cost compared to petroleum diesel fuel, being not properly commercialized in India.
- ✗ Lower heat value than petroleum diesel causing an increase in BSFC.
- ✗ Biodiesel tends to crystallize at low temperature and results in a problem in cold weather operations.
- ✗ Storage and handling are difficult, particularly stability in long term storage.

2.7 CONCLUSIONS FROM LITERATURE REVIEW

Prior to deciding upon the detailed activity of the present work, the information from different kinds of literature was analyzed. It is evident from the literature survey that conventional fuels such as diesel cannot meet the stringent performance and emissions requirements of modern CI engines and also the depletion of the petroleum reserves. Among the various alternative fuels, vegetable oils are found to be the most suitable. Most of the esterified oils tried in diesel engines were edible oils in Indian context like soyabean, sunflower, rapeseed, palm etc. So the use of biodiesels from these oils as a substitute for diesel fuel may lead to a concept of self-sufficiency in vegetable oil production, which India has not yet attained.

From the literature, it is also found that abundance of forest and tree-borne non-edible oils are available in India. It is also reported 75 plants contains 30% or more oil in their seed, fruit or nut on which not much attempt has been made to use esters of these non-edible oils as a substitute for diesel. Apart from this physiochemical properties, they need to be studied for the selection of oil as a diesel substitute. The experiments are mostly subjected to error-prone if proper attention is taken off and each experiment is subjected to costly instrumentation.

2.8 NEED FOR PRESENT WORK

In our country the ratio of diesel to gasoline fuel is 7:1, depicting a highly skewed situation. Thus it is essential to replace fossil diesel fuel by alternative fuel. From the literature, it is found vegetable oil presents a very promising scenario of functioning as alternative fuels to fossil diesel fuel. The scientists & researchers conducted several tests by using different oils and their blends with diesel. The use of non-edible vegetable oils compared to edible oils is very significant in developing countries like India, because of the tremendous demand for edible oils as foods – they are far too expensive to be used as fuel at present. As it is also reported there are many tree species that have seeds rich in non-edible vegetable oils on which much attention is not made so far. Before selecting any vegetable oil as diesel substitute it is necessary to find the physiochemical properties and compare with the properties of standard diesel fuel so that the engine may run with little or no modification. But most of the methods for detecting physiochemical properties are arduous and expensive; the values obtained are mostly subjected to some experimental error.

So, to find a solution to this problem it was decided to study two non-edible oils'; jatropha curcas and karanja (*pongamia pinnata*). It is also tried to develop certain equations for predicting different physiochemical properties that are much easier to find out in comparison to standard methods. At last, the values obtained are compared with the existing values.

2.9 STATEMENT OF THE PROBLEM

On the basis of literature survey as discussed previously, an experimental study was conducted to determine the physiochemical properties of the fuel under consideration and then the performance and exhaust emission characteristics of a compressed ignition engine using those fuels so that a significant thought can be made as a diesel substitute.

After a thorough study of the existing literature related to the field, it was decided to carry out the following experimental investigations to assess the potential of using selected biodiesel in direct injection compressed ignition engine.

The various phases of the activity considered are as follows:

- Conversion of raw jatropha and karanja oil into Jatropha Oil Methyl Ester (biodiesel) and Karanja Oil Methyl Ester (biodiesel) respectively by transesterification process.
- Development of a test rig for a detailed investigation on straight diesel operation as well as with diesel biodiesel blend. The engine chosen for this experiment was a single cylinder, air cooled, direct injection engine
- The fuel and air measuring system are incorporated into the engine system.
- Physiochemical properties of the biodiesel that has been prepared are measured and compared with the standard values of Fossil diesel fuel.

- A mathematical model has been developed to find the cetane number which is highly essential for determining the performance of CI engine and the cetane number obtained through the developed model was validated with the published experimentally obtained cetane number.
- Separate mathematical models have been developed to predict some of the fundamental fuel properties like viscosity, density and High Heat Value (HHV) and the values obtained from the model were validated with the published experimentally obtained values.
- The necessary data for analyzing the engine performance over a wide range of load variation is generated. The comprehensive experimental activities are carried out for baseline diesel, diesel-biodiesel blend and their exhaust emission is also studied.
- The engine performance, combustion and exhaust emission characteristics at various diesel-biodiesel proportions are analyzed at different loads.
- Engine performance, combustion, and exhaust emission characteristics are compared and analyzed to decide on the optimum performance of fuel blends.

The next chapter briefly explains the development of engine test rig and its associate accessories and instrumentation developed. It also describes the engine parameters and combustion characteristics that were measured and techniques employed, at different phases of this work for the generation of the experimental data.

CHAPTER 3

PRODUCTION METHODOLOGY OF BIODIESEL

3.1 PRODUCTION OF BIODIESEL

Jatropha and karanja oil are procured from commercial suppliers situated at Kolkata. Methanol and sodium hydroxide are purchased from Merck. A 7 litre capacity small reactor (figure 3.1 – 3.3) with oil bath for the transesterification is designed and fabricated, consisting of the heating element, reaction flask, made of glass and a motor driven stirrer. The reactor consists of three necks: centrally one for stirrer and also for the inlet of reactant, one for the condenser and one for the thermocouple to measure inside reaction temperature placed on both sides to the central one. The flask has a stopcock at the bottom for the removal of the glycerol and a tapping is provided at the side for the collection of the biodiesel.



Plate 3.1: 7 litre capacity reactor with oil bath



Plate 3.2: Reactor from top

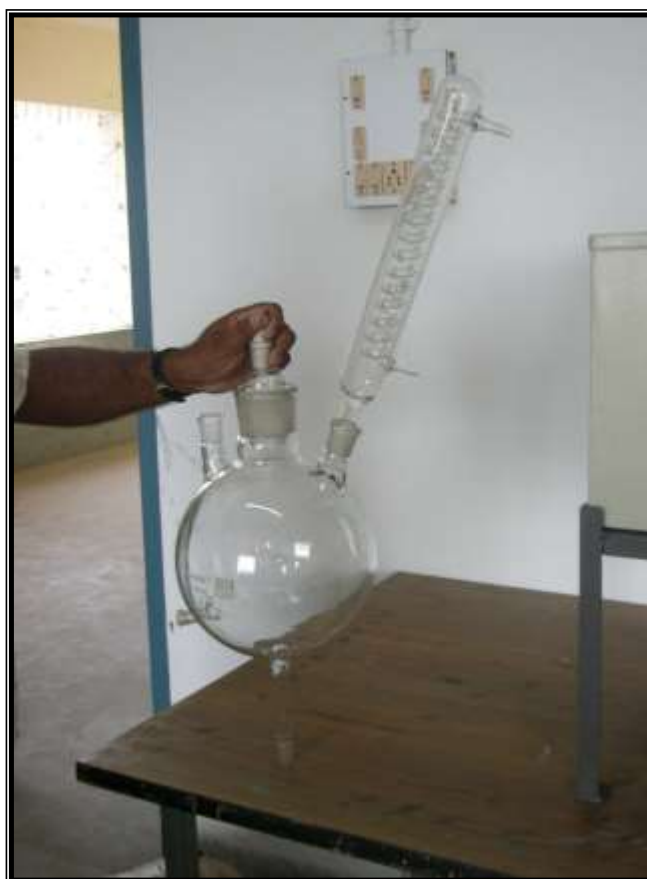


Plate 3.3: Reactor with internal view

3.1.1 Procedural steps for the production of biodiesel

i. Transesterification:

- a) The untreated 5 litre vegetable oil (karanja) is heated in the reactor at 65°C in order to remove the moisture.
- b) Methoxide solution is prepared with 7.5 litres of methanol and 450 gm NaOH.
- c) Karanja oil and the prepared methoxide solution mixed properly in the reactor.
- d) The mixtures are maintained at a temperature around 70°C to speed up the reaction and continuously stirred the mixture for around three hours.
- e) The oil is converted into Karanja Oil Methyl Ester (KOME) by transesterification. The same proportion and process conditions maintained for the production of KOME in a large capacity (50 gallons capacity, shown in plate: 3.4) biodiesel reactor plant. In this reactor, 25 litres of karanja oil is fed for the production of KOME.

ii. Separation

- f) The refinement of the product from the production of biodiesel is a crucial part that can increase the cost of production. For the purity of the biodiesel, that will meet the international standard, free fatty acids, alcohol, free and bound glycerine, the water content in the biodiesel must be kept to a minimum level. Therefore, the main object is to separate the esters from the mixture conforming high purity of products. Practically, in transesterification process two major products are formed: biodiesel and glycerol, each having a substantial amount of methanol as excess methanol is used in the reaction. The alcohol recovery is done by vacuum distillation process. As the glycerine is much denser than biodiesel the products of the reaction are allowed to settle down for around 24 hours. Two distinct layers, glycerine at the bottom and biodiesel at the top are found. The layer of glycerine settled at the bottom is carefully taken out and the upper layer is the biodiesel which is tapped separately. The remaining esters contain some amount of catalyst and alcohol and this can be further purified by washing.



Plate 3.4: Biodiesel reactor plant of 200 litre capacity

iii. **Washing:**

g) Washing of biodiesel is done for the removal of any residual catalyst or methanol presents. The amount of water required for washing is found to be approximately 8 – 10 times the volume of biodiesel.

iv. **Vacuum distillation:**

h) After washing, the biodiesel is heated for approximately 2 hours in the absence of air for the removal of any traces of moisture. This process is known as vacuum distillation. The temperature kept during the process is

around 95° – 98° C. After vacuum distillation, the biodiesel is kept for cooling and ready to use.

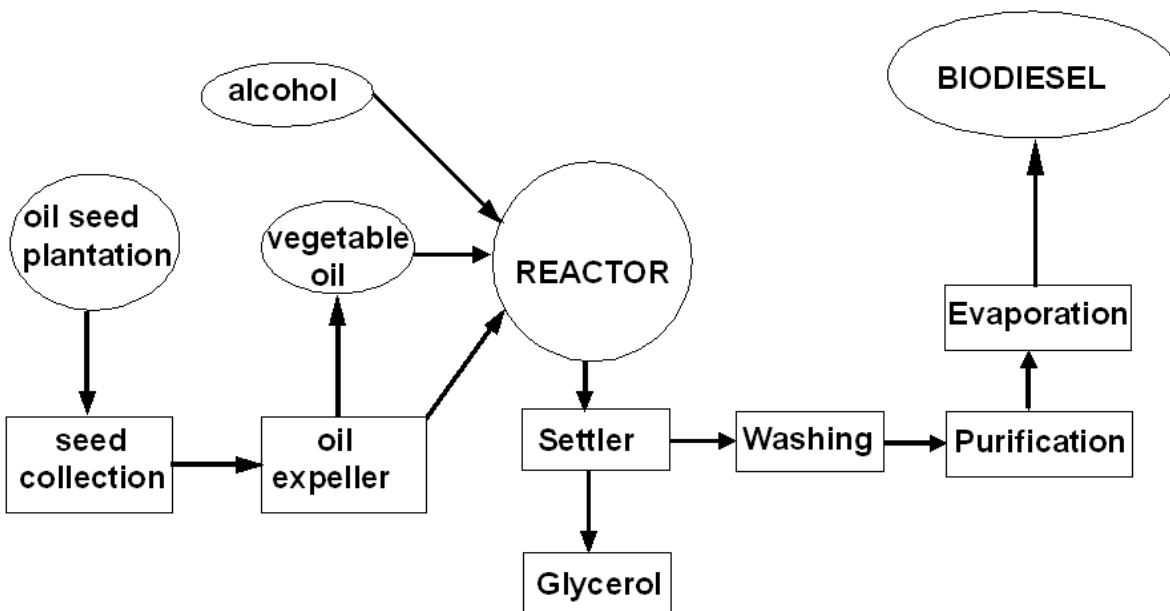


Figure 3.1 Process cycle of biodiesel

The general process cycle of biodiesel from the seed plantation is shown in figure 3.1.

3.2 BIODIESEL SPECIFICATIONS AND PROPERTIES

Biodiesel is defined as a fuel comprised of mono-alkyl esters of long chain fatty acids derived from vegetable oils or animal fats, designated B100. A mono-alkyl ester is the product of the reaction of a straight chain alcohol, such as methanol or ethanol, with a fat or oil (triglyceride) to form glycerol (glycerin) and the esters of long chain fatty acids.

3.3 PROPERTY REQUIREMENTS AND SPECIFIED METHODS FOR B100

The values of the various biodiesel properties specified by ASTM D 6751 are listed in Table 3.1. Each of these properties and the test method used to measure it, are described below.

Table 3.1 ASTM D – 6751 SPECIFICATIONS

Property	Method	Limits	Units
Flash Point, closed cup	D93	130 min	°C
Water & Sediment	D2709	0.05 max	% volume
Kinematic Viscosity at 40°C	D445	1.9 – 6.0	mm ² /s
Sulfated Ash	D874	0.020 max	wt %
Total Sulfur	D5453	0.05 max	wt %
Copper strip corrosion	D130	No. 3 max.	
Cetane number	D613	47 min	
Cloud point	D2500	Report to customer	°C
Carbon Residue	D4530	0.050 max	wt %
Acid Number	D664	0.80 max	mg KOH/g
Free Glycerin	D6584	0.020 max	wt %
Total Glycerin	D6584	0.240 max	wt %
Phosphorus Content	D4951	0.001 max	wt %
Vacuum Distillation end point	D1160	360 max	°C

3.3.1 ASTM D93- Flash point, closed cup

Requirement: 130 °C min

The flash point is defined as the “lowest temperature corrected to a barometric pressure of 101.3kPa (760 mm Hg), at which application of an ignition source causes the vapours of a specimen to ignite under specified conditions of the test.” This test, in part, is a measure of residual alcohol in the B100. The flash point is a determinant for

flammability classification of materials. The typical flash point of pure methyl esters is > 200°C, classifying them as non-flammable. However, during production and purification of biodiesel, not all the methanol may be removed, making the fuel flammable and more dangerous to handle and store if the flash point falls below 130°C. Excess methanol in the fuel may also affect engine seals and elastomers and corrode metal components.

3.3.2 ASTM D 2709 – Water and sediment

Requirement: 0.050 % volume max

Water and sediment is a test that determines the volume of free water and sediment in middle distillate fuels having viscosities at 40 °C in the range 1.0 to 4.1 mm²/s and densities in the range of 700 to 900 kg/m³. This test is a measure of cleanliness of the fuel. For B100 it is particularly important because water can react with the esters, making free fatty acids, and can support microbial growth in storage tanks. Water is usually kept out of the production process by removing it from the feed stocks. However, some water may be formed during the process by the reaction of the sodium or potassium hydroxide catalyst with alcohol. If free fatty acids are present, water will be formed when they react to either biodiesel or soap. Finally, water is deliberately added during the washing process to remove contaminants from the biodiesel. This washing process should be followed by a drying process to ensure the final product will meet ASTM D 2709.

3.3.3 ASTM D 445 – Kinematic viscosity, 40 ° C

Requirement: 1.9 – 6.0 mm²/s

Kinematic viscosity is the resistance to the flow of a fluid under gravity. [The kinematic viscosity is equal to the dynamic viscosity/density] The kinematic viscosity is a basic design specification for the fuel injectors used in diesel engines. Too high a viscosity will cause injectors malfunction. Dynamic viscosity is the ratio between applied shear stress and rate of shear strain of a liquid.

3.3.4 ASTM D 874 – Sulfated Ash

Requirement: 0.020 wt. %, max

Sulfated ash is the residue remaining after a [fuel] sample has been carbonized, and the residue subsequently treated with sulfuric acid and heated to a constant weight. This test monitors the mineral ash residual when a fuel is burned. For biodiesel, this test is an important indicator of the quantity of residual metals in the fuel that came from the catalyst used in the esterification process. Producers that use a base catalyzed process may wish to run this test regularly. Many of these spent sodium or potassium salts have low melting temperatures and may cause engine damage in combustion chambers.

3.3.5 ASTM D5453 – Total sulfur

Requirement: 0.05 wt. %, max

This method covers the determination of total sulfur in liquid hydrocarbons, boiling in the range from approximately 25^o to 400°C, with viscosities between approximately 0.2 and 20 cSt (mm²/s) at room temperature. Biodiesel feed stocks typically have very little sulfur, but this test is an indicator of contamination of protein material and/or carryover catalyst material or neutralization material from the production process.

3.3.6 ASTM D 130 – Copper strip corrosion

Requirement: No. 3, max

The copper strip corrosion is used for the detection of the corrosiveness to copper of fuels and solvents. This test monitors the presence of acids in the fuel. For B 100, the most likely source of a test failure would be excessive free fatty acids, which are determined in accordance with an additional specification.

3.3.7 ASTM D 613 – Cetane number

Requirement: 47, min

The cetane number is a measure of the ignition performance of a diesel fuel obtained by comparing it to reference fuels in a standardized engine test. Cetane for diesel engines is analogous to the octane rating in a spark ignition engine – it is a measure of how easily the fuel will ignite in the engine.

3.3.8 ASTM D 2500 – Cloud point

Requirement: Report in °C to customer

The cloud point is the temperature at which a cloud of wax crystals first appears in a liquid when it is cooled down under conditions prescribed in this test method. The cloud point is a critical factor in cold weather performance for all diesel fuels. The chemical composition of some biodiesel feed stocks leads to a B100 that may have higher cloud points than customer's desire. Since the saturated methyl esters are the first to precipitate, the amounts of these esters, methyl palmitate, and methyl stearate, are the determining factors for the cloud point.

3.3.9 ASTM D 4530 – Carbon residue

Requirement: 0.050 wt%, max

In petroleum products, the part remaining after a sample has been subjected to thermal decomposition is the carbon residue. The carbon residue is a measure of how much residual carbon remains after combustion. The test basically involves heating the fuel to a high temperature in the absence of oxygen. Most of the fuel will vaporize and be driven off, but a portion may decompose and pyrolyze to hard carbonaceous deposits. This is particularly important in diesel engines because of the possibility of

carbon residues clogging the fuel injectors. The most common cause of excess carbon residues in B 100 is an excessive level of total glycerin.

3.3.10 ASTM D 664 – Acid number

Requirement: 0.80 mg KOH/g, max

The acid number is the quantity of base, expressed as milligrams of potassium hydroxide per gram of sample, required to titrate a sample to a specified end point. The acid number is a direct measure of free fatty acids in B100. The free fatty acids can lead to corrosion and may be a symptom of water in the fuel. Usually, for a base catalyzed process, the acid value of production will be low since the base catalyst will strip the available free fatty acids. However, the acid value may increase with time as the fuel degrades due to contact with air or water.

3.3.11 ASTM D 6584 – Free glycerin

Requirement: 0.020 wt. %

Free glycerol is the glycerol present as molecular glycerol in the fuel. Free glycerol results from the incomplete separation of the ester and glycerol products after the transesterification reaction. This can be a result of imperfect water washing or other approaches that do not effectively separate the glycerol from the biodiesel. The free

glycerol can be a source of carbon deposits in the engine because of incomplete combustion.

3.3.12 ASTM D 6584 – Total glycerin

Requirement: 0.240 wt. %

Total glycerol is the sum of free and bonded glycerol. Bonded glycerol is the glycerol portion of the mono-, di-, and triglyceride molecules. Elevated total glycerol values are indicators of incomplete esterification reactions and predictors of excessive carbon deposits in the engine.

3.3.13 ASTM D 4951 – Phosphorus

Requirement: 0.0010 wt. %

This test covers the quantitative determination of barium, calcium, copper, magnesium, phosphorus, sulfur, and zinc in unused lubricating oils and additive packages. In the case of B100, phosphorus can come from the incomplete refining of the phospholipids (or gums) from the vegetable oil and from bone and proteins encountered in the rendering process.

3.3.14 ASTM D 1160 – Vacuum distillation end point

Requirement: 360 °C max, at 90 % liquid distilled

The vacuum distillation end-point test covers the determination, at reduced pressures, of the range of boiling points for petroleum products that can be partially or completely vaporized at a maximum liquid temperature of 400° C.

Petroleum fractions have several individual compounds mixed together. The distillation curves are used to characterize the broad chemistry of a given crude oil source in terms of the boiling temperatures of its constituent compounds. In B100 there are, at most, ten different esters present, and they can be identified using gas or liquid chromatography. The same chromatograph that determines free and total glycerin can determine the esters composition in the B100.

All fuels are subject to degradation over time when they are stored. This degradation may be due to microbial action, water intrusion, air oxidation, etc. The standard and the test methods for determining storage stability for B100 are still in the development stage within the ASTM process.

3.4 MEASURED FUEL PROPERTIES

Different fuel properties are measured with the standard methods and instruments, whose major specifications are shown in Appendix 1.

3.4.1 Kinematic viscosity (centistokes, cSt)

The resistance to flow exhibited by fuel blends is expressed in various units of viscosity. It is a major factor of consequence in exhibiting their suitability for the mass transfer and metering requirements of engine operation. Higher viscosity results in low volatility and poor atomization of oil during injection in CI engine, that results in incomplete combustion and ultimately carbon deposits on injector nozzle as well as in the combustion chamber. The viscosities of Karanja oil, as well as derived biodiesel, are measured by Red Wood Viscometer (As per IP70, shown in plate: 3.5) and a comparative study is made at a different temperature. Different temperature dependent viscosities are shown in table 3.2 and a comparison between the viscosities of biodiesel and raw karanja oil at different temperatures are plotted in figure 3.2. It is clearly observed that the transesterification results in a large amount of reduction in viscosity and as the temperature increases the viscosity reduces.

Table 3.2 Viscosity dependency on temperature variation of biodiesel and karanja

RAW KARANJA OIL		BIODIESEL	
Temp(⁰ C)	Viscosity(cSt)	Temp(⁰ C)	Viscosity(cSt)
30	29.65	30	8.73
45	17.34	45	7.44
60	14.62	60	5.97
75	11.74	75	5.34
90	10.63	90	4.62



Plate 3.5: Redwood viscometer

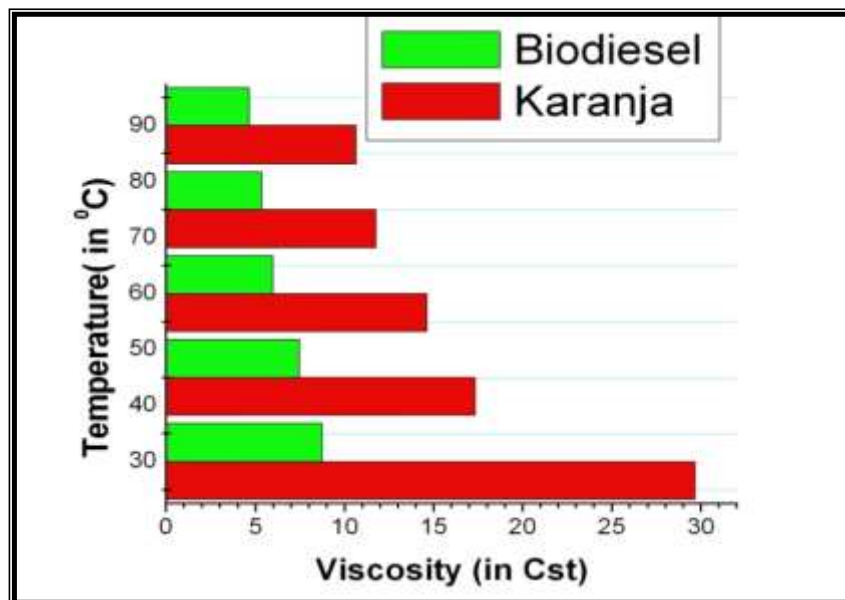


Figure 3.2 Comparative study of viscosities at different temperature

3.4.2 Calorific value (kj/kg)

The calorific value of a fuel is the thermal energy released per unit quantity of fuel when the fuel is burned completely and the products of combustion are cooled back to the initial temperature of the combustible mixture. It measures the energy content in a fuel. This is an important property of the biodiesels that determines the suitability of the material as an alternative to diesel fuels.

The heating value of the prepared biodiesel is determined with the help of Bomb Calorimeter (followed by the specification IP 12 and ASTM D4809), shown in plate 3.6. A known amount of fuel is burnt in a bomb and the temperature difference noted down. The effective heat capacity (water equivalent) of the system is also determined using the same procedure with dry and pure benzoic acid (6324calories/gm or 26460 kj/kg).



Plate 3.6: Bomb calorimeter

Table 3.3 Observation table for bomb calorimeter

TIME	MINUTES	TEMP °C		TEMP. DIFFERENCE PER MINUTES(°C)
Preliminary period	0	$T_0 = 28.00$		0.01°C (const.)
	1	$T_1 = 28.01$		
	2	$T_2 = 28.02$		
	3	$T_3 = 28.03$		
	4	$T_4 = 28.04$		
	5	$T_5 = 28.05$		
Chief period	6	$T_6 = 29.11$		Observed rise of Temp(T):- $T = T_{13} - T_5$ (°C) = 30.43 – 28.05 = 2.38°C
	7	$T_7 = 29.72$		
	8	$T_8 = 29.99$		
	9	$T_9 = 30.18$		
	10	$T_{10} = 30.32$		
	11	$T_{11} = 30.42$		

	12	$T_{12} = 30.44$		
	13	$T_{13} = 30.43$		
After period	14	$T_{14} = 30.42$		Rate of change of temp =Take the difference in two consecutive temp., which occurs maximum Nos. =0.01°C
	15	$T_{15} = 30.41$	0.01	
	16	$T_{16} = 30.41$	0	
	17	$T_{17} = 30.41$	0	
	18	$T_{18} = 30.41$	0	
	19	$T_{19} = 30.40$	0.01	
	20	$T_{20} = 30.39$	0.01	
	21	$T_{21} = 30.38$	0.01	
	22	$T_{22} = 30.37$	0.01	
	23	$T_{23} = 30.36$	0.01	
	24	$T_{24} = 30.35$	0.01	

Calculation:

Total water equivalent of the system = 2985

Biodiesel (m_f) = 0.2 gm

Calorific value of the biodiesel (C.V) = C.V

Heat developed due to Biodiesel = $m_f \times C.V$

- Correction for Nitric Acid = 10 calories [41.84J]
- Correction for heat of ignition = 20 calories [83.68J]
(Cotton +Ni-chrome wire)

Total heat = $m_f \times C.V + 10 + 20$ calories

$$= m_f \times C.V + 41.84 + 83.68 \text{ J}$$

The corrected rise of temperature = Observed rise of Temp. ($T_{13} - T_5$) denoted as T +
Cooling correction (T_c) + Thermometer correction (T_t)

The average rate of change of Temp. during the AFTER PERIOD (ΔT_2):-

$$\Delta T_2 = \frac{\text{total rate of change of Temp.}}{\text{No. of reading taken}}$$

$$= \frac{0.01+0.0+0.0+0.0+0.01+0.01+0.01+0.01+0.01+0.01}{10}$$

$$= 0.007^\circ \text{C}$$

Cooling correction (T_c) = ($n \times \Delta T_2$) = $8 \times 0.007 = 0.056^\circ \text{C}$

(n = Number of minutes during Chief period)

The corrected rise of temp. = ($T + T_c + T_t$) = $2.38 + 0.056 + 0.01$

Total heat = total water equivalent x corrected rise in temperature

$$0.2 \times C.V + 125.52 = 2985 \times 2.446$$

$$C.V = 35878.95 \text{ kJ/gm} \approx 35879 \text{ kJ/gm}$$

3.4.3 Specific gravity

Otherwise known as the relative density, specific gravity refers to the ratio of the density of a fuel to the density of water at the same temperature. With it, other properties could

be judged. The density of the fuels is measured by means of a capillary stopper relative density bottle of 20ml capacity.

Table 3.4 Specific gravity of raw karanja and biodiesel

Karanja oil	Volume (ml)	Weight (gm)	Specific	Density
Raw	20	18.240	0.912	912
Transesterified	20	17.640	0.882	882

3.4.4 Cloud point and pour point (°C)



Plate 3.7: Cloud and pour point apparatus

Cloud point is that temperature expressed as a multiple of 1°C , at which a cloud or haze of wax crystals appears at the bottom of the test jar when the oil is cooled under the prescribed conditions. Pour point is the lowest temperature, expressed as multiple of 3°C at which the oil is observed to flow when cooled and examined under prescribed conditions.

These two temperatures are of great importance in understanding the behaviour of fuels in a cold weather. These properties are determined by the standard instrument for measuring cloud and pour point apparatus followed by IP15, as shown in plate 3.7.

Table 3.5 cloud and pour points of raw karanja and biodiesel

RAW KARANJA OIL		BIODIESEL	
Property	Temp($^{\circ}\text{C}$)	Property	Temp($^{\circ}\text{C}$)
Cloud point	7	Cloud point	6
Pour point	3	Pour point	3

3.4.5 Flash and Fire point ($^{\circ}\text{C}$)

Flash point is the lowest temperature corrected to a standard atmospheric condition at which application of a test flame causes the vapour of a specimen to ignite under specified conditions of the test.

Fire point is the lowest temperature at which a specimen will sustain burning for 5 seconds.

These two parameters have great importance while determining the fire hazard (temperature at which fuel will give off inflammable vapour). Flash point and fire point of the samples measured by Cleveland open Cup Tester (followed by the specifications IP 36, ASTM D92, IS: 1448) as shown in plate 3.8.

Table 3.6 Flash point and fire points

Properties	Karanja oil	Biodiesel
Flash point (°C)	241	217
Fire point (°C)	253	223



Plate 3.8: Flash and fire point apparatus

3.4.6 Cetane number

The physical and chemical properties of fuel play very important role in delay period. The cetane number (CN) of the fuel is one such important parameter which is responsible for the delay period. Cetane number of a fuel is defined as the percentage by volume of normal cetane in a mixture of normal cetane and α -methyl naphthalene which has the same ignition characteristics (ignition delay) as the test fuel, when combustion is carried out in a standard engine under specified operating condition. A fuel of higher cetane number gives lower delay period and provides smoother engine operation. American Petroleum Institute (API) and National Bureau of Standards jointly devised an arbitrary scale expressing the gravity or density of liquid petroleum product in terms of degree API. For current fuel, it is found to be degree API as 28.93 and Diesel index as 47.79. The cetane number is calculated as more than 56.64, which proves the suitability as a diesel fuel. Aniline point apparatus is shown in plate 3.9.

Aniline point = 74°C = 165.2°F, sp. Gravity = 0.882;

50% boiling point (°C) = 364

The measuring scale is calibrated in terms of degrees API.

$$\text{Degrees API gravity} = \frac{141.5}{\text{specific gravity}} \text{ at } 60^{\circ} F - 131.5 = 28.93$$

Diesel Index: the diesel index is related to the aniline point as

$$DI = \frac{API_{gravity}(60^{\circ}F) \times aniline\ point(^{\circ}F)}{100} = 47.79$$

Cetane number: the Cetane number, in turn, is related to the diesel index as

$$CN = \frac{2}{3}DI + 0.068 [50\% \text{ boiling point } (^{\circ}F)] - 22$$

$$= \frac{2}{3} \times 47.79 + 0.068 [688] - 22$$

$$= 56.64$$



Plate 3.9: Anniline point apparatus

3.5 ANALYSIS OF FUEL PROPERTIES

Table 3.7 Comparative study of fuel properties

Properties	Karanja oil	Biodiesel	Diesel
Viscosity (cSt) at 30°C	29.65	8.73	2.5
Calorific value (kj/kg)	-	35879	43500
Flash point (°C)	241	217	52
Fire point (°C)	253	223	63
Cloud point (°C)	7	6	5
Pour point (°C)	3	3	4
Specific gravity	0.912	0.882	0.835

As shown in table 3.7, viscosity and specific gravity of biodiesel obtained are very high compared to the suitability in CI engine; therefore it is evident that dilution or blending of biodiesel with other fuels like diesel fuel would bring the viscosity and density close to a specification range. Therefore biodiesel obtained from karanja is blended with diesel oil in varying proportions to achieve the required viscosity and density close to that of a diesel fuel. The important physical and chemical properties of the biodiesel thus prepared are given in table 3.8.

Table 3.8 Properties of the fuels selected for engine experiment (KOME)

% of biodiesel (v/v)	% of diesel oil (v/v)		Viscosity (cSt) at 30°C	Specific gravity	Calorific value (kj/kg)	observation
0	100	Diesel	2.5	0.835	43500	Stable mixture
5	95	B5	2.78	0.837	43119	Stable mixture
10	90	B10	2.89	0.840	42738	Stable mixture
15	85	B15	3.06	0.842	42357	Stable mixture
20	80	B20	3.64	0.844	41956	Stable mixture
25	75	B25	3.98	0.847	41595	Stable mixture
100	0	B100	8.73	0.882	35879	Stable mixture

3.6 PRODUCTION OF BIODIESEL FROM JATROPHA

In the same manner, biodiesel is produced from jatropha oil transesterification, different fuel properties measured and tabulated in table 3.9 – 3.12. The cetane numbers of jatropha derived biodiesel calculated as 57.12 and calorific value to be 42640 Kj/kg. After transesterification, the colour of jatropha oil changes from deep brown to reddish yellow. A comparative study of jatropha derived biodiesel and diesel is made in table 3.13. In a similar way, biodiesel obtained from jatropha is blended with diesel oil in varying proportion to achieve the required viscosity and density close to that of diesel fuel. The important physical and chemical properties of the jatropha derived biodiesel thus prepared are given in table 3.14.

Table 3.9 viscosity dependency on temperature variation of biodiesel and jatropha

RAW JATROPHA OIL		BIODIESEL	
Temp(^o C)	Viscosity(cSt)	Temp(^o C)	Viscosity(cSt)
30	53.79	30	7.2
45	35.20	45	5.37
60	24.85	60	4.14
75	14.55	75	3.32
90	8.23	90	2.96

Table 3.10 Specific gravity of raw jatropha and biodiesel

Jatropha oil	Volume (ml)	Weight (gm)	Specific	Density
Raw	20	18.044	0.902	902
Transesterified	20	17.524	0.876	876.2

Table 3.11 Cloud and pour points of raw jatropha and biodiesel

RAW JATROPHA OIL		BIODIESEL	
Property	Temp(^o C)	Property	Temp(^o C)
Cloud point	7	Cloud point	6
Pour point	4	Pour point	4

Table 3.12 Flash point and fire points

Properties	Jatropha oil	Bio diesel
Flash point (^o C)	261	248
Fire point (^o C)	302	295

Table 3.13 Comparative study of fuel properties of diesel and biodiesel

Properties	Jatropha oil		Diesel
	Raw	Derived biodiesel	
Viscosity(cSt) at 30°C	53.79	7.2	2.5
Calorific value (kj/kg)	39570	42640	43500
Flash point (°C)	261	248	52
Fire point (°C)	302	295	63
Cloud point (°C)	7	6	5
Pour point (°C)	4	4	4
Specific gravity (at	0.902	0.876	0.835
Cetane Number	36	57.12	51

Table 3.14 Properties of the fuels selected for engine experiment (JOME)

% of biodiesel (v/v)	% of diesel oil (v/v)		Viscosity (cSt) at 300C	Specific gravity	Calorific value (kj/kg)	Observation
0	100	diesel	2.5	0.835	43500	Stable mixture
10	90	B10	2.99	0.8391	43414	Stable mixture
20	80	B20	3.5	0.8432	43328	Stable mixture
30	70	B30	3.81	0.8473	43242	Stable mixture
40	60	B40	4.31	0.8514	43156	Stable mixture
50	50	B50	4.51	0.8555	43070	Stable mixture
60	40	B60	5.34	0.8596	42984	Stable mixture
70	30	B70	5.78	0.8637	42898	Stable mixture
80	20	B80	6.21	0.8678	42812	Stable mixture
90	10	B90	6.98	0.8719	42726	Stable mixture
100	0	B100	7.2	0.8760	42640	Stable mixture

CHAPTER 4

MATHEMATICAL MODELING FOR PREDICTING FUEL PROPERTIES

4.1 INTRODUCTION

Vegetable oils are produced from numerous oil seed crops. The mono-alkyl esters of vegetable oils or animal fats, known as biodiesel have got a significant attention as an alternative diesel fuel. It is observed that the fuel properties of biodiesel play a significant role in the combustion process. For combustion analysis of biodiesels, the fuel properties are to be studied thoroughly before it is being selected. Therefore the prediction of biodiesel properties is the first and foremost stimulating task for the studies of biodiesel as a diesel substitute.

One of such properties is persuaded of the cetane number (CN) on the combustion process and on engine performance. The cetane number of a diesel fuel depends on both the chemical and the physical characteristics of the fuel. As an indicator of ignition delay, the CN is a prime indicator of fuel quality in the realm of diesel engines. The CN of a diesel fuel (DF) is related to ignition delay time, i.e. the time that passes between injection of the fuel into the cylinder and to set off the ignition. The ignition delay time and cetane number are inversely related to each other. Cetane number is measured using blends of two reference fuels, a long straight chain hydrocarbon ($C_{16}H_{34}$; trivial

name n –cetane)^[46] is the high quality standard on the cetane scale with an assigned CN of 100 and a highly branched compound 2,2,4,4,6,8,8 heptamethylnonane (HMN, also C₁₆H₃₄), a compound with poor ignition quality is the low quality standard and has an assigned CN of 15. The cetane number is calculated by determining which mixture of cetane and isocetane (2,2,4,4,6,8,8-heptamethylnonane) will result in the same ignition delay to that of reference fuel.

Physical properties of fuel like viscosity, density of biodiesel reported by different authors are high compared to the suitability in diesel engines. On the other side chemical property like high heat value (HHV) is an important parameter for the combustion efficiencies.

The aim of the present work is to theoretically predict few fuel properties like cetane number, viscosity, density and high heat value (HHV) of different biodiesels from their fatty acid methyl ester (FAME) composition.

4.2 PREDICTION OF CETANE NUMBER

In the present study, methyl ester of canola, linseed, rapeseed and sunflower oil that are primary sources of biodiesel are considered as reference fuels. Initially, the cetane index is found out for those reference biodiesels as per ASTM D976 and ASTM D4737. Secondly, regression equations are developed from the physical properties of FAME for predicting CN. Boiling point, viscosity, the heat of combustion, carbon

number and cetane number for the esters are taken from Knothe,2005^[46] and data for a melting point from Michael S. Graboski et al. ^[47], and density values from Aldrich catalog. Finally, another model is being developed relating CN to the composition of FAME and a comparative study has been made using different methods proposed by ASTM.

4.2.1 CN prediction by ASTM D 976 and ASTM D 4737: The distillation temperature, viscosity, and density of the four reference biodiesels are presented in table 4.1 ^[8].

Table 4.1 Distillation temperature, density and viscosity of reference fuels

Samples	Density at 25° C (gm/ml)	Distillation temperature (°C)			Viscosity (cP)
		10% (T10)	50% (T50)	90% (T90)	
Canola methyl ester (CME)	0.875	194.1 ± 8.4	231.5± 6.0	251.7 ± 3.2	3.79 ± 0.06
Linseed methyl ester (LME)	0.887	188.8	229.5	246.7	3.32
Rapeseed methyl ester (RME)	0.877	206.9	251.8	293.6	5.18
Sunflower methyl ester (SME)	0.882	192.9	236.1	>350	4.24

The cetane indexes for the above biodiesels are found as per ASTM D 976 and ASTM D 4737 are given in table 4.2. A comparison is made with the available literature values and it is observed that using boiling point and density for the calculation of cetane number of petroleum products, is inaccurate for vegetable oils and fatty acid esters.

Hence investigation is done to develop alternative equations for estimation of the cetane index of a single fatty acid ester and a mixture of known composition.

Table 4.2 Comparative studies of cetane number

Samples	Cetane Index/CN		CN based on literature review
	ASTMD976	ASTMD4737	
Canola methyl ester (CME)	30.24205	25.81588	53.9, 55 [48]
Linseed methyl ester (LME)	26.29271	20.15647	63.6[49]
Rapeseed methyl ester (RME)	35.44224	32.35473	54.5 ^[50] , 53 ^[51]
Sunflower methyl ester (SME)	29.69168	33.69594	58 [52] ,50 ^[51]

4.2.2 CN prediction from the physical properties of FAME:

Physical properties and their cetane numbers are listed in table 4.3^{[47],[46]}. By using physical properties as variable X and measured cetane number as Y variables, regression analyses are done for the prediction of CN and accordingly regression equations are generated. Regression equations and associated statistical data that relate the CN of the esters from physical properties are shown in table 4.4. Based on R² value, the descending order of precision for predicting CN from physical properties is viscosity > heat of combustion > carbon number > melting point > boiling point and density. The viscosity equation has the highest R² and lowest standard errors. So this equation is one of the best choices for finding cetane number. Other equations could also be employed to find out the CN with a minimum error.

Table 4.3 Physical properties of pure fame

Fatty acid esters	Viscosity cst @ 40°C	Heat of combustion Kg-cal/mol	Melting point in °C	Boiling point in °C	Density gm/ml	Carbon number	Cetane number
Methyl octanoate (C ₉ H ₁₈ O ₂)	1.19	1313	-40	193	0.877	8	33.6
Methyl Caprate (C ₁₁ H ₂₂ O ₂)	1.72	1625	-18	224	0.873	10	47.2
Methyl Laurate (C ₁₃ H ₂₆ O ₂)	2.43	1940	5.2	266	0.870	12	61.4
Methyl Myristate (C ₁₅ H ₃₀ O ₂)	3.23	2254	19	295	0.855	14	66.2
Methyl palmitate (C ₁₇ H ₃₄ O ₂)	4.38	2550	30	415	0.852	16	74.5
Methyl Stearate (C ₁₉ H ₃₈ O ₂)	5.51	2859	39.1	442	-	18	86.9

Table 4.4 Regression equations based on physical properties of FAME

Physical property	Predicted equation	R ²	Std. error
Viscosity	$Y = -22.33479 + 63.27386 * X + (-15.39704) * X^2 + 1.36385 * X^3$	0.9979	1.39
Heat of combustion	$Y = -27.12221 + 0.05366 * X + (-0.00001) * X^2$	0.9857	2.95
Carbon number	$Y = -24.75143 + 8.48143 * X + (-0.13214) * X^2$	0.9854	2.97
Melting point	$Y = 57.94667 + 0.62663 * X$	0.9785	3.12

Boiling point	$Y = -66.10523 + 0.67479 * X + (-0.00077) * X^2$	0.9540	5.28
Density	$Y = 1189.02462 + (-1308.57941) * X$	0.8151	8.06

A graphical representation of the variation of CN with respect to their regression equations along with the actual CN is shown in figure 4.1 – figure 4.6. The best regression equation based on viscosity, applied for reference fuels and to other biodiesels investigated by different researchers is shown in table 4.5. A major variation is observed between the predicted CN value and the values obtained from the different researchers, may be due to the reason that the regression equations are based on the saturated fatty esters, while most of the biodiesels are a mixture of saturated and unsaturated FAME.

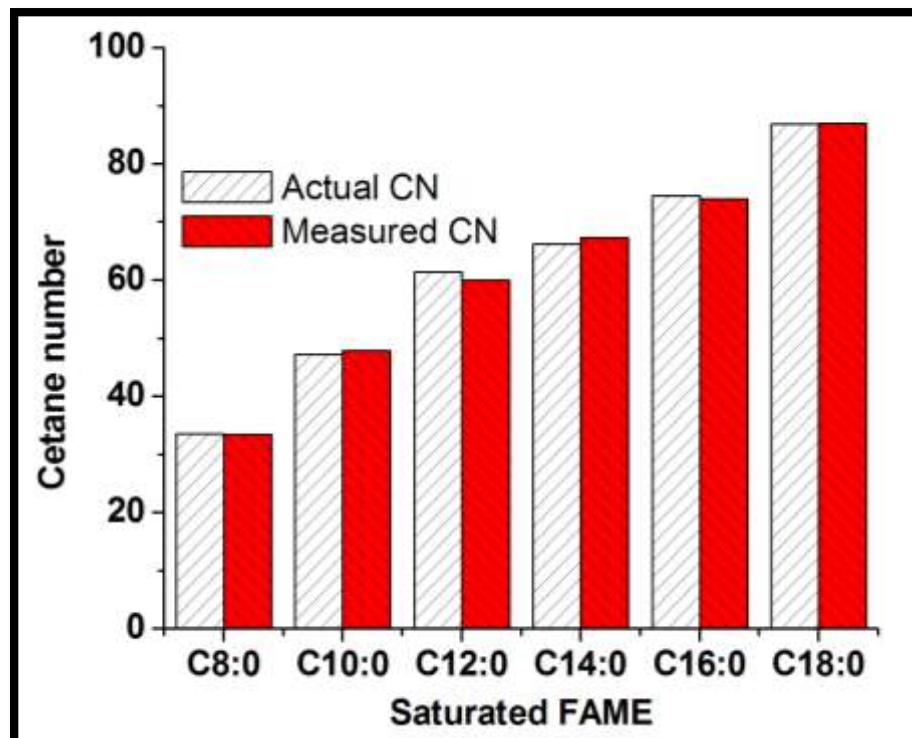


Figure 4.1 Plot of CN VS. Viscosity for saturated FAME

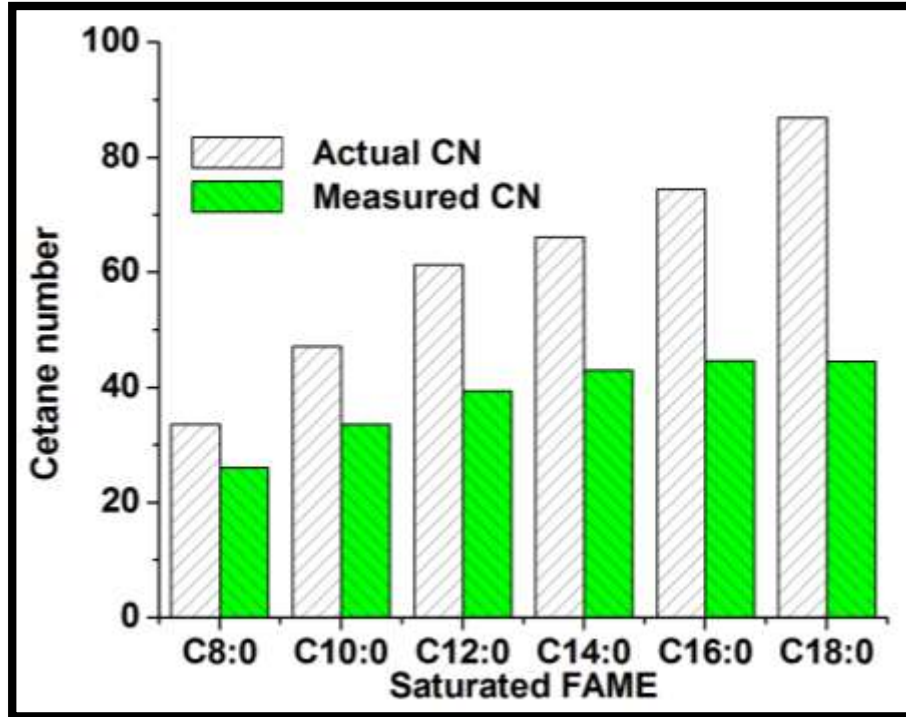


Figure 4.2 Plot of CN VS. Heat of combustion for saturated FAME

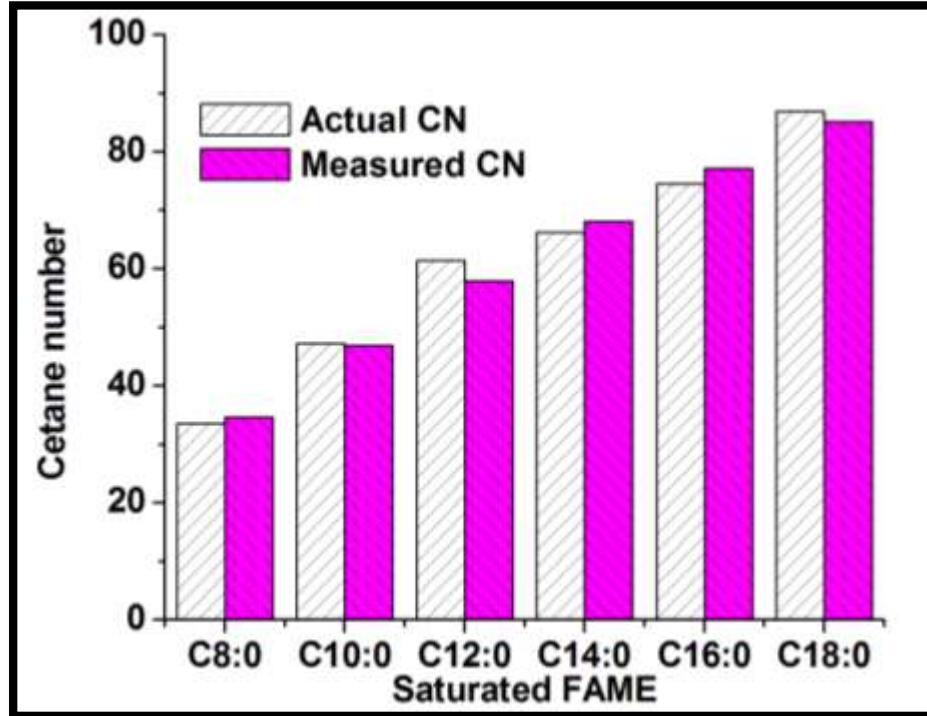


Figure 4.3 Plot of CN VS. Carbon number for saturated FAME

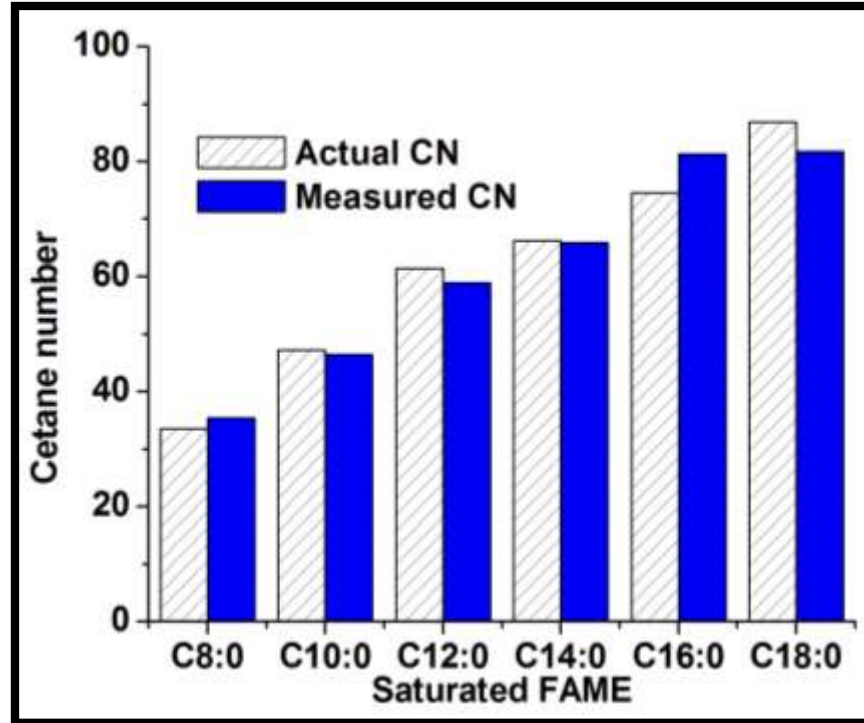


Figure 4.4 Plot of CN VS. Boiling point for saturated FAME

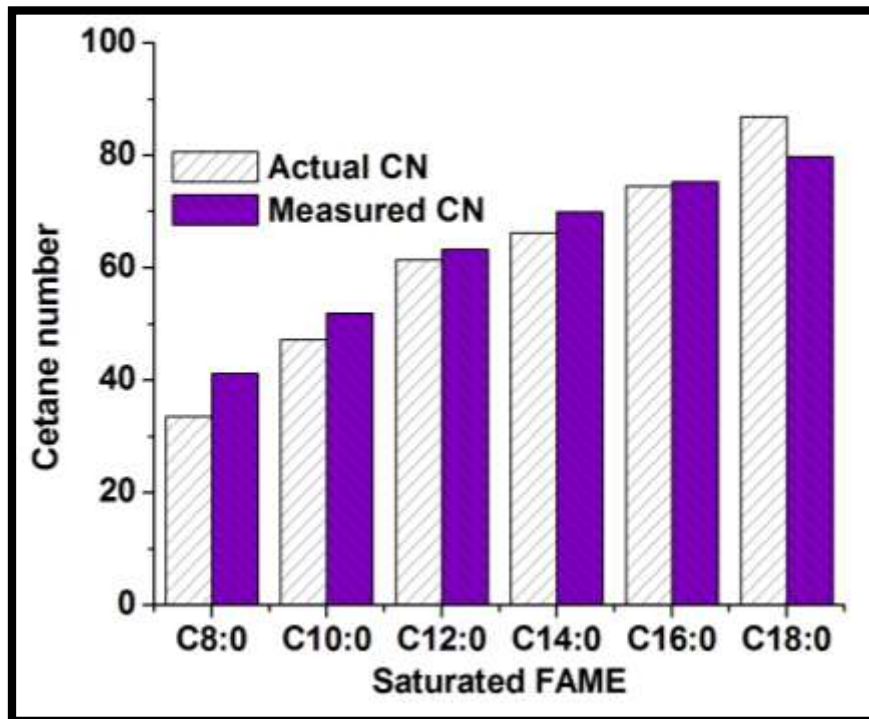


Figure 4.5 Plot of CN VS. Melting point for saturated FAME

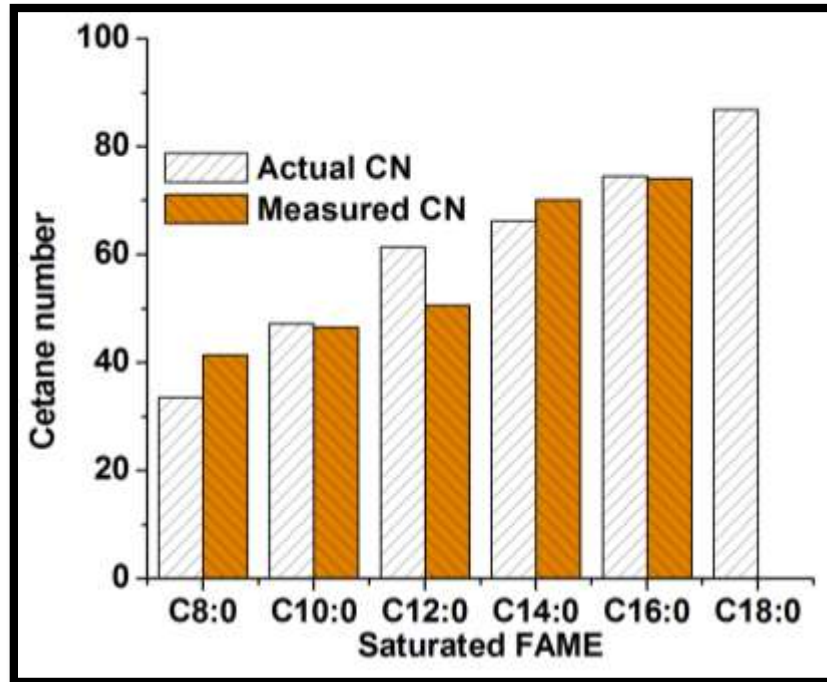


Figure 4.6 Plot of CN VS. Density for saturated FAME

Table 4.5 Predicted CN values from the regression equation

Samples	Viscosity, Cst	Predicted CN
Canola methyl ester	4.33 ^[8]	73.68
Sunflower methyl ester	4.30 ^[8]	73.49
Rapeseed methyl ester	4.83 ^[47]	77.76
Linseed methyl ester	3.74 ^[8]	70.29
Soybean methyl ester	4.08 ^[47]	72.15
Palm oil methyl ester	4.50 ^[47]	74.89
Tallow methyl ester	4.80 ^[47]	77.46

4.2.3. CN prediction from the average percentage composition of FAME:

Cetane number for the pure FAME and reference biodiesels are obtained from different kinds of literature from testing laboratories using ASTM D 613 as shown in table 4.6.

Table 4.6 Fatty acid compositions and the experimental cetane numbers of esters

CN	Lauric	Myristic	Palmitic	Stearic	Palmitoleic	Oleic	Linoleic	Linolenic
61.4 ^[46]	100	0	0	0	0	0	0	0
66.2 ^[46]	0	100	0	0	0	0	0	0
74.5 ^[46]	0	0	100	0	0	0	0	0
86.9 ^[46]	0	0	0	100	0	0	0	0
51.0 ^[49]	0	0	0	0	100	0	0	0
55.0 ^[46]	0	0	0	0	0	100	0	0
42.2 ^[53]	0	0	0	0	0	0	100	0
22.7 ^[53]	0	0	0	0	0	0	0	100
55.0 ^[48]	0 ^[8]	0 ^[8]	4.2 ^[8]	2.2 ^[8]	0 ^[8]	67.2 ^[8]	18.9 ^[8]	7.4 ^[8]
58.0 ^[54]	0 ^[51]	0 ^[51]	8.6 ^[51]	1.93 ^[51]	0 ^[51]	11.58 ^[8]	77.89 ^[8]	0 ^[51]
54.5 ^[50]	0 ^[51]	0.1 ^[51]	4.8 ^[51]	0.4 ^[51]	0.2 ^[51]	61.6 ^[51]	20.6 ^[51]	9.2 ^[51]
63.6 ^[49]	0 ^[8]	0 ^[8]	5.2 ^[8]	3.2 ^[8]	0 ^[8]	14.5 ^[8]	15.3 ^[8]	61.9 ^[8]

A nine by twelve matrix is formed with CN as the dependent variable and the FAME composition as the independent variables for the regression analysis. The linear regression equation used is as follows:

$$\text{CN} = K + Ax_1 + Bx_2 + Cx_3 + Dx_4 + Ex_5 + Fx_6 + Gx_7 + Hx_8 \quad (4.1)$$

Where K, A, B, C, D, E, F, G, and H are constants to be determined from regression analysis; x_1, x_2, \dots, x_8 are percentage compositions of FAME. For example, x_1 is the percentage of Lauric acid methyl ester present, x_2 is the percentage of Myristic acid methyl ester present and so on. Using MATLAB the regression equation becomes:

$$\text{CN}^{[55]} = 19.2656 + 0.4213x_1 + 0.4694x_2 + 0.5666x_3 + 0.6833x_4 + 0.3174x_5 + 0.3885x_6 + 0.2969x_7 + 0.1546x_8 \quad (4.2)$$

Equation (4.2) shows the relationship between the CN and the FAME composition.

4.2.4 Results and Discussion:

From the equation, it is observed that the coefficient for the saturated FAME increases with the increase in carbon number from lauric (C12:0) to stearic (C18:0) methyl ester. This suggests an increase in the CN number with an increase in the composition of the saturated FAME. However, the coefficients of the unsaturated FAME reduce with increase in carbon number and unsaturation. This equation is a good agreement with the findings of other authors that saturated compounds have higher CN than the unsaturated compounds ^{[56][57]}. The results of the prediction of CN values on the basis of test data and the findings of other authors are plotted in figure 4.7. It is observed from the plot that the equation developed from the percentage FAME composition has the ability to predict the CN quite accurately.

Table 4.7 Experimental and predicted cetane numbers of some biodiesels

Feed-stock	C12:0	C14:0	C16:0	C18:0	C16:1	C18:1	C18:2	C18:3	CN from literature	Predicted CN
SOME ^[48]	0	0.9	10.54	3.75	1.3	23.18	48.92	1.16	52 ^[59]	52.34
PME ^[58]	0.3	0.9	43.32	3.81	0.2	40.57	10.25	0.25	62.4	65.94
TME ^[51]	0.1	2.8	23.3	19.4	0	42.4	2.9	0.9	64.8 ^[51]	64.55
COME ^[51]	0.1	0.7	20.1	2.6	0	19.2	55.2	0.6	52	56.74

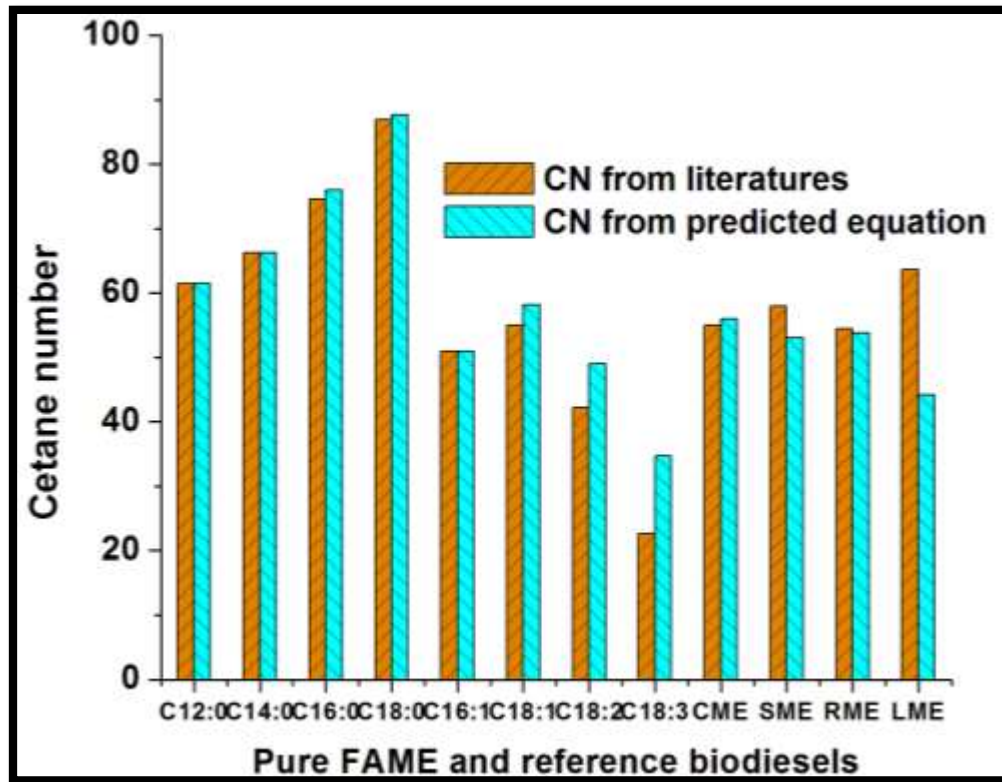


Figure 4.7 Comparison between measured and predicted
Values of CN

The equation developed, applied to other results obtained by different researchers is shown in table 4.7. The obtained results give an indication of variation of the CN due to its percentage variation in FAME composition. Soybean methyl ester (SOME) is rich in unsaturated acid, oleic and linoleic. The CN of pure oleic acid is 55, while that of linoleic acid is 42.2. The CN of SOME obtained from the literature is 52 while the predicted value is 52.34. The CN values are very close and the small variation may be due to either experimental error or oxidation of the fuel before use. Some reports have already been established that an increase in CN with an increase in peroxide value of the biodiesel up

to 82 ^[57] or change in the oxidation level of the biodiesel may change the CN value ^[6]. Similarly, palm oil methyl esters (PME) is rich in both saturated (palmitic, 43.32%) and unsaturated (oleic, 40.57%) acid. The CN of methyl palmitate acid is 74.5 while that of pure methyl oleate is 55. The predicted CN value is 65.94 while that of obtained from literature is 62.4. The value of the CN follows the same trend in the composition of FAME compounds of Tallow methyl ester (TME) and cotton seed methyl ester (COME).

It is observed from the result that a biodiesel with high in saturated fatty esters always has a high CN value, while biodiesel rich in unsaturated fatty esters have lower CN value. This evokes a profound effect of fatty acid composition on the CN of the biodiesel. It further supports the fact that the CN value is dependent on the percentage composition of FAME.

4.3 PREDICTION OF VISCOSITY, DENSITY AND HHV

In the present study, ten biodiesels (corn, cottonseed, linseed, rapeseed, safflower, soybean, sunflower, mahua, jatropha and palm) are considered as reference fuels and their viscosity, density and HHV along with their FAME composition are tabulated from the published literature^{[61],[62],[47],[63],[64],[65]} in table 4.8 and table 4.9.

Table 4.8 FAME compositions in different biodiesels

SI No.	Biodiesel	Percentage weight of FAME's							
		Palmitic 16:0	Palmitoleic 16:1	Stearic 18:0	Oleic 18:1	Linoleic 18:2	Linolenic 18:3	Arachidic 20:0	Others
01.	Corn	11.8	0	2.0	24.8	61.3	0	0.3	0
02.	Cottonseed	28.7	0	0.9	13.0	57.4	0	0	0
03.	Linseed	5.1	0.3	2.5	18.9	18.1	55.1	0	0
04.	Rapeseed	3.5	0	0.9	64.1	22.3	8.2	0	0
05.	Safflower	7.3	0	1.9	13.6	77.2	0	0	0
06.	Soy bean	13.9	0.3	2.1	23.2	56.2	4.3	0	0
07.	Sunflower	6.4	0.1	2.9	17.7	72.9	0	0	0
08.	Mahua	24.5	0	22.7	37.0	14.3	0	1.5	0
09.	Jatropha	14.7	1.3	9.5	39.1	34.6	0.3	0.3	0.2
10.	Palm	43.6	0	4.5	40.5	10.1	0.2	0	0.1

Table 4.9 Properties of different biodiesels

SI No.	Biodiesel	Properties of FAME		
		Viscosity(mm ² /s)	Density (kg/m ³)	HHV(MJ/kg)
01.	Corn	3.62	873	41.14
02.	Cottonseed	3.75	871	41.18
03.	Linseed	2.83	885	40.84
04.	Rapeseed	4.6	857	41.55
05.	Safflower	4.03	866	41.26
06.	Soy bean	4.08	865	41.28
07.	Sunflower	4.16	863	41.33
08.	Mahua	5.1	876	36.91
09.	Jatropha	5.65	880	38.45
10.	Palm	3.94	867	41.24

4.3.1 Correlation analysis: Correlation is a procedure for examining the relationship between two variables. This procedure involves two variables where the values for one variable are paired with the values for the other variable. The degree of association or strength of the relationship between two variables is represented by a number called a correlation coefficient. The Pearson product-moment correlation coefficient is a measure of the linear relationship between two variables, X and Y , and is denoted by r_{XY} or simply r . The value of a correlation coefficient can range from 1 to -1. A value of 1 denotes a perfect positive relationship; whereas -1 refers to the perfect negative relationship.

Table 4.10 Pearson product moment correlation coefficient (R) between viscosity, density, HHV Vs. FAME's composition

Sl. No.	r value	Percentage weight of FAME's								
		Palmitic 16:0	Palmitoleic 16:1	Stearic 18:0	Oleic 18:1	Linoleic 18:2	Linolenic 18:3	Arachidic 20:0	Others	
01.	Viscosity vs FAME	0.081	0.515	0.607	0.530	-0.163	-0.580	0.498	0.566	
02.	Density vs FAME	0.069	0.478	0.388	-0.291	-0.313	0.522	0.344	0.315	
03.	HHV vs FAME	-0.194	-0.404	-0.955	-0.209	0.419	0.121	-0.892	-0.363	

To evaluate the degree of linear relationship between the fuel properties (viscosity, density, and HHV) and its FAME composition correlation analysis is performed and their corresponding r values are tabulated in table 4.10. The scattered plots of fuel properties against FAMEs, fitted with the regression lines are plotted in figure 4.8, figure 4.9, and figure 4.10.

4.3.2 Pearson product moment of correlation coefficient(r):

From the correlation analysis (table 4.10), it is observed that palmitoleic, stearic, oleic and arachidic acid has a moderate positive linear relationship with the viscosity, whereas linolenic acid bears a moderate negative linear relationship with viscosity. Palmitic and linoleic acid has also a weak linear relationship with viscosity. Figure 4.8 shows the scattered plot of viscosity and FAMEs with the fitted regression line. The correlation analysis between the density and FAMEs show that palmitoleic, stearic, linolenic and arachidic acid are moderately positively correlated with density. The linoleic acid is moderately negatively correlated and palmitic and oleic acid is weakly correlated with the density. Figure 4.9 shows the scattered plot of density and FAMEs with the fitted regression line. From the correlation analysis between the HHV and FAMEs, it is observed that stearic and arachidic acid has a high degree of negative correlation with HHV. The linoleic acid has a moderate degree of positive correlation and palmitoleic acid has a moderate degree of negative correlation with HHV. Figure 4.10 shows the scatter plot of HHV and FAMEs with the fitted regression line.

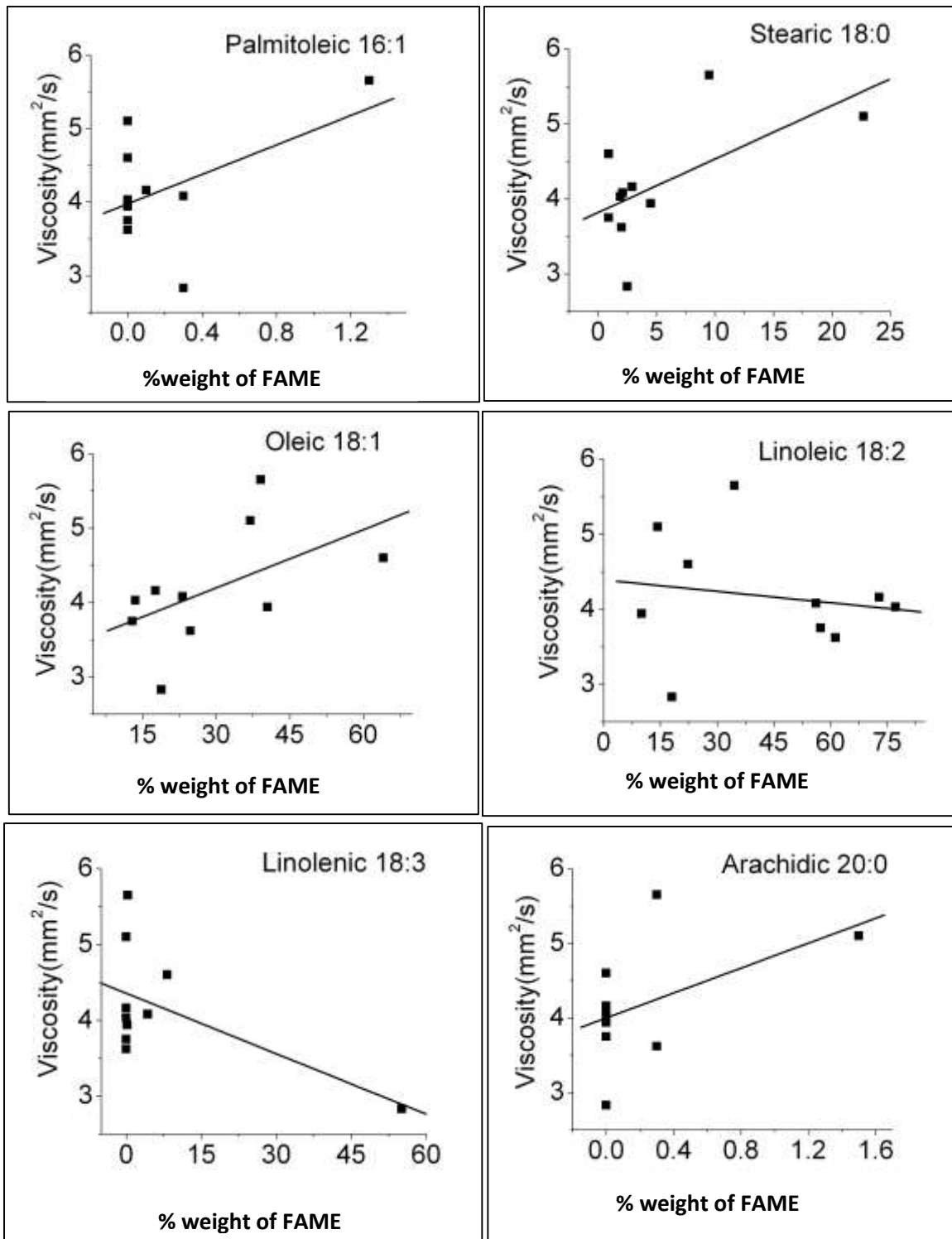


Figure 4.8 Scatter plot of viscosity vs. FAME with fitted regression line

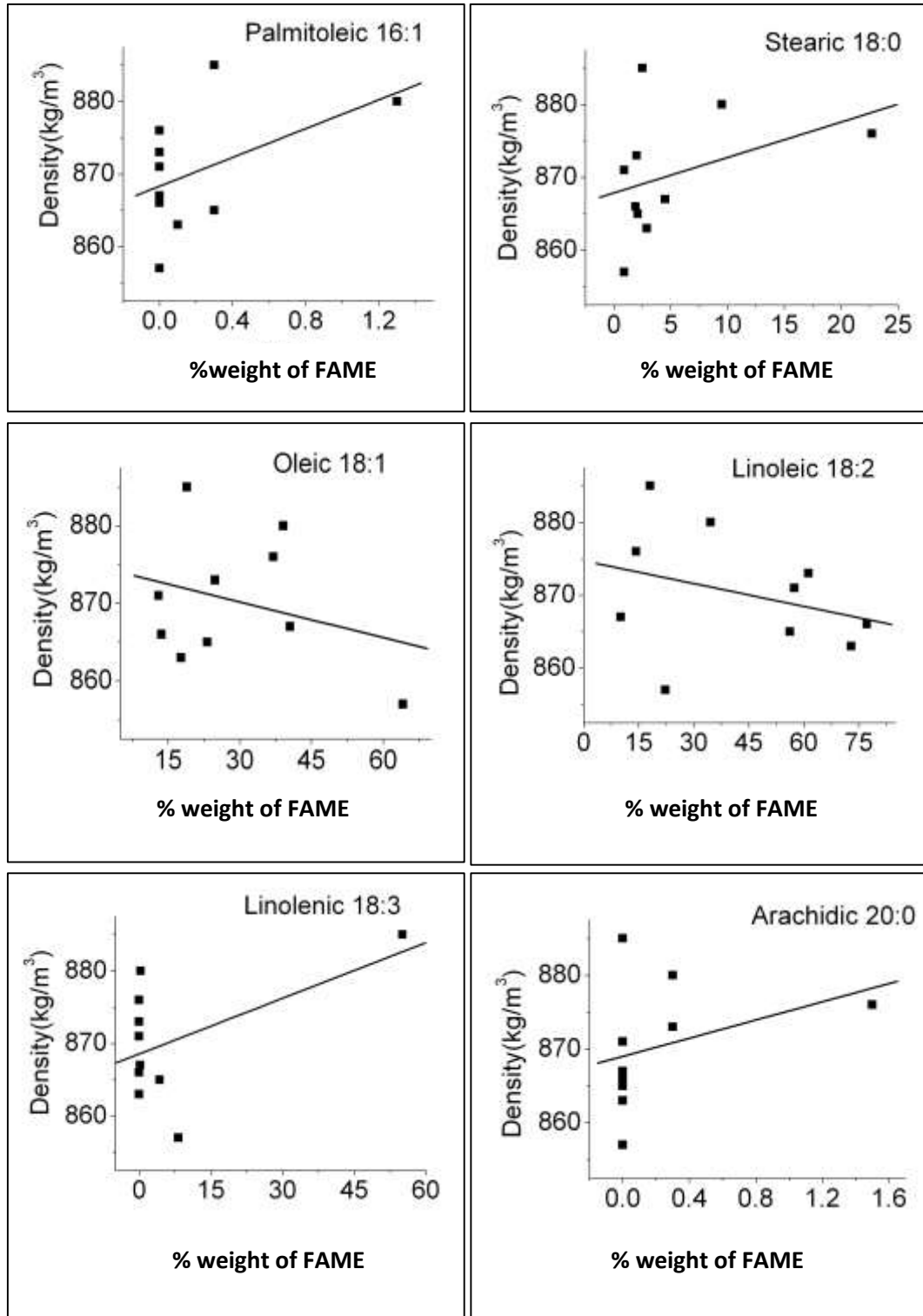


Figure 4.9 Scatter plot of density vs. FAME with fitted regression line

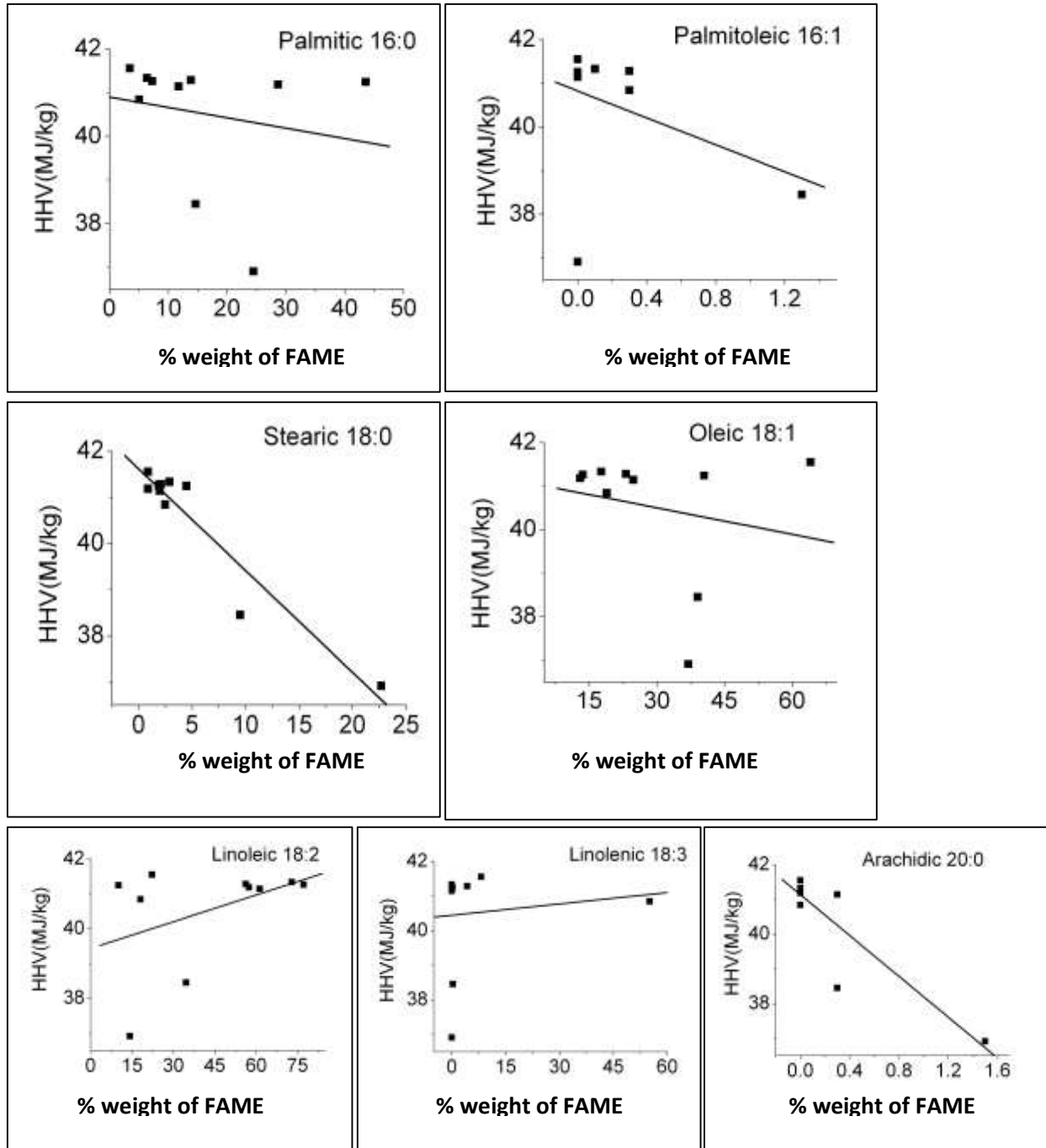


Figure 4.10 Scatter plot of HHV VS. FAME with fitted regression line

4.3.3 Regression model

After the evaluation of r value, three regression models as given by Eqs. (4.3), (4.4) and (4.5) are developed for the prediction of viscosity, density, and HHV of biodiesels.

$$\text{Viscosity}^{[66]} = 373.4774 - (3.7096 \times P) - (0.0993 \times PL) - (3.812 \times S) - (3.7431 \times OL) - (3.6808 \times L) - (3.717 \times LL) + (0.1131 \times A) - (10.8943 \times \text{Oth}) \quad (4.3)$$

$$\text{Density}^{[66]} = 2204.5 - (13.2 \times P) - (1.4 \times PL) - (16 \times S) - (13.8 \times OL) - (13.3 \times L) - (12.9 \times LL) + (39.7 \times A) + (72.2 \times \text{Oth}) \quad (4.4)$$

$$\text{HHV}^{[66]} = -518.5 + (5.5977 \times P) + (0.4859 \times PL) + (5.8637 \times S) + (5.6976 \times OL) + (5.5723 \times L) + (5.5799 \times LL) - (3.5537 \times A) + (10.8667 \times \text{Oth}) \quad (4.5)$$

Where, P = Palmitic, PL = Palmitoleic, S = Stearic, OL = Oleic, L = Linoleic, LL = Linolenic, A = Arachidic, Oth = Others.

4.3.4 Results and Discussion:

The relationship between predicted fuel properties and FAME composition is investigated. For viscosity Eq. (4.3) shows an increase with increasing chain length and decrease with increasing degree of unsaturation. In other words, viscosity decreases nonlinearly with the increase in the number of double bonds. Eq. (4.4) shows a decrease in the density with increasing carbon number and increases with increasing degree of unsaturation. For HHV Eq. (4.5) shows an increase with increasing chain length.

The determined and predicted viscosity values using Eq. (4.3) of selected biodiesels are tabulated in table 4.11 and compared in figure 4.11. It is observed from the table 4.11 that

a maximum error of 2.857% is obtained for the fitted values in the case of cottonseed oil methyl ester. Table 4.12 shows the list of determined and predicted density values by using Eq. (4.4) for the biodiesels. From figure 4.12 it is observed that a maximum error of 0.388% is obtained in the comparison between determined and predicted values of density in case of sunflower oil methyl ester. Figure 4.13 shows the comparison of the determined and the predicted HHV using Eq. (4.5) while the table 4.13 lists the same for different biodiesels showing a maximum error of 0.415% for the fitted values in the case of soybean oil methyl ester.

Table 4.11 Comparison between determined and predicted viscosity of biodiesel

Sl No.	Biodiesel	Viscosity (mm ² /s) determined	Viscosity (mm ² /s) predicted	% error
01.	Corn	3.62	3.65	0.888
02.	Cottonseed	3.75	3.64	-2.857
03.	Linseed	2.83	2.82	-0.181
04.	Rapeseed	4.6	4.57	-0.673
05.	Safflower	4.03	4.09	1.504
06.	Soy bean	4.08	4.19	2.818
07.	Sunflower	4.16	4.09	-1.730
08.	Mahua	5.1	5.10	-0.014
09.	Jatropha	5.65	5.63	-0.314
10.	Palm	3.94	3.98	1.025

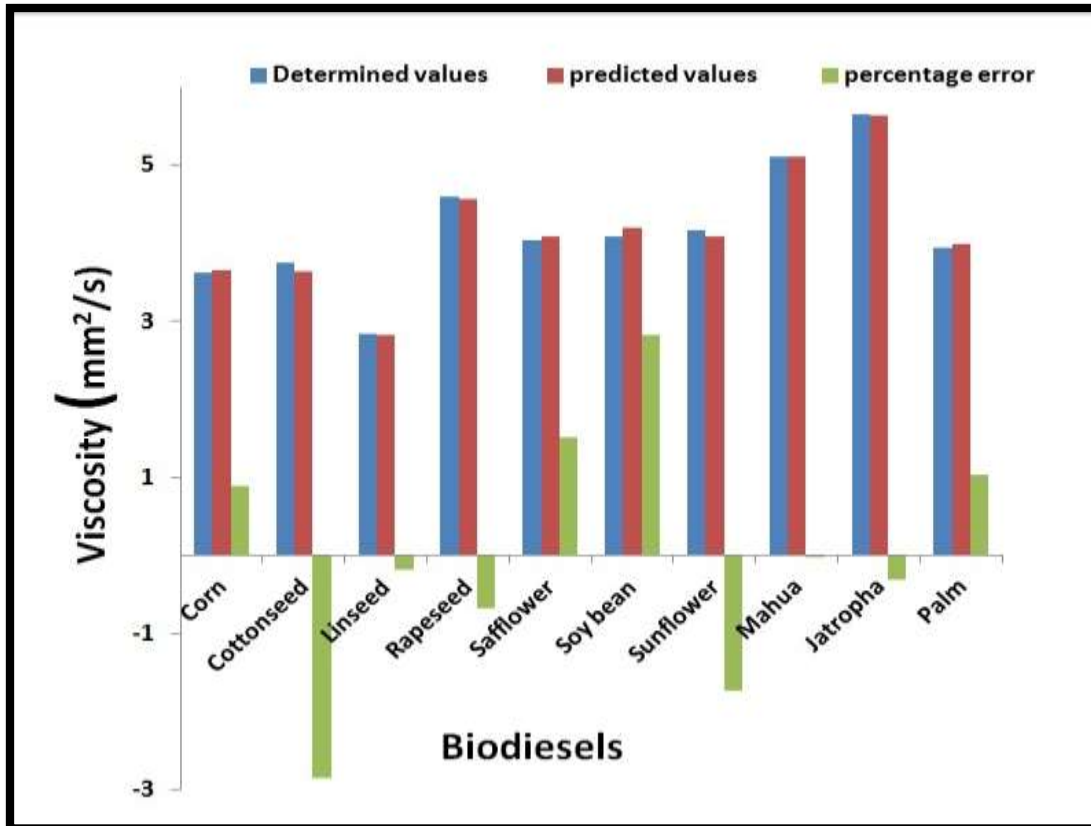


Figure 4.11 Determined and predicted viscosity value of biodiesels

Table 4.12 Comparison between determined and predicted density of biodiesel

Sl No.	Biodiesel	Density (kg/m ³) determined	Density (kg/m ³) predicted	% error
01.	Corn	873	871.12	-0.215
02.	Cottonseed	871	868.44	-0.294
03.	Linseed	885	884.42	-0.066
04.	Rapeseed	857	856.95	-0.006
05.	Safflower	866	863.3	-0.312
06.	Soy bean	865	863.91	-0.126
07.	Sunflower	863	859.65	-0.388
08.	Mahua	876	876.66	0.075
09.	Jatropha	880	879.36	-0.073
10.	Palm	867	868.39	0.160

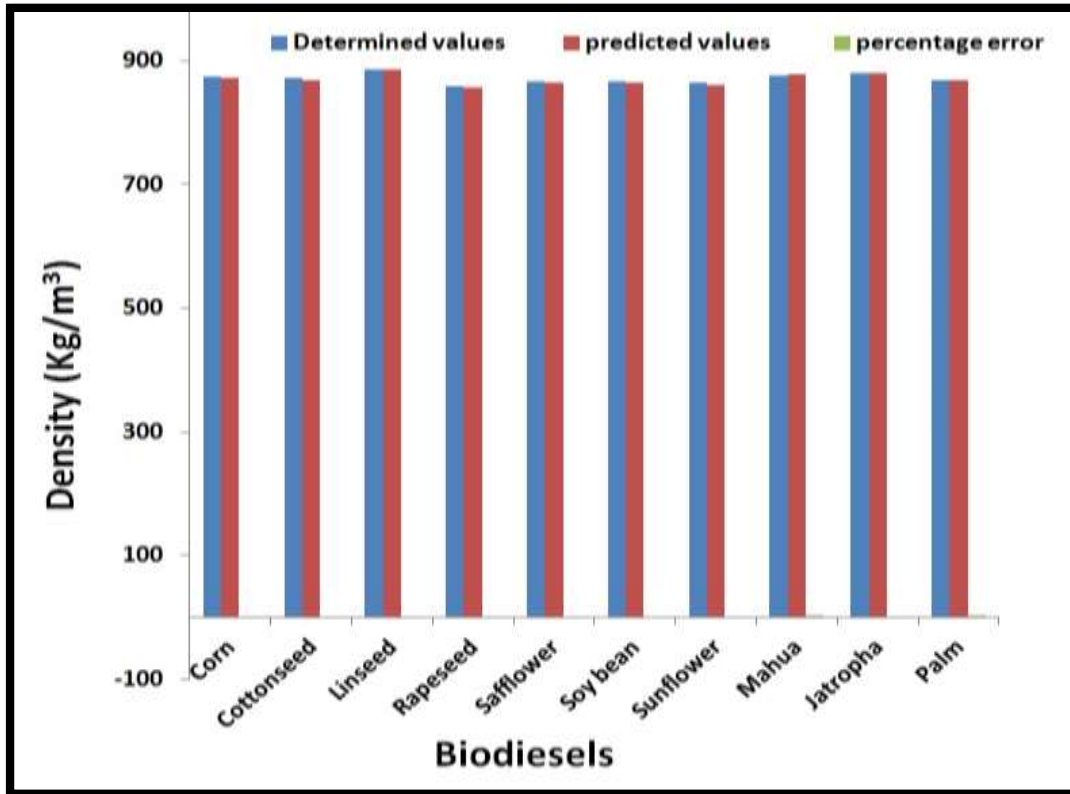


Figure 4.12 Determined and predicted density value of biodiesels

Table 4.13 Comparison between determined and predicted HHV of biodiesel

Sl No.	Biodiesel	HHV (Mj/kg) determined	HHV (Mj/kg) predicted	% error
01.	Corn	41.14	41.10	-0.105
02.	Cottonseed	41.18	41.35	0.413
03.	Linseed	40.84	40.85	0.022
04.	Rapeseed	41.55	41.60	0.127
05.	Safflower	41.26	41.17	-0.210
06.	Soy bean	41.28	41.11	-0.415
07.	Sunflower	41.33	41.45	0.283
08.	Mahua	36.91	36.91	0.011
09.	Jatropha	38.45	38.48	0.083
10.	Palm	41.24	41.18	-0.141

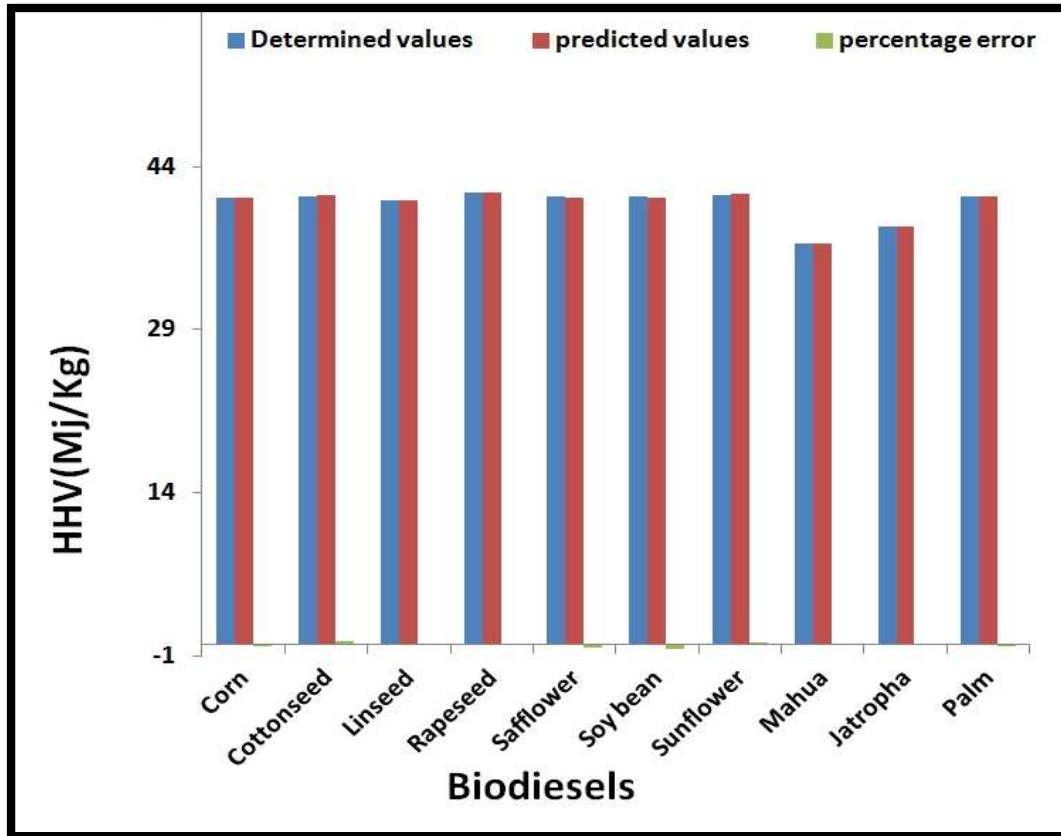


Figure 4.13 Determined and predicted HHV of biodiesels

4.3.5 Evaluation and comparison of HHV of biodiesels from their predicted equation and available published models

Ayhan Demirbas ^[62] has developed a model to predict HHV of biodiesel from the viscosity value. The model is given by,

$$\text{HHV} = 0.4625 \text{ VS} + 39.45, \text{ where VS} = \text{viscosity.} \quad (4.6)$$

S.M. Sadrameli ^[64] has developed another model to predict HHV of fatty acid present in biodiesel from its density value. The model is given by,

$$\text{HHV} = 93.4 \text{ DN} + 122.6, \text{ where DN} = \text{density.} \quad (4.7)$$

Table 4.14 comparison between predicted and published models of HHV

Sl No.	Biodiesel	HHV (MJ/kg) Predicted by Eq. (4.5)	HHV (MJ/kg) Predicted by Ayhan Demirbas	HHV (MJ/kg) Predicted by S.M. Sadrameli
01.	Corn	41.10	41.12	41.31
02.	Cottonseed	41.35	41.18	41.56
03.	Linseed	40.85	40.76	40.07
04.	Rapeseed	41.60	41.58	42.63
05.	Safflower	41.17	41.31	42.04
06.	Soy bean	41.11	41.34	41.98
07.	Sunflower	41.45	41.37	42.38
08.	Mahua	36.91	41.81	40.79
09.	Jatropha	38.48	42.06	40.54
10.	Palm	41.18	41.27	41.56

Ayhan Demirbas^[61] has described HHV in terms of viscosity, and S.M. Sadrameli^[64] has defined HHV in terms of density. The HHV are calculated in both the cases considering the predicted density and viscosity values. The predicted equation of HHV is compared with the published HHV by Ayhan Demirbas^[61] and S.M. Sadrameli^[64]. Table 4.14 lists the HHV for different biodiesels by Eq. (4.5), Eq. (4.6) and Eq. (4.7). As the percentage error is quite acceptable, thus the equations for the prediction of viscosity, density, and HHV are validated. Therefore for the calculations of viscosity, density, and HHV of biodiesel Eq. (4.3), Eq. (4.4) and Eq. (4.5) are suggested respectively.

CHAPTER 5

EXPERIMENTAL TEST RIG

DEVELOPMENT & METHODOLOGY

5.1 ENGINE DETAILS

The engine used for the experiment is a single cylinder direct injection (DI) commercial diesel engine. It is an air-cooled, naturally aspirated constant speed compression ignition engine, whose major specifications are shown in Appendix 2. The engine is coupled to an eddy current dynamometer through which load has been applied. The engine is tested at 0, 25, 50, 75 and 100 percent brake load condition. The engine has the provision to run either on pure diesel or dual fuel mode. Plate 5.1 shows the experimental test rig, equipped with temperature indicator, speed indicator, air flow measuring device, fuel measuring device.



Plate 5.1: Experimental test rig

5.2 INSTRUMENTATION

5.2.1 Eddy current dynamometer



Plate 5.2: Eddy current dynamometer

Eddy current type dynamometer is used to apply the load to the engine crank shaft. The dynamometer is Dynaspede make eddy current type air cooled fitted with universal brake controller unit.

5.2.2 Engine speed

The engine speed is measured by a speed indicator fitted on the control panel. The speed sensor is installed near the flywheel of the engine. As flywheel rotates it sense the signal and converts it into proportional revolutions per minute and displayed on the indicator.

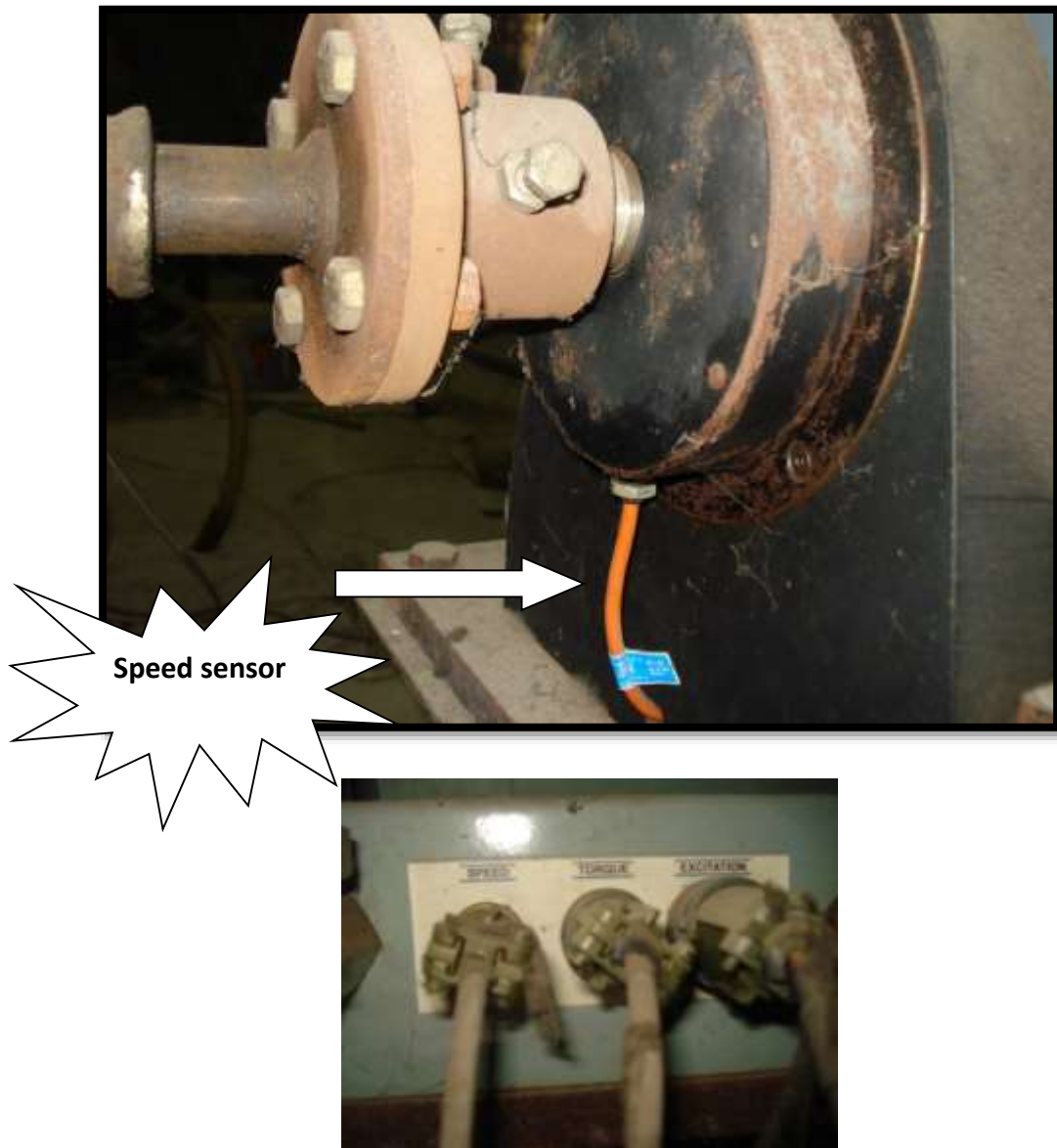


Plate 5.3: Speed sensor

5.2.3 Air flow measurement

Air surge tank fitted with orifice meter and U-tube manometer is fitted at the engine intake to measure the air flow rate to the engine. To remove the fluctuation of the water column in the manometer the tank is provided with a rubber membrane.



Plate 5.4: Surge tank fitted with orifice

5.2.4 Temperature Measurement

It consists of the Cr-Al thermocouple and digital indicator. The thermocouple is fitted at the exhaust manifold to record the exhaust gas temperature at different loading situation.

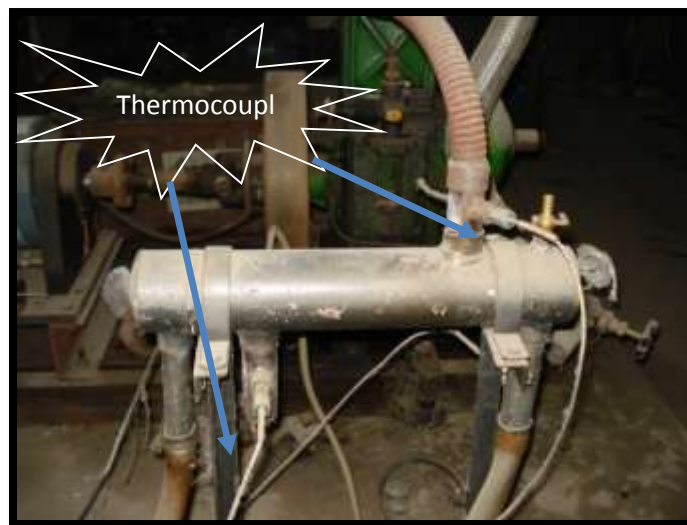


Plate 5.5: Thermocouple used for temperature measurement

5.2.5 Fuel supply Measurement

250 c.c. glass burette fitted with glass and paper filter, valve and fuel tank, is used to measure the fuel consumption of both diesel and biodiesel in dual fuel mode and the consumption of blended fuel.



Plate 5.6: Fuel supply measurement

5.2.6 Exhaust Emissions Analyzer

AVL make 5 Gas Analyzer (Model Digas 444) is used along with di-gas sampler to fitted in the exhaust line. The amount of CO, CO₂, NO_x, O₂ and HC is measured from the direct reading.



Plate 5.7: Gas analyzer

CHAPTER 6

EXPERIMENTAL RESULTS AND DISCUSSIONS

6.1 INTRODUCTION

A series of experimental works has been carried out using pure diesel and its blend of biodiesel. To study the engine performance and emission the experiments are carried out in Kirloskar make vertical cylinder, direct injected compression ignition diesel engine (Engine model – AVI). The power output of the engine is 5HP @1500 rpm, having compression ratio 16.5:1. The emission, as well as engine performance, is studied at different engine loads (25, 50, 75 and 100% of the load corresponding to load at maximum power). Test results of diesel and biodiesel blend are also compared with the pure diesel to find out the best possible alternatives as a replacement for pure diesel.

6.2 EXPERIMENTAL APPROACH

First of all, baseline data with diesel are found out experimentally to determine the engine performance and emission, shown in Appendix 5. The overall work is completed in three phases. In the first phase, the engine has been run on net diesel with varying loads.

In the second phase of work, the engine is first run on diesel for some time for warming up the engine till the diesel in the pipeline is exhausted. Then karanja derived

biodiesel blend with diesel (diesel 95% + KOME 5%, known as KB05) has been introduced by cutting off diesel supply. The fuel quantity has been adjusted manually to maintain a constant speed of 1500 rpm. Emission data and other relevant data are collected for calculating engine performance at various load conditions [shown in appendix 6]. The various performance data are compared on the basis of brake thermal efficiency, brake specific fuel consumption, brake specific engine consumption and exhaust emissions such as HC, NO_x, CO and exhaust gas temperature. The same steps are followed for the other biodiesel blends (KB10, KB15, KB20, KB25 and KB100). The main focus of this study is to find out the optimum ratio of the biodiesel-diesel blend.

In the third phase of work, jatropha-derived biodiesel is blended with diesel in varied proportions (JB10, JB20, JB30, JB40, JB50, JB60, JB70, JB80, JB90, and JB100) [JB10 means 10% JOME and 90% diesel] and similar experimental results are tabulated [Appendix 7].

6.2.1 Experiments on diesel:

The baseline data for diesel is tabulated [Appendix 5]. The maximum thermal efficiency is found to be 34.41. The NO_x and CO emission increase as the load increase in a diesel engine. The unburnt hydrocarbon and exhaust gas temperature also increase as the load increases.

6.2.2 Experiments on karanja derived biodiesel

Engine performance Test:

In the next phase, the engine is run with varied KOME blends (KB05, KB10, KB15, KB20, KB25, and KB100) and their respective performance and emission parameters are noted down. The variation of BSFC with varied torque for different karanja derived biodiesel diesel blend is shown in figure 6.1 and figure 6.2 shows the variation of BSFC with percentage of KOME in the blend for different load conditions. The fuel consumption of an engine fundamentally depends on the heating value of the fuel, the air-fuel ratio and the efficiency of the engine process. The BSFC is a comparative parameter that explains how effectively an engine is converting fuel into the work. The total fuel consumption is determined by measuring the volume or weight of fuel consumed by the engine under the given test condition. The specific fuel consumption is determined by dividing the total fuel consumption per hour by the power developed, the brake power being used. The fuel consumption of an engine depends principally on the heating value of the fuel, the air-fuel ratios and the efficiency of the engine process. It is clear from the figure 6.1 that at maximum load the BSFC of biodiesel (KB100) is higher as compared to that of diesel due to the higher heating value of the diesel in comparison to KB100 since the air-fuel ratio and engine efficiency remain constant. The BSFC of diesel at peak load is 0.2405 kg/kWh and that of biodiesel is 0.3599 kg/kWh. On the other hand in case of blending of 5%, 10%, 15%, 20% and 25%, it comes out to be 0.2485 kg/kWh, 0.2570 kg/kWh, 0.2577 kg/kWh, 0.2668 kg/kWh and 0.2764 kg/kWh respectively.

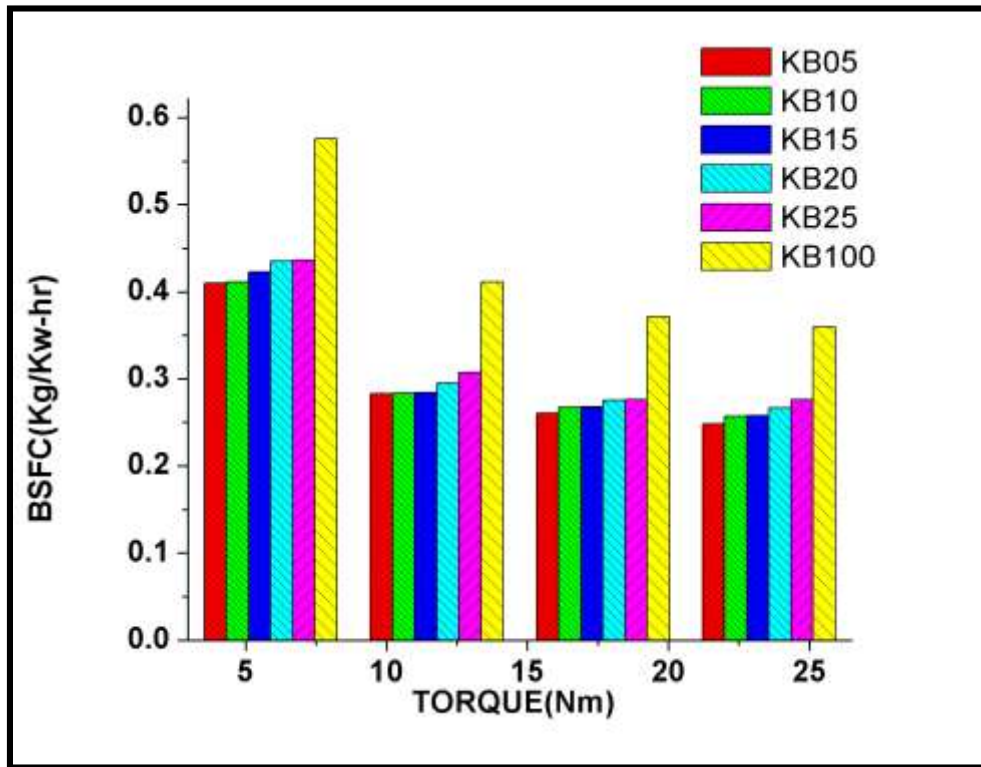


Figure 6.1 Variation of BSFC with varied torque for diesel KOME blend

Figure 6.2 explains the trends of BSFC for different KOME blends at a particular load i.e. 25%, 50%, 75%, and 100%. The figure shows that for a particular load, the BSFC increases as the blending proportion increases (i.e. KB05, KB10, KB15 and so on) and the overall values of BSFC are reduced as the percentage of load increases. The above discussion reveals that the only major influencing parameter is the heating value of fuel that is responsible for the variation of BSFC.

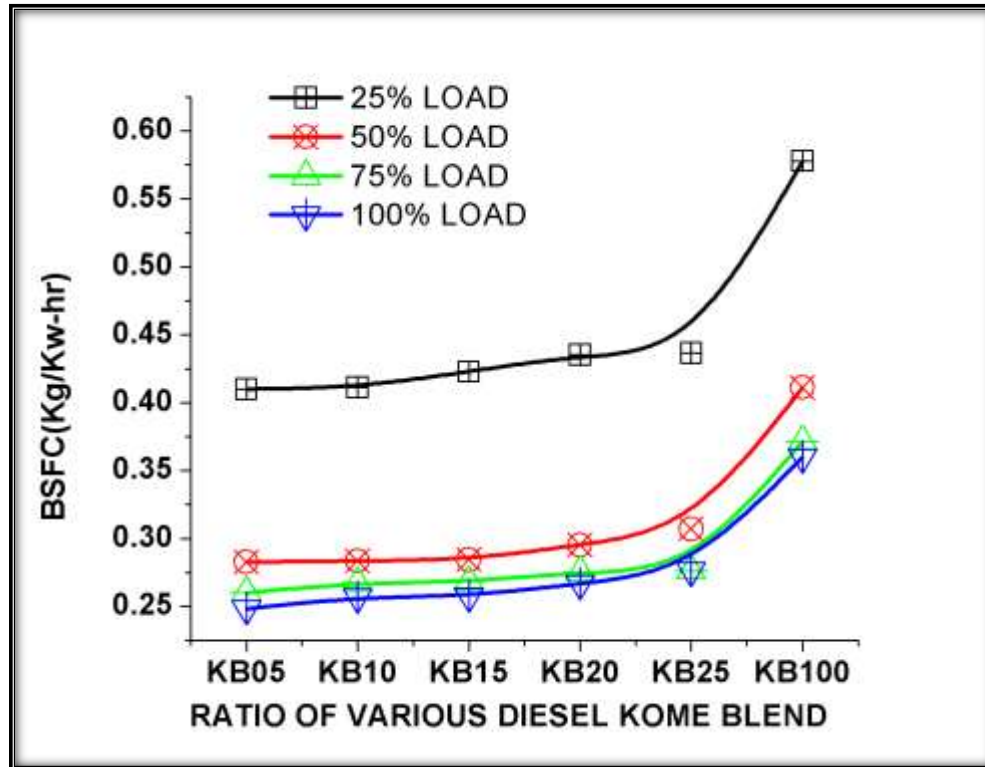


Figure 6.2 Variation of BSFC with percentage of KOME in the blend for different load conditions

The variation of BSEC with varied torque for different karanja derived biodiesel diesel blend is shown in figure 6.3 and figure 6.4 shows the variation of BSEC for different KOME blends at different load condition. It is observed from these figures that BSEC increases with increase in the blend. The maximum increase of BSEC is observed in the case of KB100. With biodiesel blends having a higher proportion of biodiesel the BSEC tends to increase. This is attributed to lower gross heat values of these blends than that of reference fuel. Figure 6.4 explains the change in BSEC with respect to varied biodiesel blends for a particular load. It is observed from the figure 6.4 that the BSEC deteriorate as the load increases from partial to full throttle. The energy content of the fuel tends to

decrease by increasing biodiesel proportion from KB05 to KB25 and KB100. This consequently affects the fuel economy. It can be seen from figure 6.3 the minimum increase in BSEC is for KB25. Therefore it is concluded that KB25 is the optimum fuel blend as compared to all test fuels.

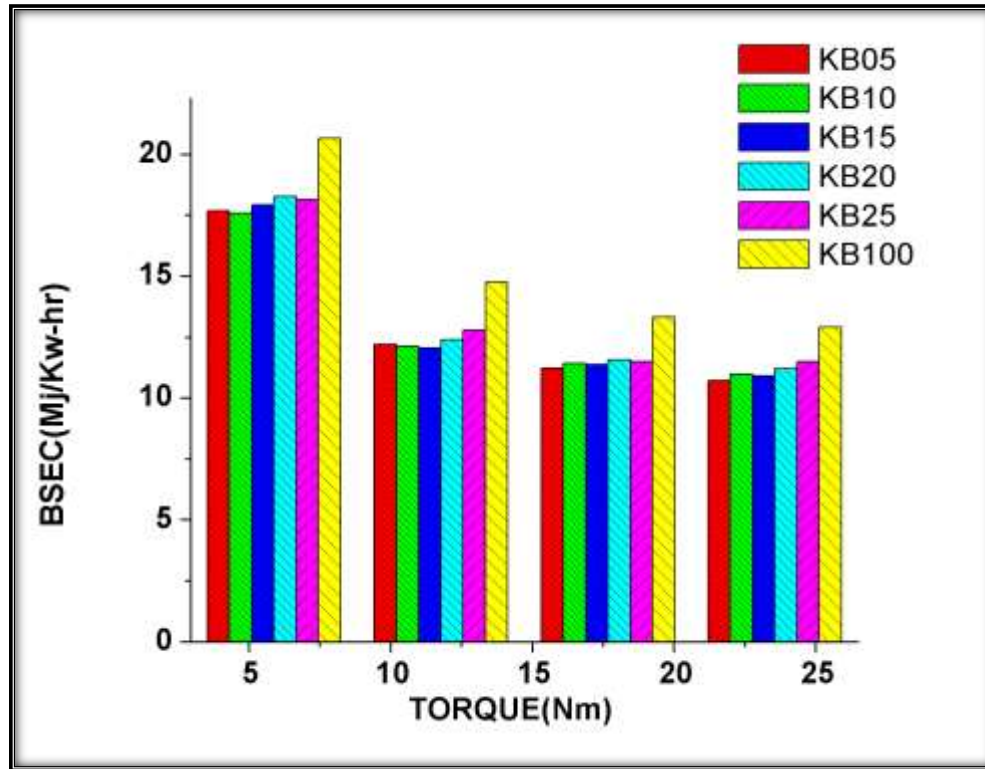


Figure 6.3 Variation of BSEC with varied torque for diesel KOME blend

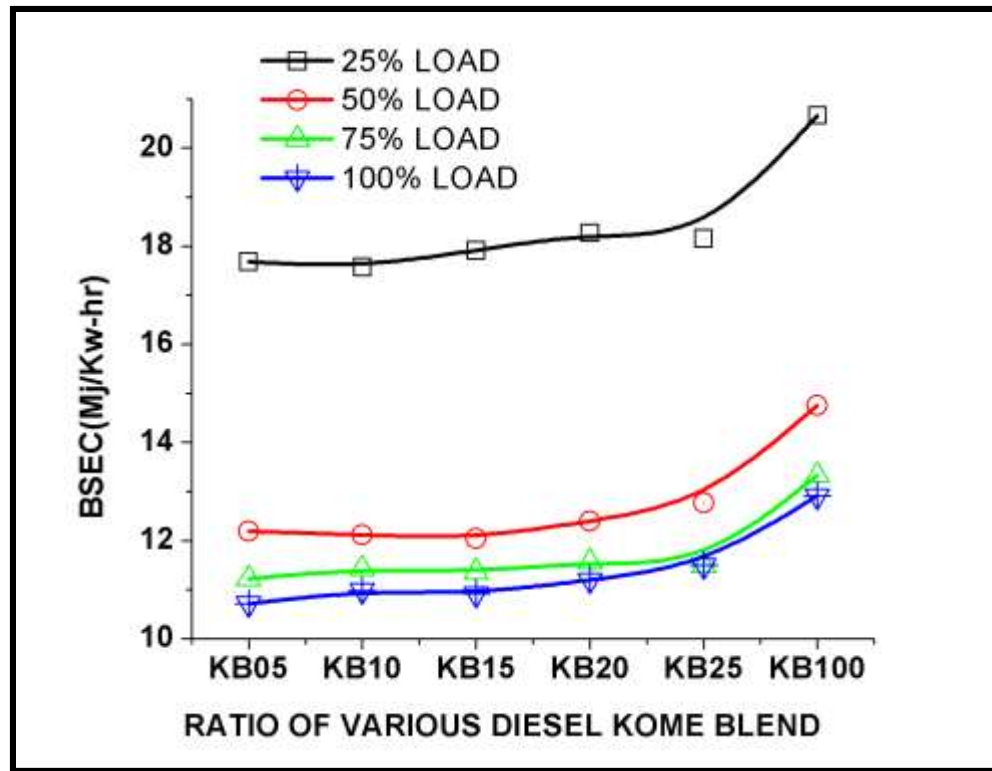


Figure 6.4 Variation of BSEC with percentage of KOME in the blend for different load conditions

The variation of brake thermal efficiency with varied torque for different karanja derived biodiesel diesel blend is shown in figure 6.5 and figure 6.6 shows the variation of brake thermal efficiency at different engine load for respective biodiesel blends. The mixture formation is poor as a result of low volatility and slightly higher viscosity, the thermal efficiency is lower with the methyl ester of karanja oil as compared to diesel oil. The maximum thermal efficiency with the methyl ester of karanja oil is about 27.88% whereas that of diesel is 34.41% at maximum power output. The thermal efficiencies are higher with 5%, 10%, 15%, 20% and 25% blending of biodiesel by volume as compared

to 100% biodiesel. The methyl ester of karanja oil and the blend have higher viscosity and density than the diesel. The higher viscosity leads to decreased atomization, fuel vaporization, and combustion. The calorific value of the diesel is more than that of 100% biodiesel and their different blends discussed above. Hence the thermal efficiency of 100% biodiesel is lower than that of diesel, whereas thermal efficiency is higher in the case of blending as compared to biodiesel.

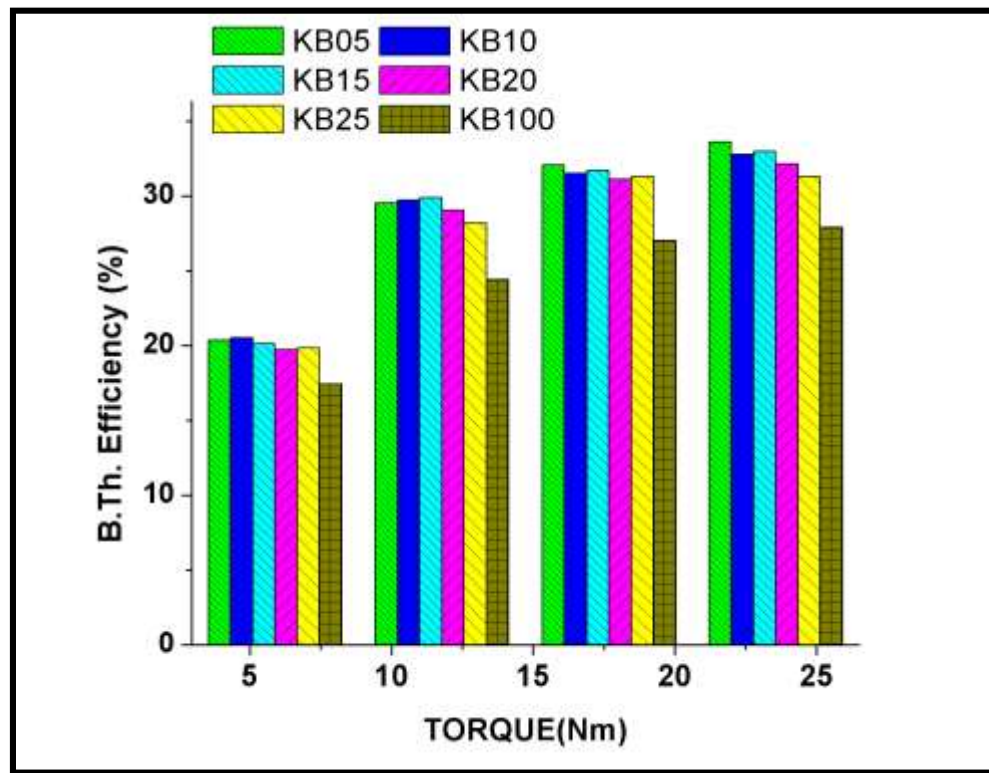


Figure 6.5 Variation of B.Th. Efficiency with varied torque for diesel KOME blend

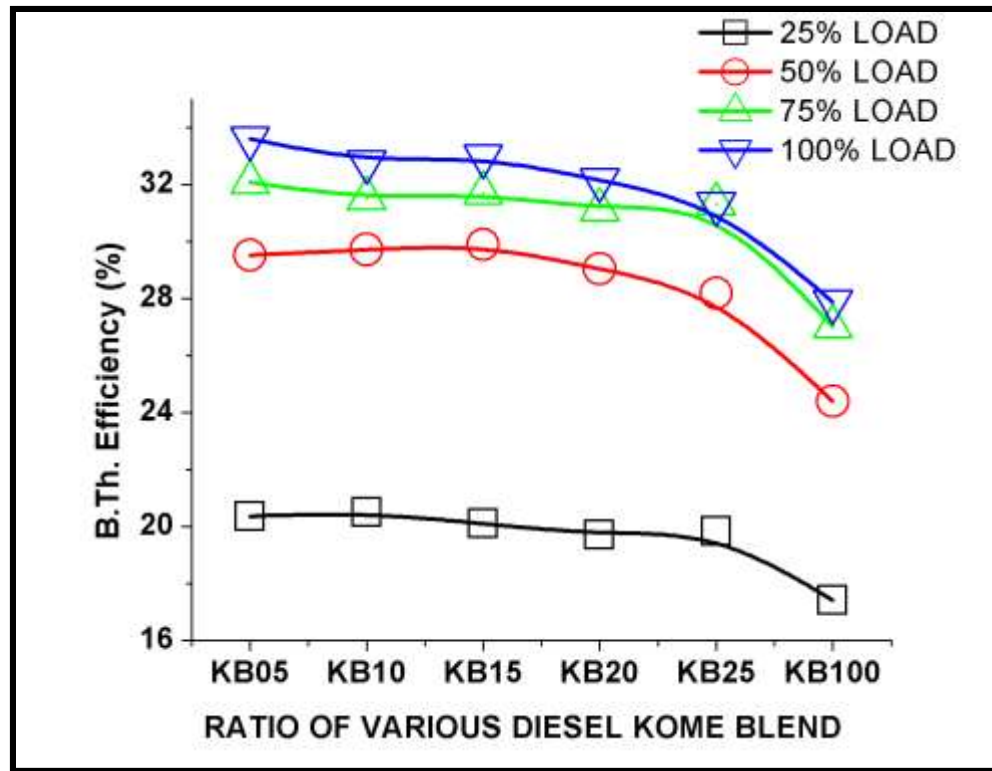


Figure 6.6 Variation of B.Th. Efficiency with percentage of KOME in the blend for different load conditions

Engine emission Test:

The variation of exhaust temperature with varied torque for different karanja derived biodiesel diesel blend is shown in figure 6.7 and figure 6.8 shows the variation of exhaust temperature at different engine load for respective biodiesel blends. Exhaust temperature is higher with biodiesel than diesel. This is due to oxygen present in the ester molecule which enhances the combustion process thus increasing temperature. The maximum temperature of exhaust gas at peak load is 318°C with the methyl ester of karanja oil and 312°C with the diesel.

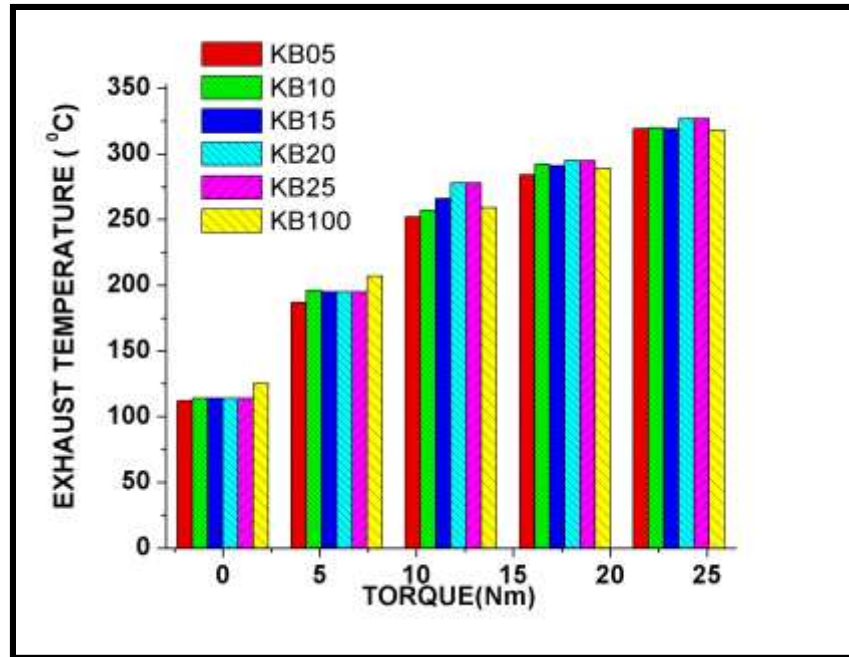


Figure 6.7 Variation of exhaust temperature with varied torque for diesel KOME blend

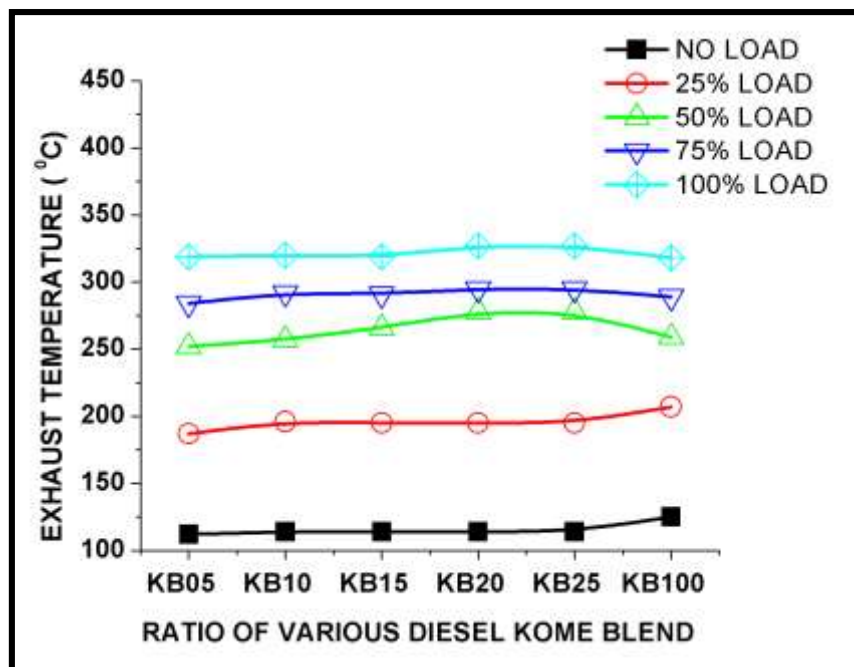


Figure 6.8 Variation of exhaust temperature with percentage of KOME in the blend for different load conditions

The variation of CO with varied torque for karanja derived biodiesel diesel blend is shown in figure 6.9 and figure 6.10 shows the variation of CO at different engine load for respective biodiesel blends. The figure shows a decrease in the trend of CO emission for a particular karanja derived biodiesel diesel blend as the load is increased. It further shows that when the percentage of biodiesel is increased in a biodiesel diesel blend, the CO emission is further decreased. The CO emission of diesel at full load is 0.024% whereas that of karanja derived biodiesel is 0.016% i.e. there is a reduction in 34% CO emission in case of karanja derived biodiesel than diesel fuel. However, the CO emissions are higher for blends as compared to pure biodiesel.

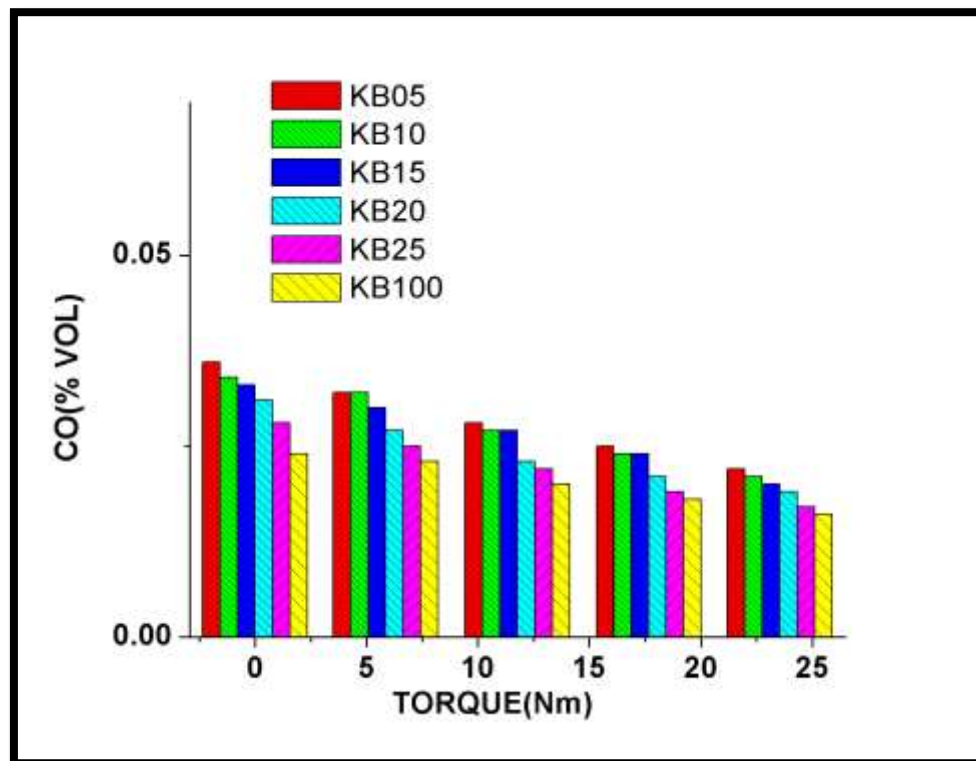


Figure 6.9 Variation of CO with varied torque for diesel KOME blend

The emissions are 0.022%, 0.021%, 0.020%, 0.019% and 0.017% with blends of 5%, 10%, 15%, 20% and 25% respectively at maximum load. Factors causing such trends are, in biodiesel being an oxygenated fuel contents additional oxygen enhances a complete combustion; thus reducing CO emissions. Another major reason is the higher cetane number of biodiesel that means the lower the probability of fuel-rich zone formation, hence exhibits the lower CO emissions.

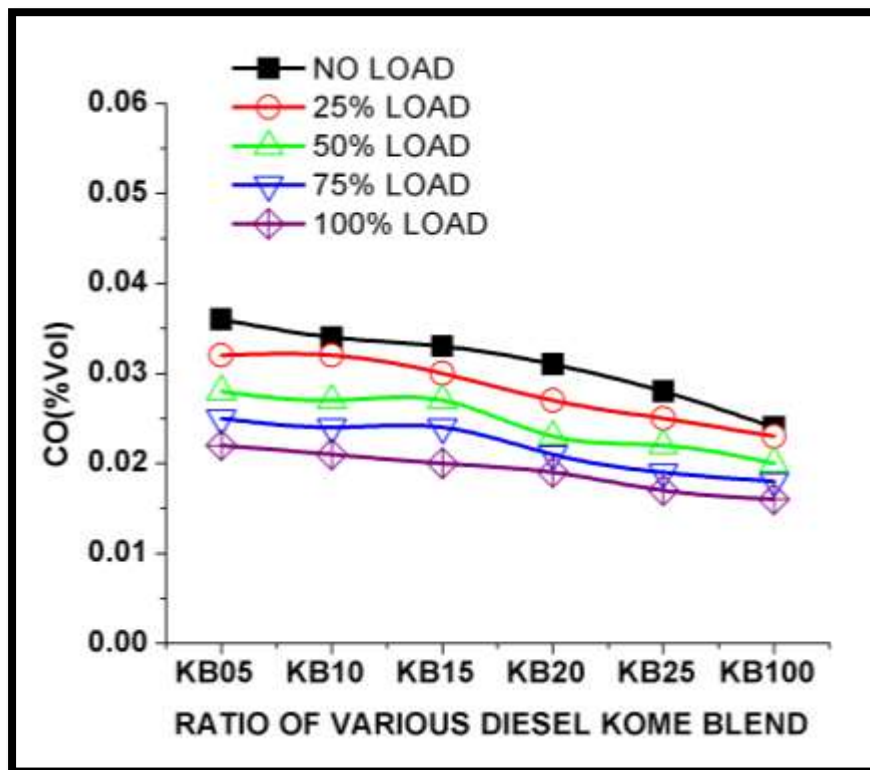


Figure 6.10 Variation of CO with percentage of KOME in the blend for different load conditions

The variation of HC with varied torque for karanja derived biodiesel diesel blend is shown in figure 6.11 and figure 6.12 shows the variation of HC at different engine load for respective biodiesel blends. Biodiesel exhibits lower HC emission as compared to standard diesel operation. The HC emission of diesel at maximum load is 32 ppm

whereas that of biodiesel is 23 ppm. However, the HC emission is lower with the biodiesel-diesel blend as compared to diesel. Emission has been found to be 30 ppm, 29 ppm, 27 ppm, 26 ppm and 24 ppm with blend 5%, 10%, 15%, 20% and 25% respectively at maximum load. The reduction in HC is mainly due to the result of complete and cleaner combustion of biodiesel blends within the combustion period due to the presence of excess oxygen atom in biodiesel. Another reason is the higher cetane number of biodiesel; reduces the combustion delay, and such reduction has been related to the decrease in HC emission.

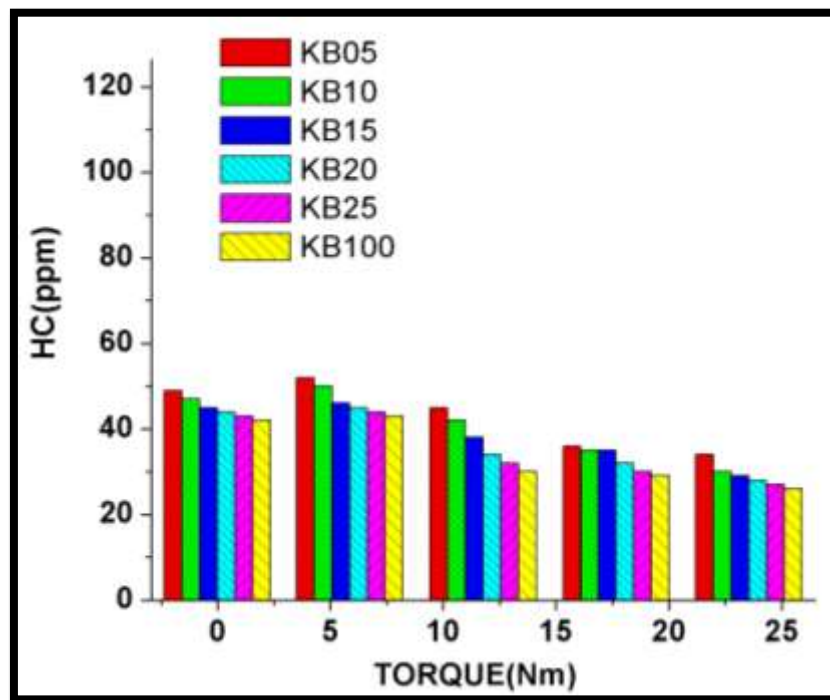


Figure 6.11 Variation of HC with varied torque for diesel KOME blend

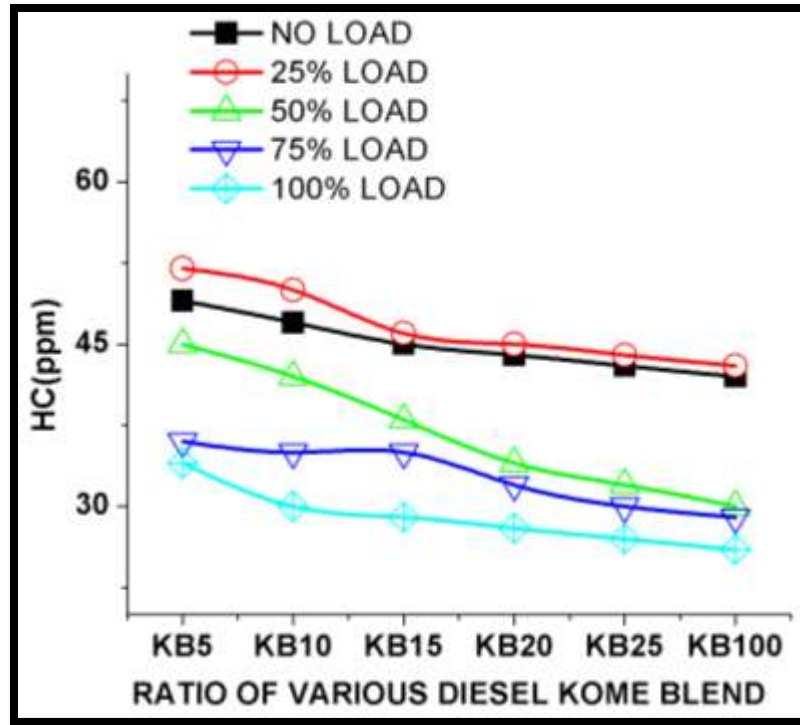


Figure 6.12 Variation of HC with percentage of KOME in the blend for different load conditions

The variation NO_x with varied torque for karanja derived biodiesel diesel blend is shown in figure 6.13 and figure 6.14 shows the variation of NO_x at different engine load for respective biodiesel blends. From the NO_x curves, two observations can be made. First NO_x emission is a direct function of engine loading. This is expected because on increasing load the temperature of the combustion chamber increases and NO_x formation is strongly temperature dependent phenomena. The second important observation is that the NO_x emission in the case of biodiesel fuel is higher; this may be due to the higher temperature of biodiesel combustion chamber. This is also evident from higher exhaust temperature from the biodiesel engine. The NO_x emission for the diesel at maximum load is 557 ppm, whereas for 100% biodiesel it is 627 ppm. This difference is obviously due to

the higher temperature of the combustion chamber for biodiesel. The NO_x emission is a function of temperature which in turn is a function of engine loading – this statement is quite justified in figure 6.14. At 100% load, the NO_x emission for the 100% biodiesel and their blend varies from 595 ppm to 627 ppm. Whereas for the 25% load, it varies from 203 ppm to 297 ppm and for 50% and 75% load the variation are from 347 ppm to 409 ppm, and from 479 ppm to 536 ppm respectively.

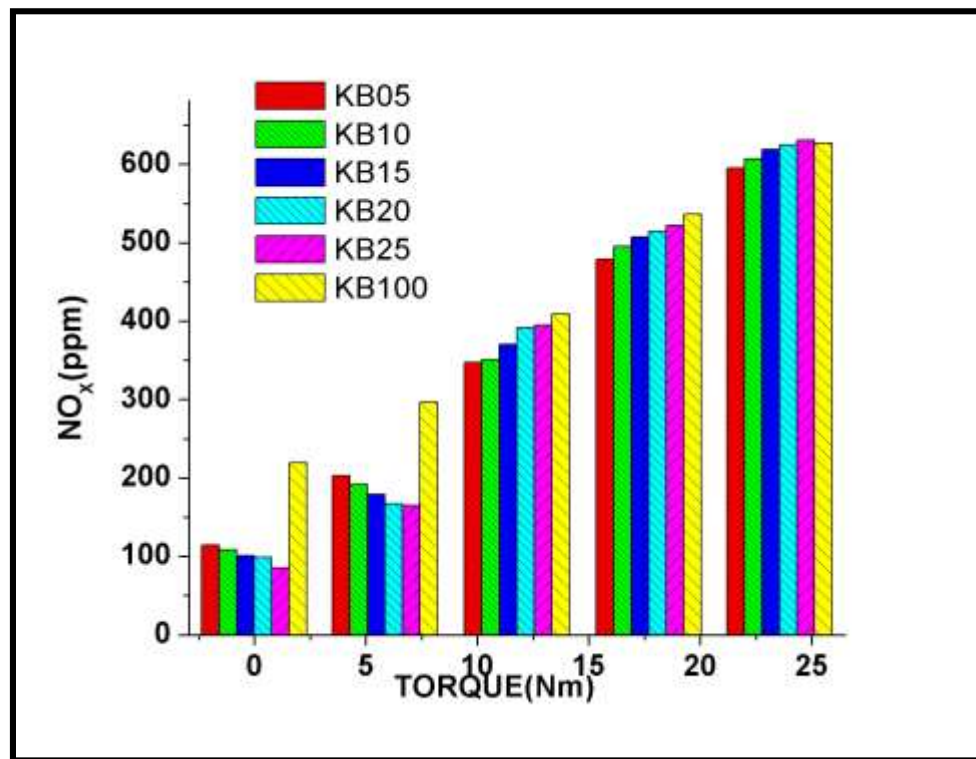


Figure 6.13 Variation of NO_x with varied torque for diesel KOME blend

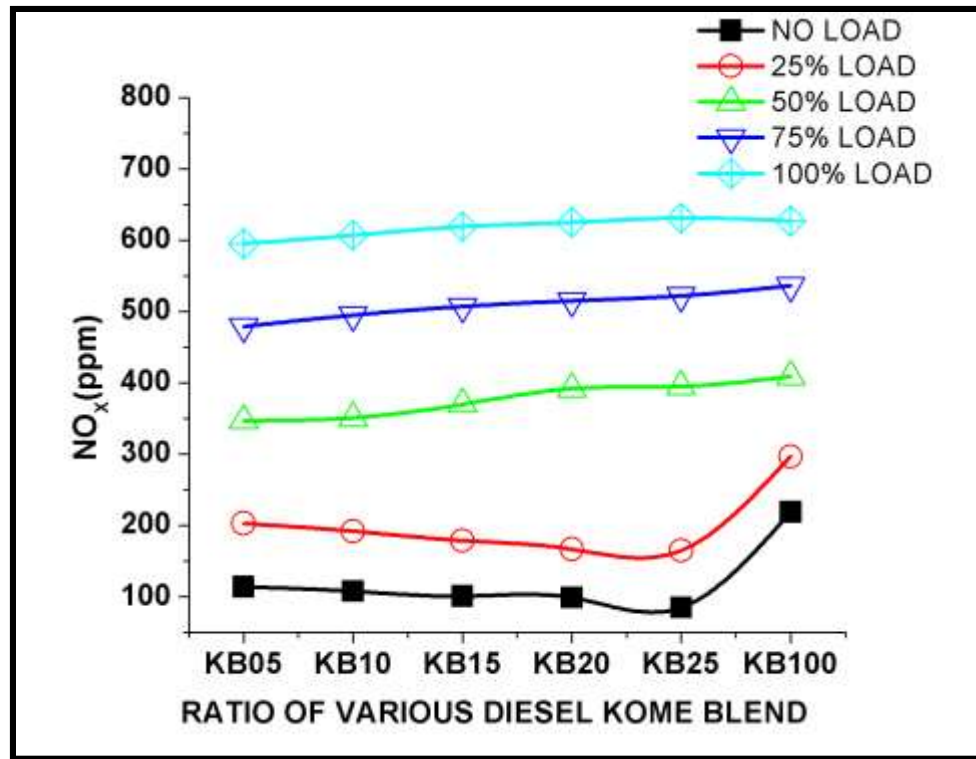


Figure 6.14 Variation of NO_x with percentage of KOME in the blend for different load conditions

6.2.3 Experiments on jatropha derived biodiesel

Engine performance Test:

In the third phase, the engine is run with varied JOME blends (JB10, JB20, JB30, JB40, JB50, JB60, JB70, JB80, JB90, and JB100) and their respective performance and emission parameter are noted down. The variations of BSFC with varied torque are shown in figure 6.15. It is observed that the maximum BSFC at peak load is 0.33 kg/KWh (JB100) that is higher than that of the diesel. This is due to the fact that pure diesel has a higher heating value than the JB100. On the other hand in case of blending (from JB10

to JB100) the BSFC at maximum load varies from 0.2568 kg/KWh to 0.3050 kg/KWh. Figure 6.16 explains the trend of BSFC for different JOME diesel blends at different load. It is observed that for a fixed load (say 25%) the BSFC increases as the blending proportion increase (say JB10, JB20 and so on) and the overall values of BSFC for a definite biodiesel blend is reduced as the percentage of the load is increased. For example the BSFC for JB10 at 25% load is 0.4214 kg/KWh, at 50% load is 0.2834 kg/KWh, at 75% load is 0.2490 kg/KWh. In all the cases the only major influencing parameter is the heating value of the respective fuel.

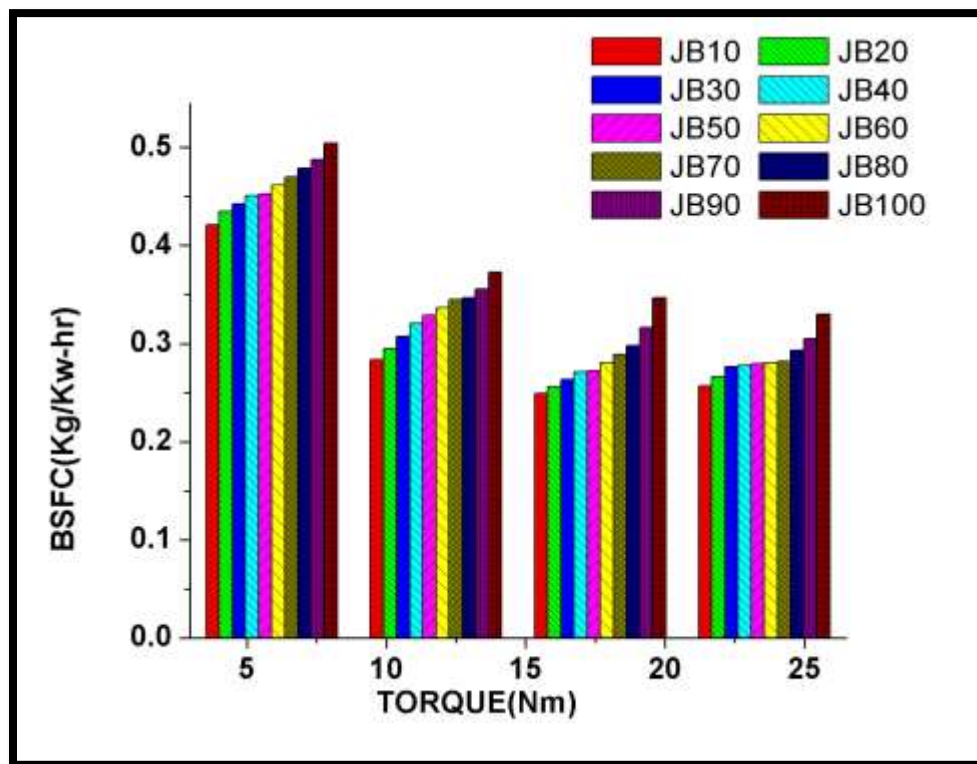


Figure 6.15 Variation of BSFC with varied torque for diesel JOME blend

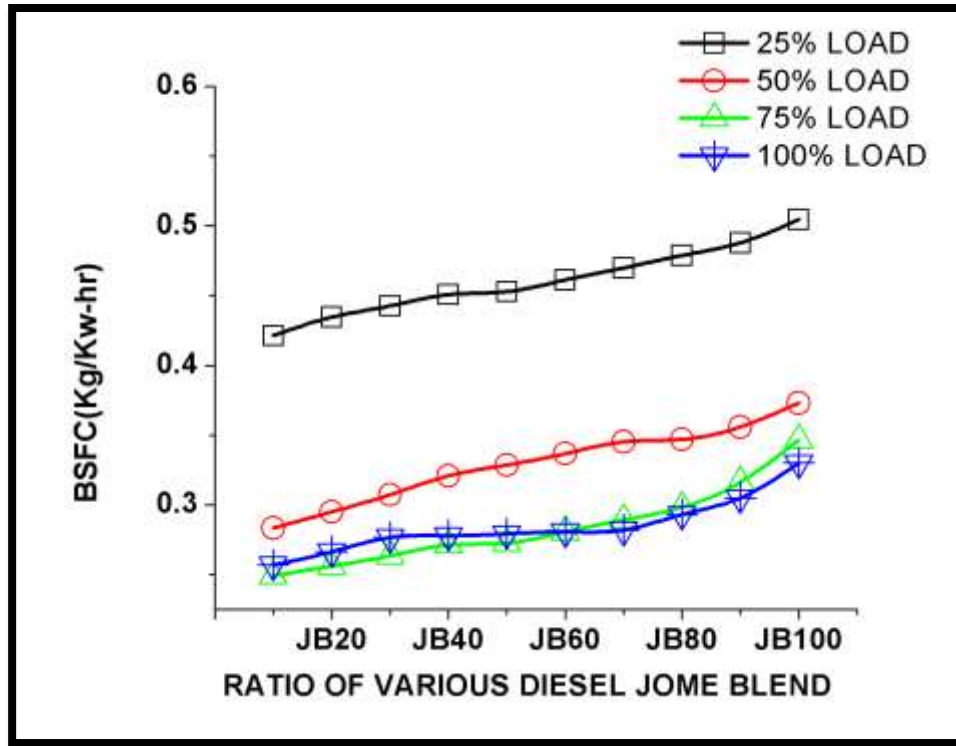


Figure 6.16 Variation of BSFC with percentage of JOME in the blend for different load conditions

Brake specific energy consumption (BSEC) is an ideal parameter for comparing engine performance. BSEC is defined as the amount of energy consumed per kilo-watt power developed in the engine in one hour. For the comparison of the economy of two fuels, brake specific energy consumption is the better way of judgment as compared to brake specific fuel consumption because the heating value and density of the fuels exhibit slight different trends. The variation of BSEC with varied torque is shown in figure 6.17 and figure 6.18 shows the variation of BSEC at different engine load for varying jatropha derived biodiesel diesel blends. It is observed from the figure 6.17 that BSEC increases with increase in blending proportion for a fixed load. The maximum increase of BSEC is observed in the case of JB100. The obtained value of BSEC for JB100 is 12845.9 kJ/kWh.

With biodiesel blends having a higher proportion of biodiesel the BSEC tends to increase.

This is attributed to lower gross heat values of these blends than that of reference fuel.

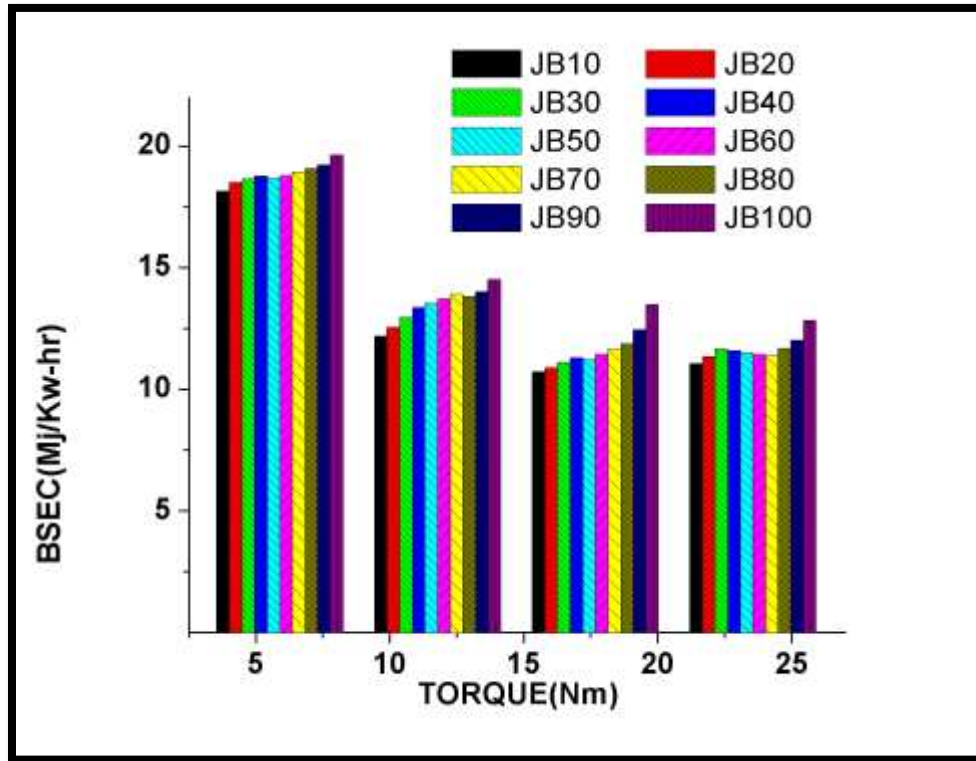


Figure 6.17 Variation of BSEC with varied torque for diesel JOME blend

Figure 6.18 explains the change in BSEC with respect to varied biodiesel blends for the different load. It is observed from the figure 6.18 that the BSEC deteriorates as the load increases from partial to full throttle. The energy content of the fuel tends to decrease by increasing biodiesel proportion from JB10 to JB100. This consequently affects the fuel economy. It can be seen from figure 6.18, BSEC value for JB50 is quite compatible with the value obtained from pure diesel as the higher jatropha derived biodiesel

blends(>JB50) may create a problem in fuel supply due to higher viscosity in the long run.

Therefore it is concluded that JB50 is the optimum fuel blend as compared to all test fuels.

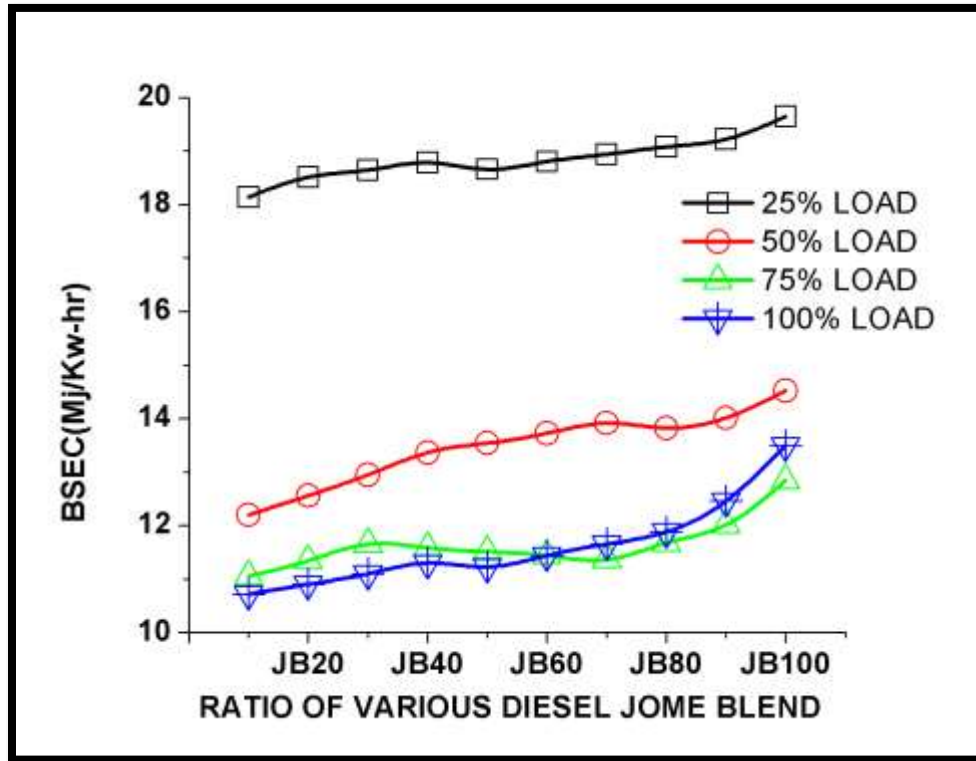


Figure 6.18 Variation of BSEC with percentage of JOME in the blend for different load conditions

The variation of brake thermal efficiency with varied torque for different jatropha derived biodiesel diesel blend is shown in figure 6.19 and figure 6.20 shows the variation of brake thermal efficiency at different engine load for respective biodiesel blends. The mixture formation is poor as a result of low volatility and slightly higher viscosity, the thermal efficiency is lower with the methyl ester of jatropha oil as compared to diesel oil. The maximum thermal efficiency with the methyl ester of karanja oil is about 28.02% whereas that of diesel is 34.41% at maximum power output. The thermal efficiencies are

higher with (10%, 20% up to 90%) different blending of biodiesel by volume as compared to 100% biodiesel. The methyl ester of jatropha oil and their blend have higher viscosity and density than the diesel. The higher viscosity leads to decreased atomization, fuel vaporization, and combustion. The calorific value of the diesel is more than that of 100% biodiesel and their different blends discussed above. Hence the thermal efficiency of 100% biodiesel is lower than that of diesel, whereas thermal efficiency is higher in the case of blending as compared to biodiesel.

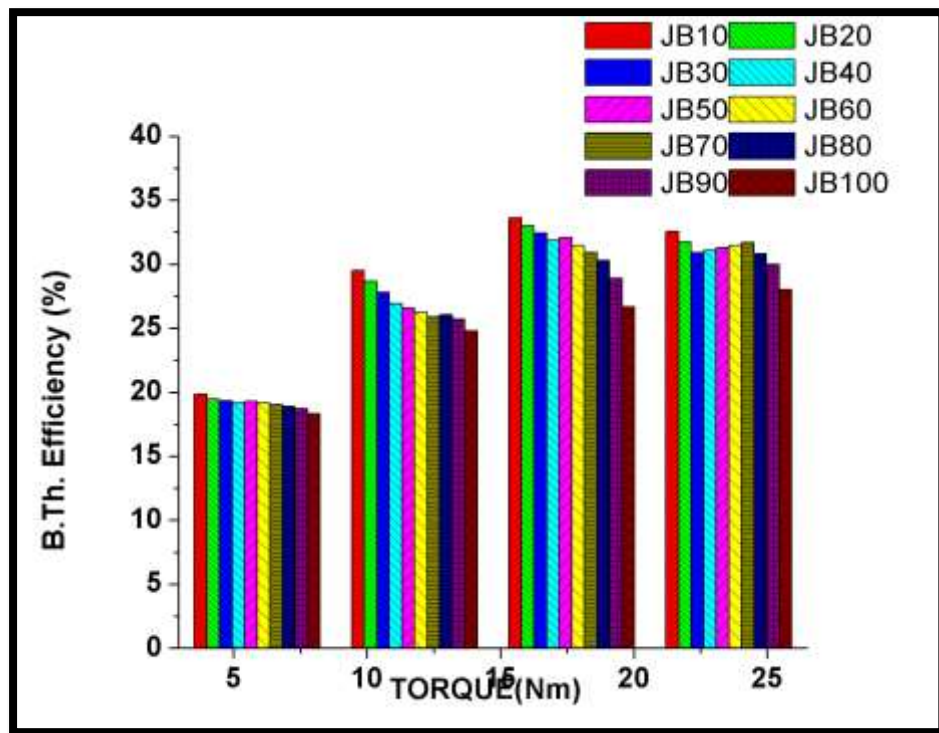


Figure 6.19 Variation of B.Th. Efficiency with varied torque for diesel JOME blend

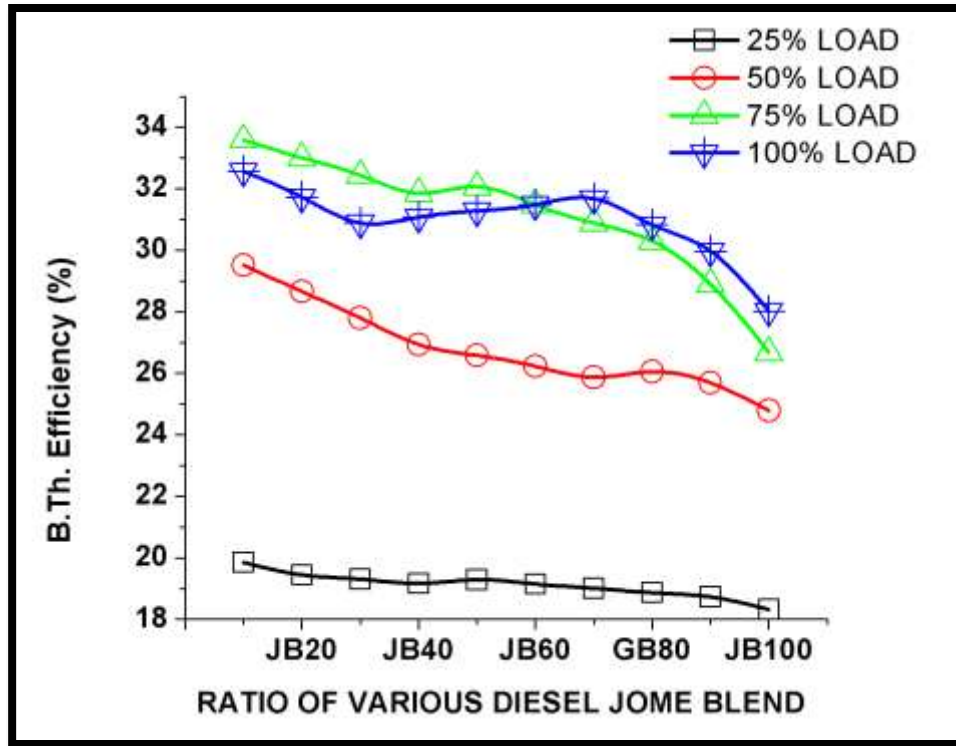


Figure 6.20 Variation of B.Th. Efficiency with percentage of JOME in the blend for different load conditions

Engine emission Test:

The variation of exhaust temperature with varied torque for different jatropha derived biodiesel diesel blend is shown in figure 6.21 and figure 6.22 shows the variation of exhaust temperature at different engine load for respective biodiesel blends. Exhaust temperature is higher with biodiesel than diesel. This is due to oxygen present in the ester molecule enhances the combustion process thus increasing temperature. The maximum temperature of exhaust gas at peak load is 547°C with the methyl ester of jatropha oil and 312°C with the diesel.

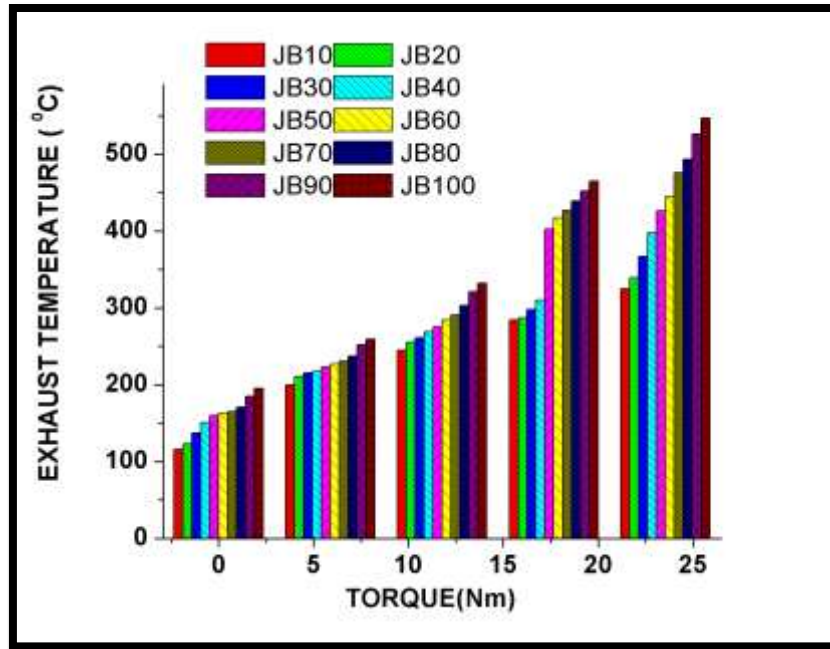


Figure 6.21 Variation of exhaust temperature with varied torque for diesel JOME blend

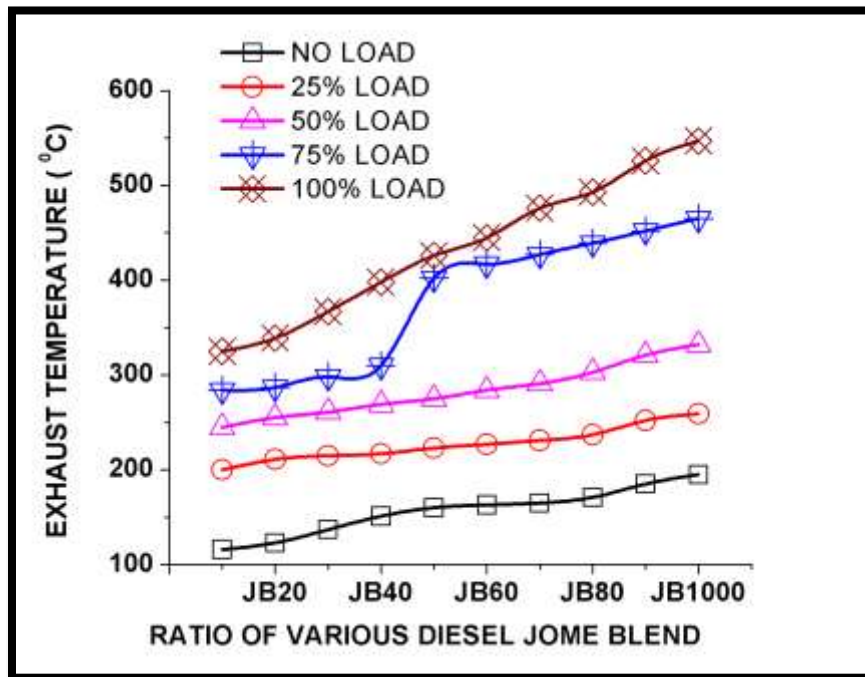


Figure 6.22 Variation of exhaust temperature with percentage of JOME in the blend for different load conditions

The variation of CO with varied torque for jatropha derived biodiesel diesel blend is shown in figure 6.23 and figure 6.24 shows the variation of CO at different engine load for respective biodiesel blends. The CO emission of diesel is 0.024% whereas that of JB100 is 0.013% at maximum load i.e. almost 50% reduction in CO emission for biodiesel in comparison to diesel fuel. However, the emissions are shown lower for blends as compared to pure biodiesel and further reduced with the increase in load.

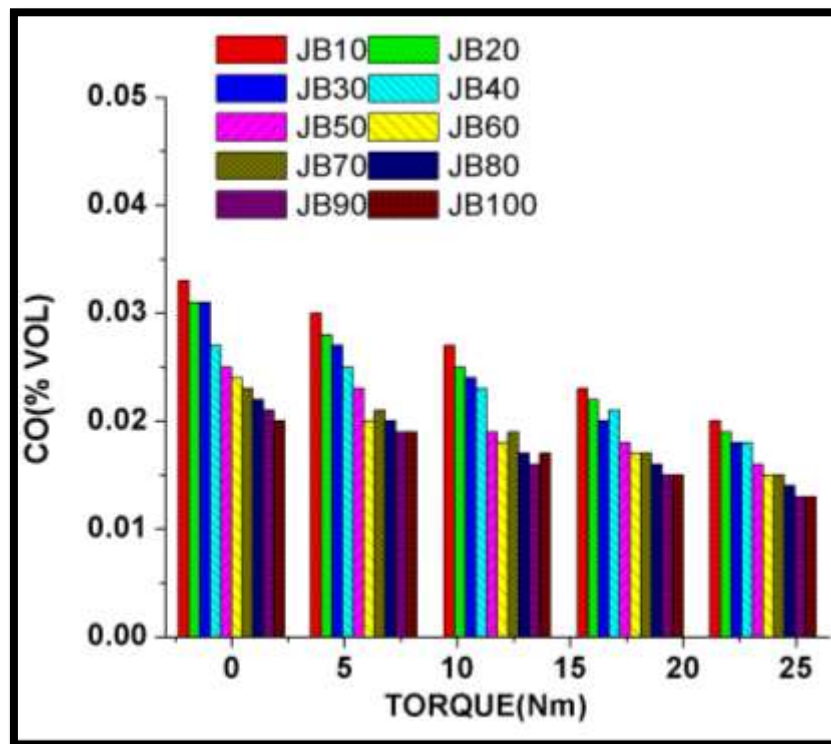


Figure 6.23 Variation of CO with varied torque for diesel JOME blend

The emissions varied from 0.020% to 0.013% with blends of 10% to 90% at maximum load. Factors causing excess oxygen in biodiesel and higher cetane number is responsible for the decreased CO emission. It is also observed that CO emission decreases gradually with the blending of higher concentration of biodiesel to diesel.

Again, this may be due to the increase in oxygen with blending of biodiesel in diesel leading to complete combustion.

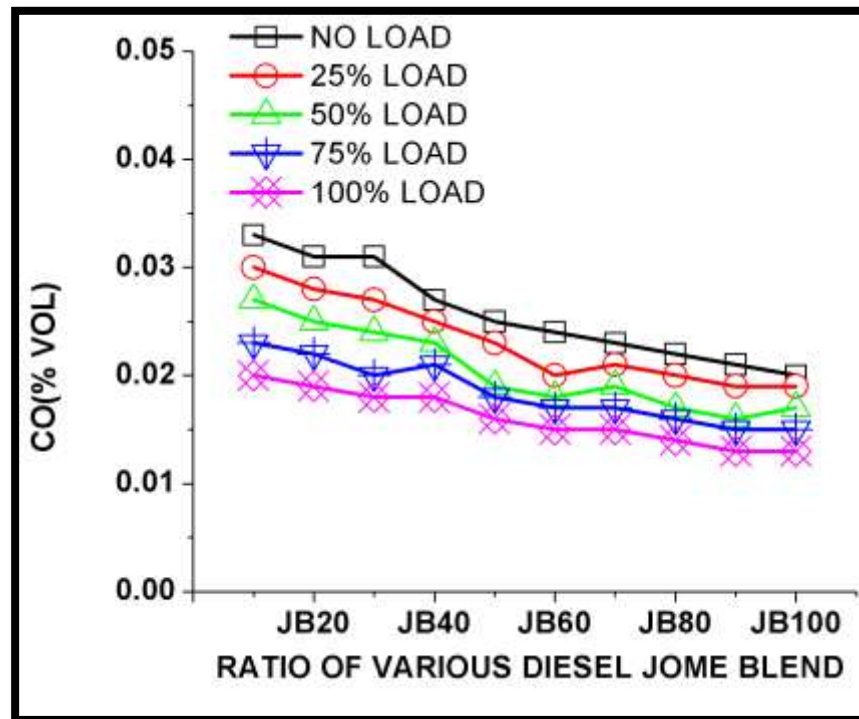


Figure 6.24 Variation of CO with percentage of JOME in the blend for different load conditions

The variation of HC with varied torque for jatropha derived biodiesel diesel blend is shown in figure 6.25 and figure 6.26 shows the variation of HC at different engine load for respective biodiesel blends. Biodiesel exhibits lower HC emission as compared to standard diesel operation. The HC emission of diesel at maximum load is 32 ppm whereas that of JB100 is 16 ppm i.e. 50% reduction in HC emission for pure biodiesel in comparison to diesel fuel. However, the emission is lower with the pure biodiesel as compared to biodiesel-diesel blend. Emission has been found to be varying from 29 ppm

to 16 ppm with blend varies from 10% to 90% at maximum load. The reduction in HC is mainly due to the result of improved combustion of biodiesel blends within the combustion period due to the presence of excess oxygen atom in biodiesel. Another major reason is the higher value of cetane number for biodiesel that reduces the combustion delay, and such a reduction has been related to decrease in HC emission.

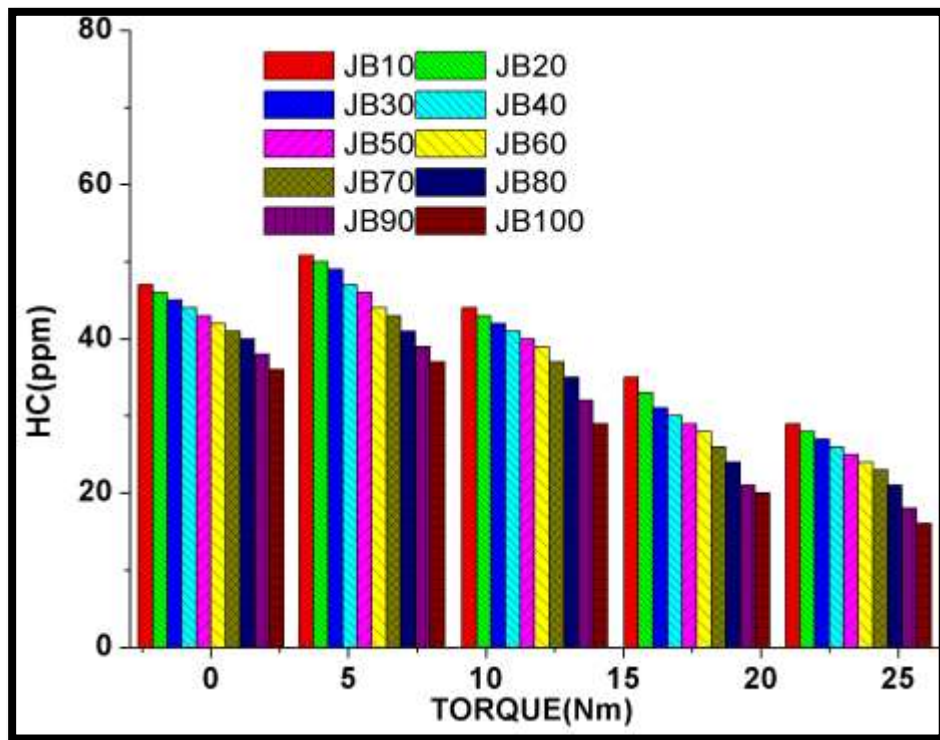


Figure 6.25 Variation of HC with varied torque for diesel JOME blend

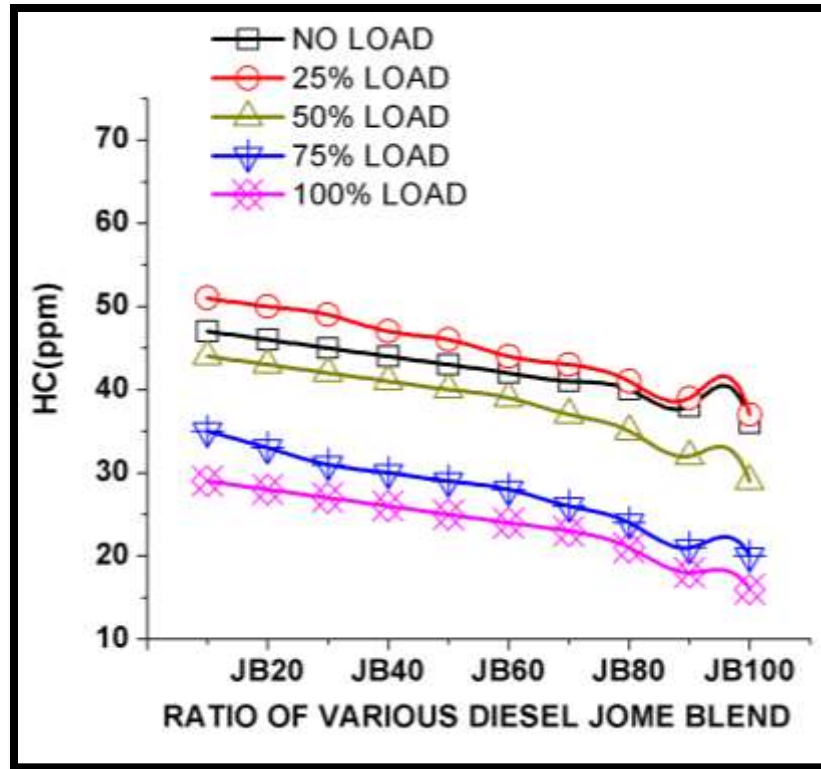


Figure 6.26 Variation of HC with percentage of JOME in the blend for different load conditions

The variation NO_x with varied torque for jatropha derived biodiesel diesel blend is shown in figure 6.27 and figure 6.28 shows the variation of NO_x at different engine load for respective biodiesel blends. From the NO_x curves, two observations can be made. First NO_x emission is a direct function of engine loading. This is expected because on increasing load the temperature of the combustion chamber increases and NO_x formation is strongly temperature dependent phenomena. Second important observation is that the NO_x emission in the case of biodiesel fuel is higher; this may be due to the higher temperature of biodiesel combustion chamber. This is also evident from higher exhaust temperature from the biodiesel engine. The NO_x emission for the diesel at maximum load

is 557 ppm, whereas, for JB100, it is 772 ppm. This difference is obviously due to the higher temperature of the combustion chamber for biodiesel. The NO_x emission is a function of temperature which in turn is a function of engine loading – this statement is quite justified in figure 6.28. At peak load the NO_x emission for the jatropha derived biodiesel blend varies from 607 ppm to 739 ppm. Whereas for the 25% load, it varies from 211 ppm to 285 ppm and for 50% and 75% load the variation are from 349 ppm to 446 ppm, and from 515 ppm to 641 ppm respectively.

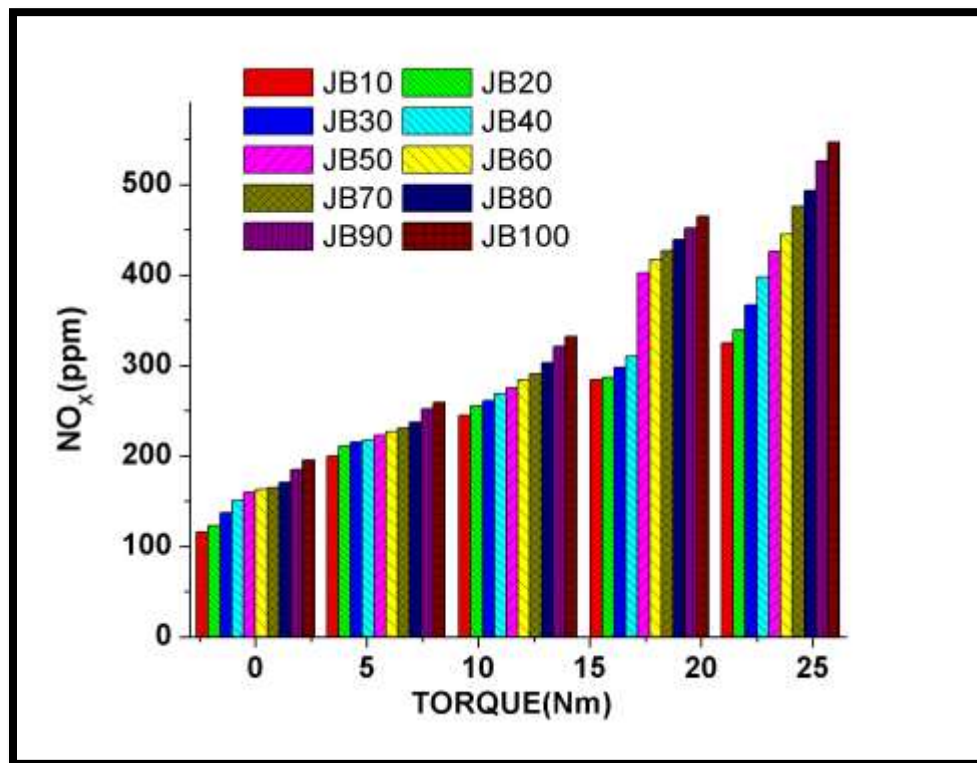


Figure 6.27 Variation of NO_x with varied torque for diesel JOME blend

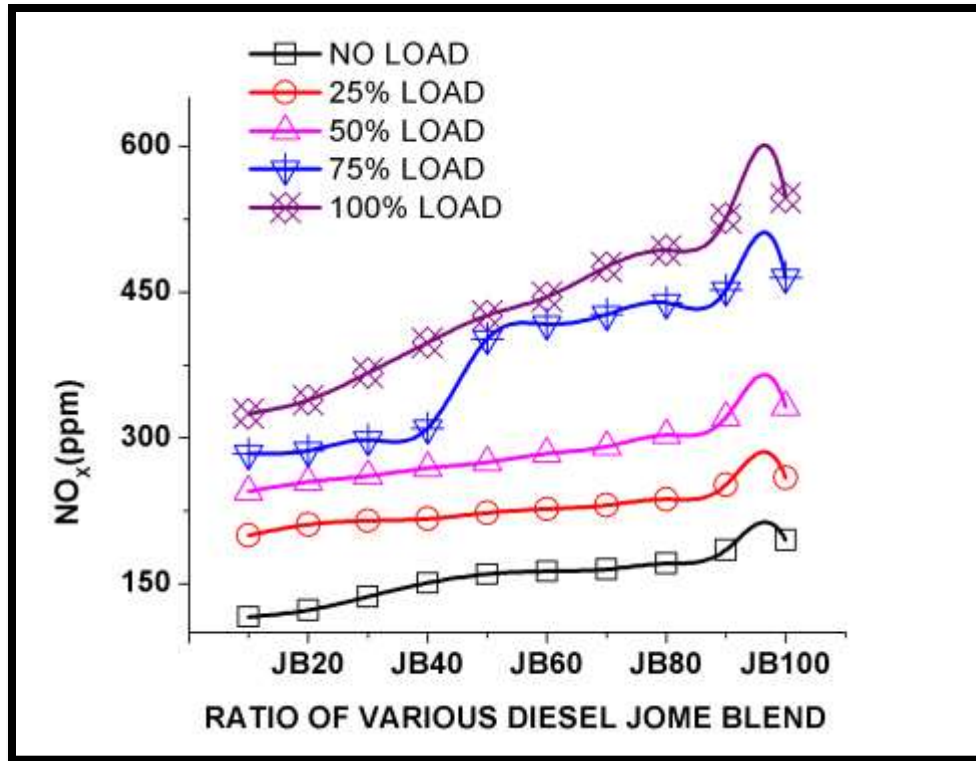


Figure 6.28 Variation of NO_x with percentage of JOME in the blend for different load conditions

6.3 COMPARISON AMONG DIESEL, KARANJA DERIVED BIODIESEL & JATROPHA DERIVED BIODIESEL:

A comparison is made among diesel, karanja derived biodiesel and jatropha derived biodiesel with respect to BSFC values in the figure 6.29. The BSFC actually explains how efficiently the fuel of an engine can be converted into work. The figure 6.29 explains the BSFC value is minimum for diesel and maximum for karanja derived biodiesel. The BSFC of diesel at peak load is 0.2405 kg/kWh and that of karanja derived biodiesel is 0.3599 kg/kWh, whereas that of for jatropha derived biodiesel it is 0.33 kg/kWh. The fuel consumption mainly depends on upon the heating values of the fuel, air-fuel ratio, and the engine efficiency. The heating value of the jatropha derived biodiesel

is nearer to the diesel and higher than karanja derived biodiesel; the BSFC value for jatropha derived biodiesel is found to be lower than karanja derived biodiesel and higher than diesel. The values of the BSFC are quite closer for the fuel under study and therefore both can be significantly thought as replacement of diesel in respect to BSFC values.

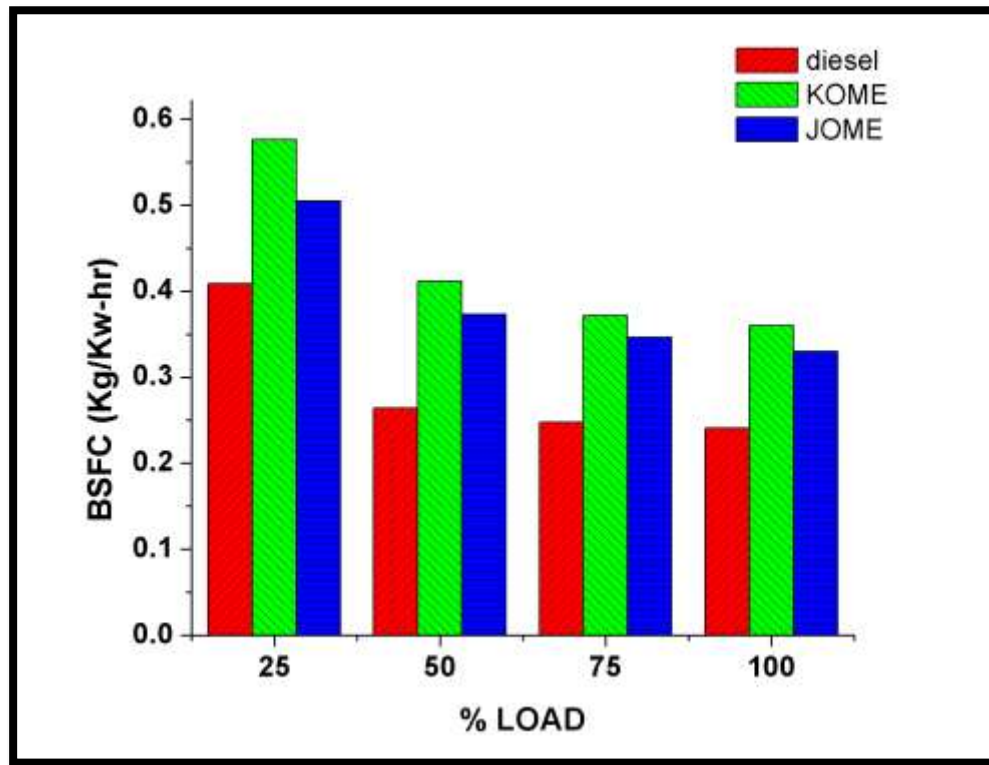


Figure 6.29 Variation of BSFC at different load for diesel, karanja derived biodiesel & jatropha derived biodiesel

The variations of brake thermal efficiency is shown in figure 6.30 among diesel, karanja derived biodiesel and jatropha derived biodiesel. The maximum thermal efficiency with karanja derived biodiesel is about 27.88% whereas that of diesel is 34.41% and for jatropha derived biodiesel is 28.02% at maximum power output. The higher viscosity leads to decreased atomization, fuel vaporization, and combustion, and hence the

thermal efficiency of 100% biodiesel is lower than that of diesel, whereas thermal efficiency is higher in the case of blending as compared to biodiesel. Hence the blending of biodiesel with diesel is a better choice than using pure biodiesel as CI engine substitute.

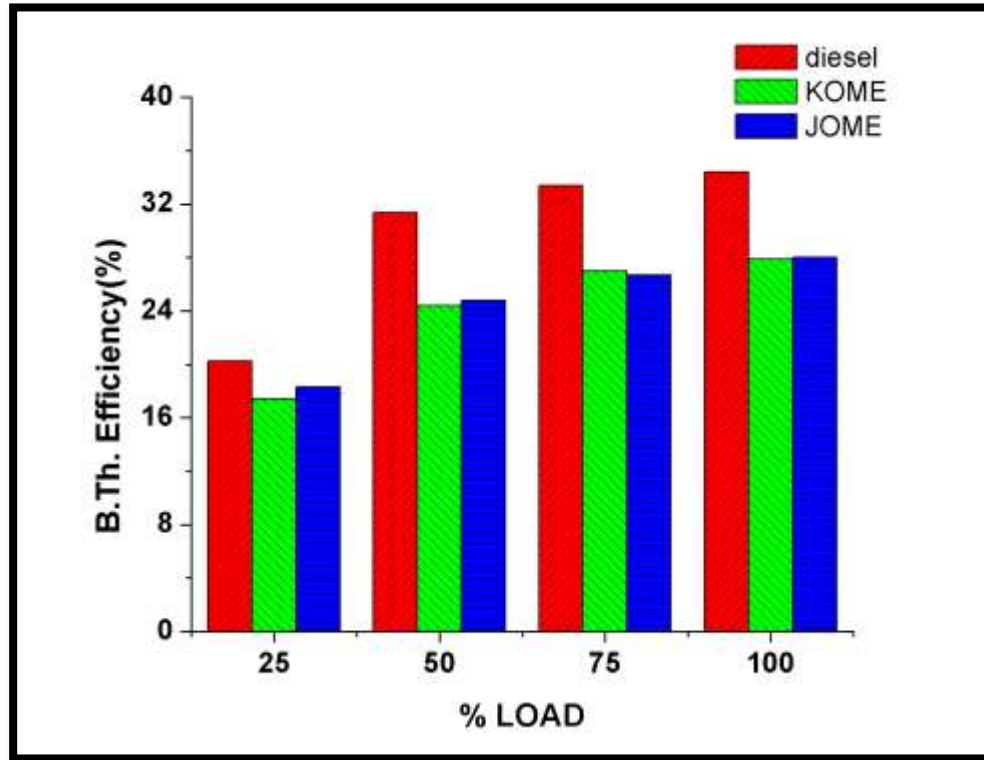


Figure 6.30 Variation of B.Th. Efficiency at different load for diesel, karanja derived biodiesel & jatropha derived biodiesel

A comparison is made among diesel, karanja derived biodiesel and jatropha derived biodiesel with respect to their exhaust gas temperature values in the figure 6.31. The maximum temperature of exhaust gas at peak load is 318°C with the karanja derived biodiesel and 312°C with the diesel and that of for jatropha derived biodiesel is 347°C. This is due to the more oxygen present in the ester molecules of jatropha than karanja oil

that enhances the complete combustion process and increased the temperature of the exhaust.

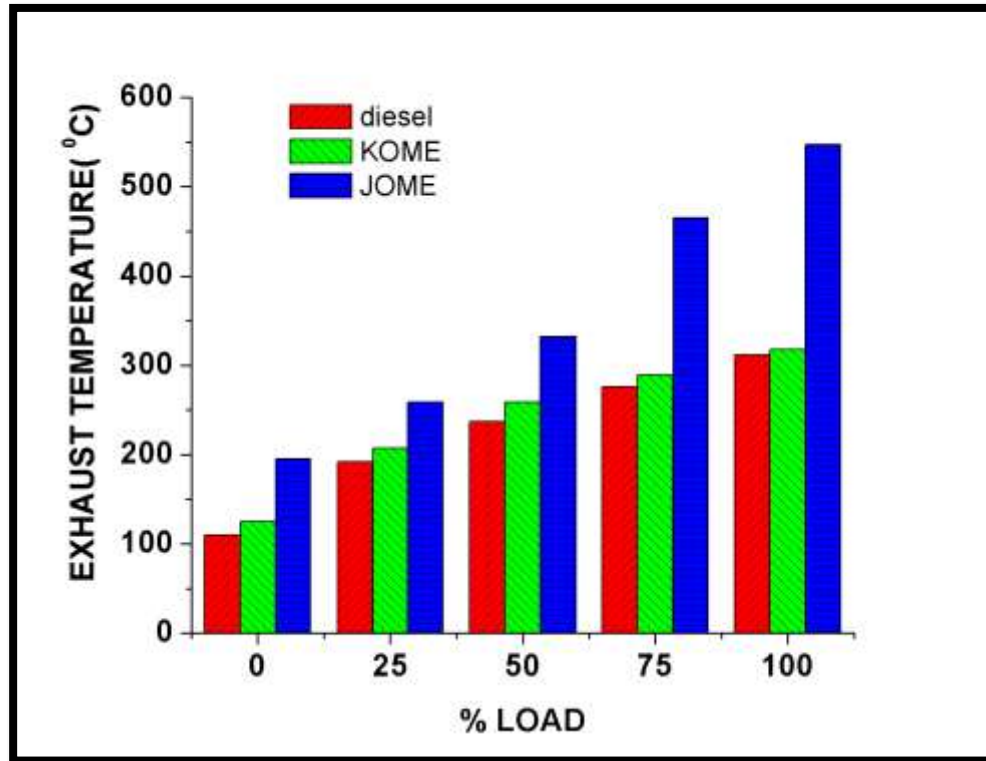


Figure 6.31 Variation of exhaust temperature at different load for Diesel, karanja derived biodiesel & jatropha derived biodiesel

The variations of CO are shown in figure 6.32 among diesel, karanja derived biodiesel (KOME) and jatropha derived biodiesel (JOME). The jatropha and karanja derived biodiesel shows less CO emission compared to diesel because of their higher cetane number that reduces the combustion delay and biodiesel being oxygenated fuel results clean and complete combustion.

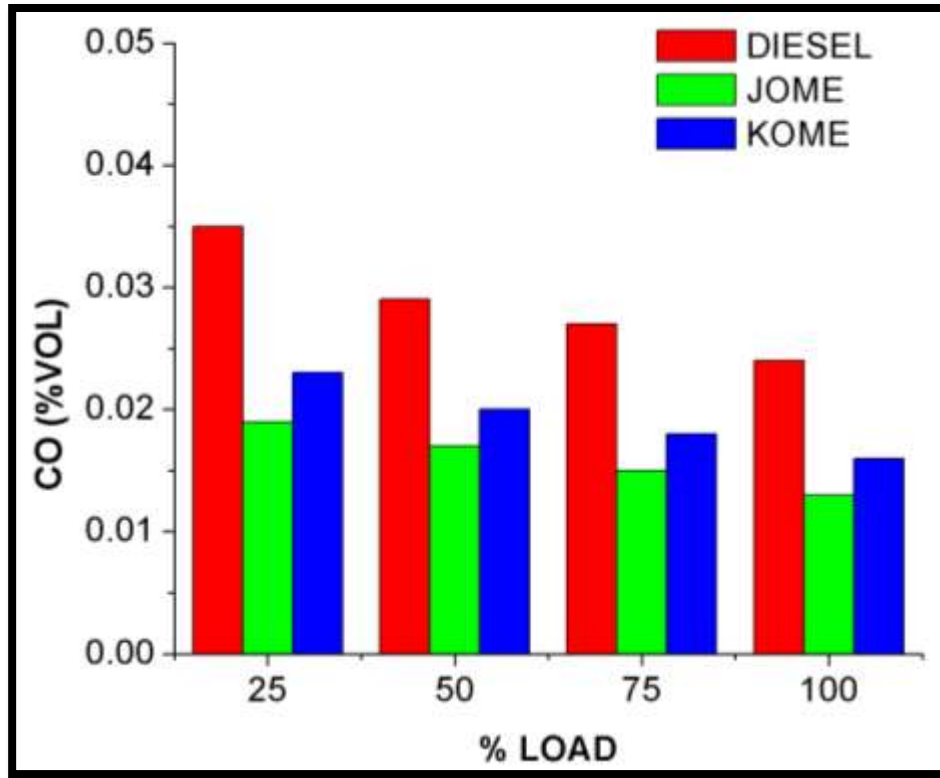


Figure 6.32 Variation of CO at different load for diesel, karanja derived biodiesel & jatropha derived biodiesel

Proper mixing with excess oxygen for biodiesel results in lower HC emission. The results are shown in figure 6.33, where the HC emission of diesel at maximum load is 32 ppm and for karanja derived biodiesel is 23 ppm whereas that of for jatropha derived biodiesel it is 16 ppm. Excess oxygen content in the biodiesel leads to a clean and complete combustion. Whereas the higher cetane number reduces the combustion delay, and such a reduction has been related to decrease in HC emission. The cetane number for jatropha derived biodiesel is found to be 57 and for karanja derived biodiesel is 56.

Therefore the HC emission for jatropha derived biodiesel is found even less than the karanja derived biodiesel.

A comparison is made among diesel, karanja derived biodiesel and jatropha derived biodiesel with respect to their NO_x values in the figure 6.34. The NO_x emission is higher in the case of biodiesel than diesel due to the higher temperature of biodiesel combustion chamber. The NO_x emission for diesel is 557 ppm whereas for karanja derived biodiesel it is 627 ppm and for jatropha derived biodiesel it is 772 ppm.

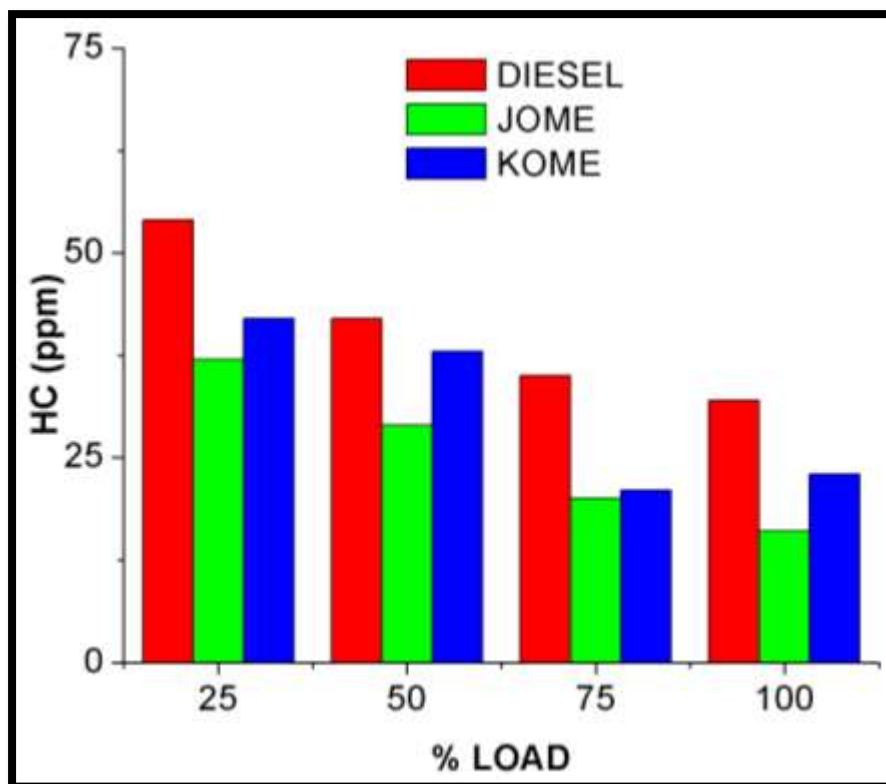


Figure 6.33 Variation of HC at different load for diesel, karanja derived biodiesel & jatropha derived biodiesel

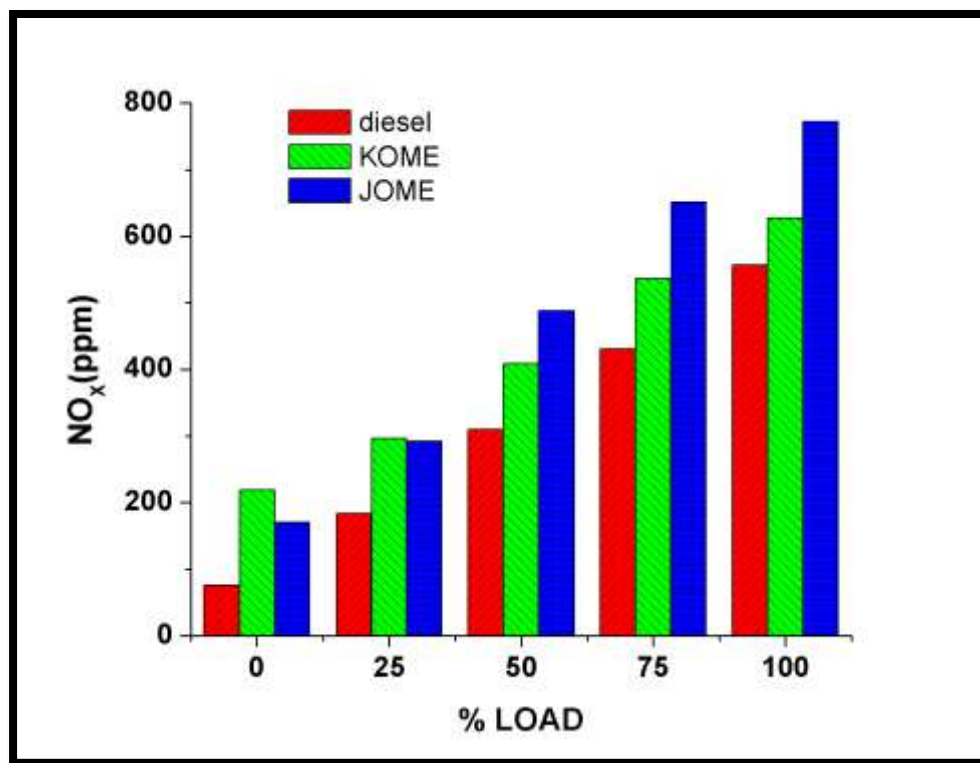


Figure 6.34 Variation of NO_x at different load for diesel, karanja derived biodiesel & jatropha derived biodiesel

6.4 COMPARISON AMONG DIESEL, OPTIMUM KOME BLEND, AND OPTIMUM JOME BLEND:

In the previous articles, while comparing among diesel, JOME, and KOME, it is found that both are quite good substitutes for the diesel fuel in terms of performance or emission. But the experiments of the biodiesel are conducted on a short-term basis. Since the viscosity, density obtained from biodiesel are quite high, it has been blended with diesel oil in varying proportions to achieve the required viscosity and density close to that of diesel fuel. Considering the properties of the diesel fuel and EURO III norms, it is found that for the karanja derived biodiesel KB25 and for the jatropha derived biodiesel JB 50

is the optimum choice. These optimum choices are further compared with the diesel fuel with respect to their performance and emission.

A comparison is made among diesel, KB25 and JB50 with respect to BSFC values in the figure 6.35. At full load, the BSFC value for diesel is 0.2405 kg/kWh and for KB25 it is 0.2764 kg/kWh whereas for JB50 it is 0.2793 kg/kWh. So around 14.92% BSFC value is increased in the case of KB25 compared to diesel at full load and 16.13% increased for JB50.

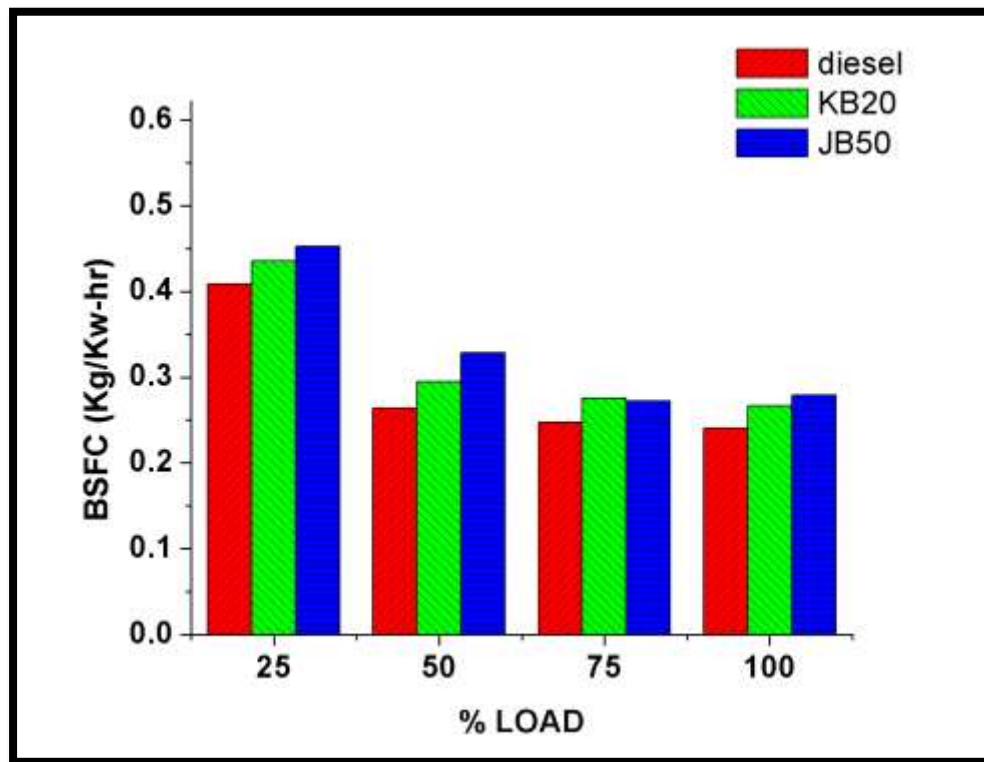


Figure 6.35 Variation of BSFC at different load for diesel, KB25 & JB50

The variations of brake thermal efficiency are shown in figure 6.36 among diesel, KB25, and JB50. The maximum thermal efficiency with KB25 is about 31.31% whereas

that of diesel is 34.41% and for JB50, it is 31.28% at maximum power output. So the blending in the both the cases results in 3% reductions in the brake thermal efficiency compared to diesel and it is quite acceptable.

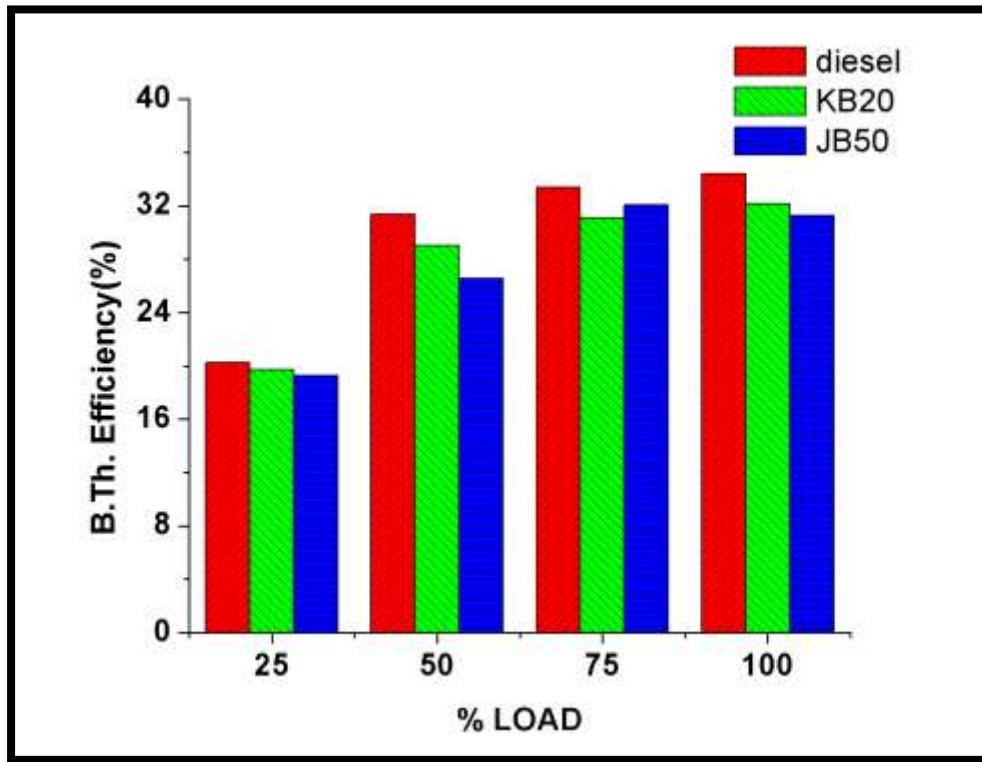


Figure 6.36 Variation of B.Th. Efficiency at different load for diesel, KB25 & JB50

Figure 6.37 to figure 6.40 explain the variations of emission parameters among diesel, KB25, and JB50. At full load, the exhaust temperature for diesel is 312°C, whereas for KB25, it is 327°C, and for JB50, it is 426°C. The exhaust temperatures for the blended biodiesels are found to be higher than diesel, as the biodiesels are oxygenated fuels. The amount of unburnt hydrocarbon for JB50 is found to be lesser than diesel fuel. This is due to proper mixing and complete combustion of the fuel. Whereas for the KB25, it is also

found the amount unburnt hydrocarbon is less as compared to diesel. The CO emission for KB25 is found less than the diesel fuel whereas the JB50 shows a much lesser CO emission than diesel. The NO_x emission for diesel is 557ppm whereas for KB25 it is 631 ppm and for JB50 it is 674 ppm.

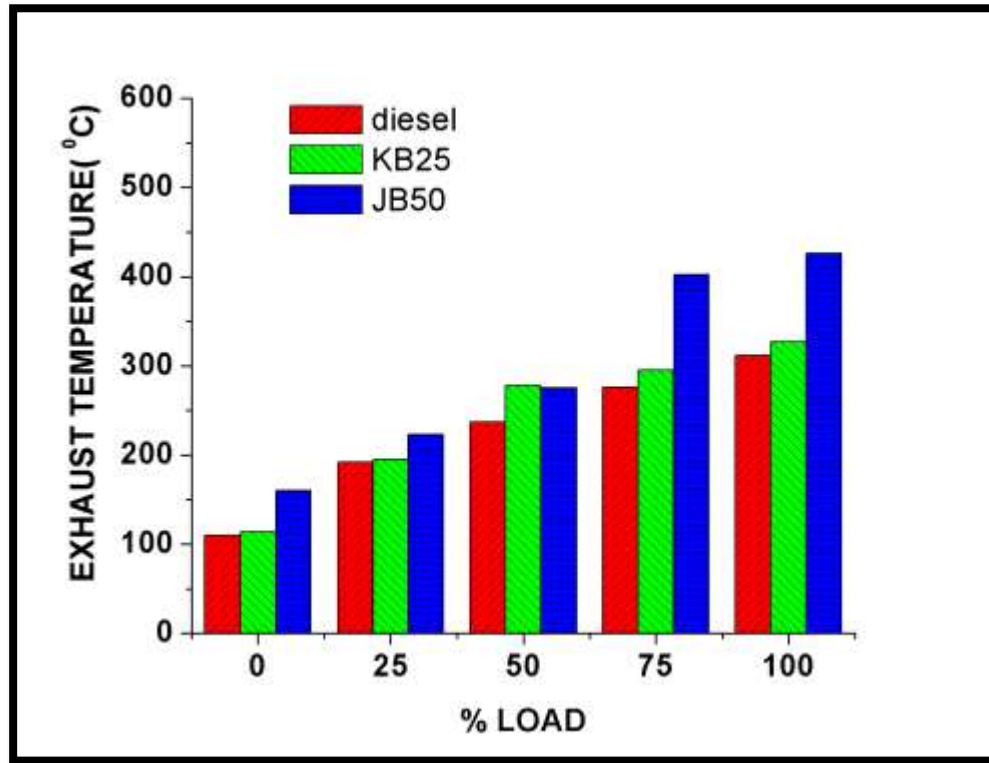


Figure 6.37 Variation of exhaust temperature at different load for diesel, KB25 & JB50

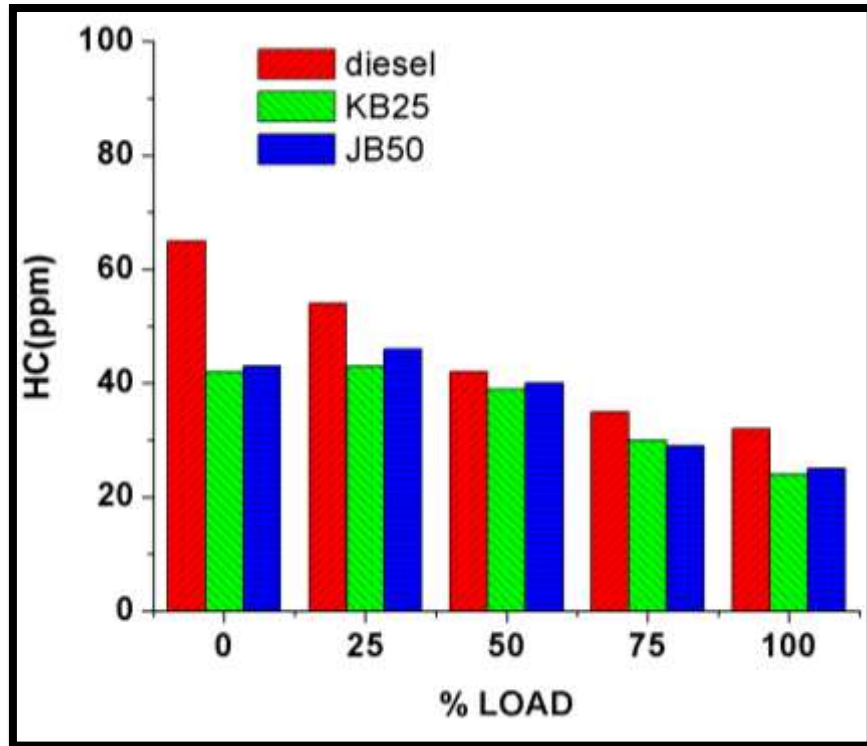


Figure 6.38 Variation of HC at different load for diesel, KB25 & JB50

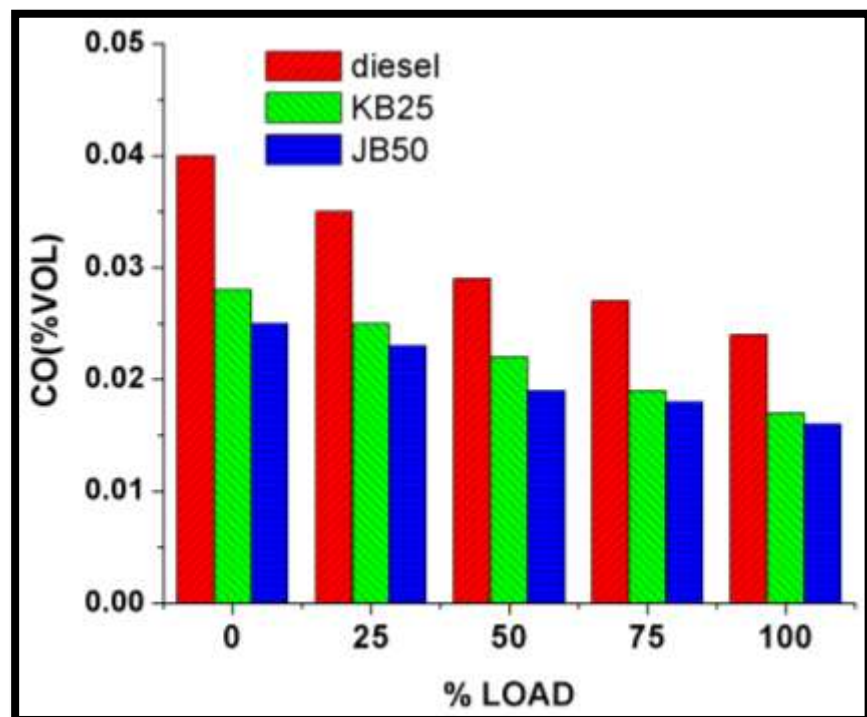


Figure 6.39 Variation of CO at different load for diesel, KB25 & JB50

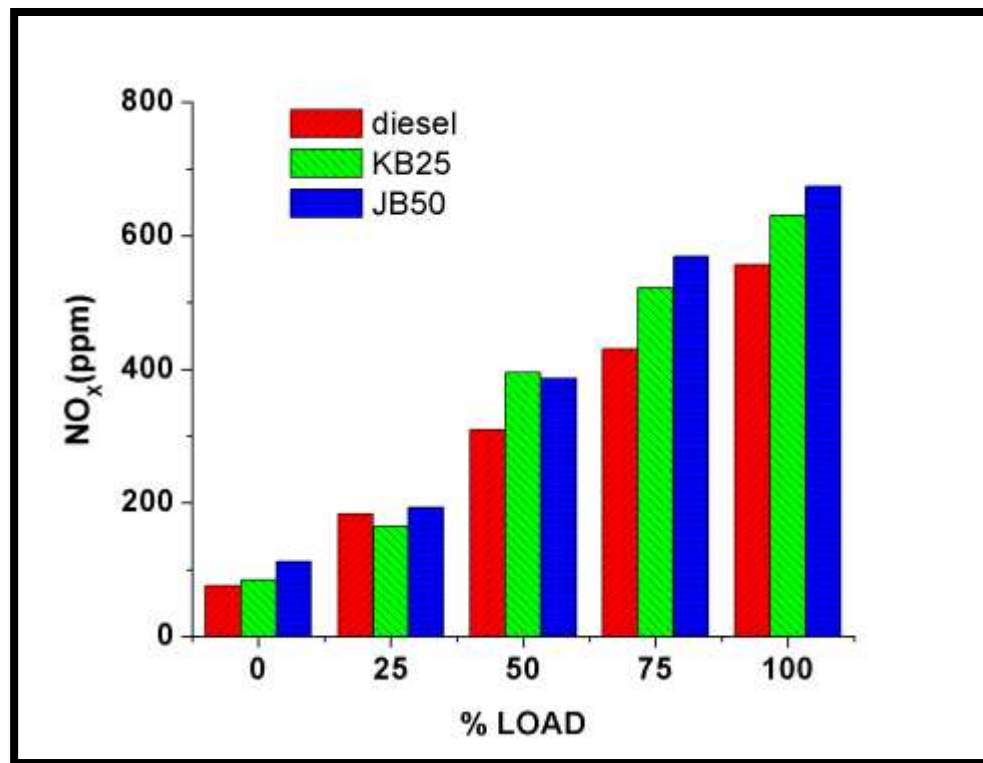


Figure 6.40 Variation of NO_x at different load for diesel, KB25 & JB50

6.5 SALIENT POINTS OF EXPERIMENTS:

a. Diesel:

- The maximum thermal efficiency is 34.41%.
- The maximum BSFC is 0.2405 kg/KWh.
- The minimum BSEC is 10462.2 kJ/KWh.
- The NO_x value increases from 76 ppm to 557 ppm as the load increases from no load to peak load.
- The CO value decreases from 0.04% by volume to 0.024% by volume as the load increases from no load to peak load.

- The HC value decreases from 65 ppm to 32 ppm as the load increases from no load to peak load.
- The exhaust temperature increases from 110°C to 312°C as the load increases from no load to peak load.

b. Karanja derived biodiesel and its blend with diesel:

- The maximum thermal efficiency for KB100 is 27.88%.
- The maximum BSFC for KB100 is 0.3599 kg/KWh.
- The minimum BSEC for KB100 is 12912.9 kJ/KWh.
- The NO_x value for KB100 increases from 219 ppm to 627 ppm as the load increases from no load to peak load.
- The CO value for KB100 decreases from 0.024% by volume to 0.016% by volume as the load increases from no load to peak load.
- The HC value for KB100 decreases from 40 ppm to 23 ppm as the load increases from no load to peak load.
- The exhaust temperature increases from 125°C to 318°C as the load increases from no load to peak load.
- The BSFC value increases for a particular load as the percentage of KOME increases in a KOME diesel blend.
- The maximum BSFC for KB25 is 0.2764 kg/KWh.

- The BSEC value increases for a particular load as the percentage of KOME increases in a KOME diesel blend.
- The minimum BSEC for KB25 is 11498.1 kJ/KWh.
- The brake thermal efficiency of a particular KOME blend increases with increase in loading.
- The brake thermal efficiency decreases for a particular load as the percentage of KOME increases in a KOME diesel blend.
- The maximum brake thermal efficiency of KB25 is 31.31%.
- The CO value for the KOME diesel blend decreases as the load increases.
- The CO value decreases for a particular load as the percentage of KOME increases in a KOME diesel blend.
- The maximum CO value for KB25 is 0.028%.
- The NO_x value for the KOME diesel blend increases as the load increases.
- The maximum NO_x value for KB25 is 631 ppm.
- The HC value for the KOME diesel blend decreases as the load increases.
- The maximum HC value for KB25 is 43 ppm.
- The exhaust temperature for the KOME diesel blend increases as the load increases.
- The maximum exhaust temperature for KB25 is 327°C.

c. Jatropha derived biodiesel and its blend with diesel:

- The maximum thermal efficiency for JB100 is 28.02%.
- The maximum BSFC for JB100 is 0.33 kg/KWh.
- The minimum BSEC for JB100 is 12845.9 kj/KWh.
- The NO_x value for JB100 increases from 170 ppm to 772 ppm as the load increases from no load to peak load.
- The CO value for JB100 decreases from 0.02% by volume to 0.013% by volume as the load increases from no load to peak load.
- The HC value for JB100 decreases from 36 ppm to 16 ppm as the load increases from no load to peak load.
- The exhaust temperature increases from 195°C to 547°C as the load increases from no load to peak load.
- The BSFC value increases for a particular load as the percentage of JOME increases in a JOME diesel blend.
- The maximum BSFC for JB50 is 0.2793 kg/KWh.
- The BSEC value increases for a particular load as the percentage of JOME increases in a JOME diesel blend.
- The minimum BSEC for JB50 is 11510.4 kj/KWh.
- The brake thermal efficiency of a particular JOME blend increases with increase in loading.

- The brake thermal efficiency decreases for a particular load as the percentage of JOME increases in a JOME diesel blend.
- The maximum brake thermal efficiency of JB50 is 31.28%.
- The CO value for the JOME diesel blend decreases as the load increases.
- The CO value decreases for a particular load as the percentage of JOME increases in a JOME diesel blend.
- The maximum CO value for JB50 is 0.025%.
- The NO_x value for the JOME diesel blend increases as the load increases.
- The maximum NO_x value for JB50 is 674 ppm.
- The HC value for the JOME diesel blend decreases as the load increases.
- The maximum HC value for JB50 is 46 ppm.
- The exhaust temperature for the JOME diesel blend increases as the load increases.
- The maximum exhaust temperature for JB50 is 426°C.

CHAPTER 7

CONCLUSIONS AND RECOMMENDATIONS

7.1 CONCLUSIONS:

The results of this research work showed that both the biodiesels (jatropha oil methyl ester and karanja oil methyl ester) are compatible for replacing the diesel oil in terms of performance and emission characters. But the experiments were carried out on a short term basis. Major problems associated with biodiesel as diesel substitute in CI engine have been recognized as its high viscosity, low volatility and poly unsaturated character. These problems are due to large molecular mass and chemical structure of vegetable oils. High viscosity and low volatility of such oil leads to excessive pumping power, in efficient combustion and poor atomization in the injector systems of a CI engine. Due to long chain unsaturated character, in a long term operation vegetable oils normally introduced the development of gumming, the formation of injector deposits, sticking of piston ring that makes incompatible with conventional diesel fuel. In such situation blending of biodiesel (JOME and KOME) is a preferred choice for the replacement of diesel in CI engine. Some of the observations are listed below:

- Blending of biodiesel and diesel shows a stable mixture.
- For blended biodiesel KB25 and JB50 are the optimum choice for the diesel fuel replacement.

- For KB25 and JB50, brake thermal efficiency is reduced by 3% compared to diesel fuel.
- Unburnt hydrocarbon for JB 50 was found to be lesser than diesel fuel.
- The KB 25 and JB50 show higher NO_x emission than the diesel fuel.
- The CO emission for KB25 was found less as that of diesel fuel.

For combustion analysis of biodiesels, the fuel properties are to be studied thoroughly before it is being selected. Therefore the prediction of biodiesel properties is the first and foremost stimulating task for the studies of biodiesel as a diesel substitute. In this research, the aim of the work was to theoretically predict few fuel properties like, cetane number, viscosity, density and high heat value (HHV) of different biodiesels from their fatty acid methyl ester (FAME) composition. The predicted results are summarized below:

- $CN = 19.2656 + 0.4213x_1 + 0.4694x_2 + 0.5666x_3 + 0.6833x_4 + 0.3174x_5 + 0.3885x_6 + 0.2969x_7 + 0.1546x_8$
- $Viscosity = 373.4774 - (3.7096 \times P) - (0.0993 \times PL) - (3.812 \times S) - (3.7431 \times OL) - (3.6808 \times L) - (3.717 \times LL) + (0.1131 \times A) - (10.8943 \times Oth)$
- $Density = 2204.5 - (13.2 \times P) - (1.4 \times PL) - (16 \times S) - (13.8 \times OL) - (13.3 \times L) - (12.9 \times LL) + (39.7 \times A) + (72.2 \times Oth)$

- $HHV = - 518.5 + (5.5977 \times P) + (0.4859 \times PL) + (5.8637 \times S) + (5.6976 \times OL) + (5.5723 \times L) + (5.5799 \times LL) - (3.5537 \times A) + (10.8667 \times Oth)$

7.2 RECOMMENDATIONS:

- The effect of delay period, heat release rates, pressure rise is definitely a better selection criterion for the biodiesel should also be researched.
- As the viscosity reduces with temperature, the preheating of the biodiesel blend and multi fuel injection will definitely cause the use of higher percentage of blend without alteration of much performance in comparison to diesel engine should also be researched.

REFERENCES:

1. Nicholas, R.J., "The challenges of Change in the Auto Industry: Why Alternative fuels?" *Alternative Fuels, Engine Performances, and Emissions*, ASME ICE, Vol. 20, pp. 3 – 10, 1993.
2. Agarwal, A. K., Rajamanoharan, K., Experimental investigations of performance and emissions of Karanja oil and its blends in a single cylinder agricultural diesel engine. *Applied Energy* 86 (2009) 106–112
3. Agrawal, A. K., Bijjwe, J., Das, L.M., " Effect of Biodiesel on wear of vital parts in compression engines", *Journal of Gas Turbines and Power*, Vol. 125, pp. 604 – 11, 2003.
4. Lapureta , M., Hernandez, J.J., Gimenez, F., "Evaluation of EGR as a Technique for Reducing Engine NO_x Emissions". *Proceeding International mechanical Engineering Part D. Journal of Automobile Engineering*, Vol. 214, pp. 88 – 93, 2000.
5. Murgesan, A., Umarani, C., Subramanian, R., Nedunchezian, N., "Bio-diesel as an alternative fuel for diesel engines – A review". *Renewable and Sustainable Energy Reviews*, Vol. 13, pp. 653 – 662, 2009.
6. International conference on bio-fuels 2012 vision to reality. *Energy Fuel Users* January – March 2006: 6 – 8.

7. Meher, L.C., Vidya Sagar, D., Naik, S.N., 2006. Technical aspects of biodiesel production by transesterification—a review. *Renewable and Sustainable Energy Reviews* 10, 248–268.
8. Lang, X., Dalai, A.K., Bakhshi, N.N., Reaney, M.J., Hertz, P.B., “Preparation and characterization of bio-diesels from various bio-oils”, *Bioresource Technology* 80 , pp. 53 – 62, 2001.
9. Meher, L.C., Vidya, S.S., Dharmagadda, Naik, S.N., “ Optimization of alkali catalyzed transesterification of *Pongamia pinnata* oil for production of biodiesel”. *Bioresour Technol* 2006; 97:1392–7.
10. Dec, J.E., “ A Conceptual Model of DI Diesel Combustion Based on Laser Sheet Imaging”, SAE Paper 970873, 1997.
11. Warnatz, j., U. Mass and R.W. Dibble, “Combustion: Physical and chemical Fundamentals, Modeling and Simulation, Experiments, Pollutants Formation”, Springer – Verlay, Berlin, ISBN 3 – 540 – 60730 – 7, 1996.
12. Loffler, S., P. Loffler, Homann, K.H., “Growth of Large Ionic Polycyclic Aromatic Hydrocarbon in Sooting Flames”, In *Soot and Models*, Springer – Verlay, Berlin, ISBN 3 – 540 – 58398 – X, 1994.
13. Frenklach, M., Clary. D. W., Gardiner, W. C., Jr., and Stein, S. E., “Twenty-First Symposium

14. Smith, O.I., "Fundamentals of Soot Formation in Flames with Application to Diesel Engines particulates Emissions", progress in Energy and Combustion Science, Vol. 7, pp.275 – 291, 1981.
15. Whitehouse, W.D., "The Development of Some Gaseous Products during Diesel Engine Combustion", SAE Paper 80028, 1980.
16. Flynn, P.E., Durett, R.P., "Diesel Combustion: An Integrated View Combining Laser Diagnostics, Chemical Kinetics, and Empirical Validation", SAE Paper 1999 – 01 – 0509, 1999.
17. Baijalwan A, Sharma CM, Kediya VK. Bio-diesel revolution. Science Reporter, January 2006. pp. 14 – 17.
18. M.E. Tat, J.H. Van Gerpen, S. Soylu, M. Canakci, A. Monyem, S. Wormley, The speed of sound and isentropic bulk modulus of biodiesel at 21 °C from atmospheric pressure to 35 MPa, JACS 77 (2000) 285–289.
19. Johnson J H, Bagley ST, Gratz LD, Leddy DG. A review of diesel particulate control technology and emission effects. SAE Transactions 1994; ISSN 0096- 736X, 103:210–244.
20. Baumgard KJ, Johnson JH. The effect of low sulfur fuel and a ceramic particle filter on diesel exhaust particle size distributions. SAE Trans 1992;101:691–9.
21. Kittelson DB. Engines and nanoparticles: a review. J Aerosol Sci 1998;29:575–88.

22. Andrews GE, Abbass MK, Abdelhalim S, Farrar KJ, Ghazikhani M, Ounzain A, et al. "Unburned liquid hydrocarbons using differential temperature hydrocarbon analysers". Soc Auto Eng 2000, 2000-01-0506.
23. Bertoli C, Del GN, Caprotti R, Smith AK., "The influence of automotive diesel back end volatility and new fuel additive technology on regulated emissions". Inst Mech Eng 1991 [C427/34/218].
24. P. F. Flynn, G. L. Hunter, L. Farrell, R. P. Durrett, O. Akinyemi, A. O. Zur Loye, C. K. Westbrook, W. J. Pitz, "THE INEVITABILITY OF ENGINE-OUT NO_x EMISSIONS FROM SPARK-IGNITED AND DIESEL ENGINES", Proceedings of the Combustion Institute, Volume 28, 2000/pp. 1211–1218.
25. Babu AK, Devaradjane D, "Vegetable oils and their derivatives as fuels for CI engines. An overview", SAE 2003 – 01- 0767, 2003.
26. Christopher W., "The practical implementation of bio-diesel as an alternative fuel in service motor coaches", SAE 973201, 1997.
27. Montague X., " Introduction of rapeseed methyl ester in Diesel fuel—the French National program", SAE 962065, 1996.
28. Senatore A., "A comparative analysis of combustion process in D. I. diesel engine fueled with biodiesel and diesel fuel", SAE 2000-01-0691, 2000.

29. Tadashi Young., "Low carbon build up, low smoke and efficient diesel operation with vegetable oil by conversion to monoesters and blending with diesel oil or alcohols", SAE 841161, 1984.
30. Baumgard KJ, Johnson JH., "The effect of low sulfur fuel and a ceramic particle filter on diesel exhaust particle size distributions". SAE Trans 1992;101:691–9.
31. Gragg K., 1994., "Effects of Environmentally Classified Diesel Fuels, RME and Blends of Diesel Fuels and RME on the Exhaust Emissions". Final Report., Swedish Environ. Prot. Agency. Bilprovning Press, Stockholm, Sweden.
32. Pangavhane DR, Kushare PB. Bio-diesel need of India, Proceedings of Recent Trends in Automotive Fuels, Nagpur, India, 2002.
33. Salvatore A, Maddaleena A., "The effect of methyl ester of rapeseed oil on combustion and emissions of D.I. diesel engines", SAE 932801, 1993.
34. Barsic NJ, Humke H. "Performance and emission characteristics of a naturally aspirated diesel engine with vegetable oil", SAE 810262, 1981.
35. Yu Zhang, Jon H Van Gerpen., "Combustion Analysis of Esters of Soybean Oil in a Diesel Engine". SAE paper 960765.
36. Labeckas G, Slavinskas S., "The effect of rapeseed oil methyl ester on direct injection diesel engine performance and exhaust emissions". Energy Conversion and Management 2006;47: 1954–67.

37. Recep Altın, Cetinkaya S, Yucesu H S, "The potential of using vegetable oil fuels as fuel for diesel engines", *Energy conversion and Management* 42(2001) 529 – 538.
38. Raheman H, Phadatare AG., "Diesel engine emissions and performance from blends of karanja methyl ester and diesel". *Biomass and Bioenergy* 2004;
39. Chitra, P., Venkatachalam, P., Sampathrajan, A., 2005. "Optimisation of experimental procedure for biodiesel production from alkaline-catalysed transesterification of *Jatropha curcas* oil". *Energy Sustain. Dev.* 9, 13–18.
40. Bari S, Yu CW, Lim TH. "Performance deterioration and durability issues while running a diesel engine with crude palm oil". *Proceedings of the Institution of Mechanical Engineers, Part D* 2002; 215:785 – 92.
41. Silvio Cade Almeida. "Performance of a diesel generator fuelled with palm oil". *Fuel* 2002; 81:2097 – 102.
42. Bhupendra Singh Chauhan, Naveen Kumar, Yong Du Jun, Kum Bae Lee. "Performance and emission study of preheated *Jatropha* oil on medium capacity diesel engine". *Energy* 35 (2010) 2484 – 2492
43. Fangrui Ma. Milford A. Bio-diesel production—review. *Bioresource Technology*, New Delhi, India, 1999.
44. Narayan CM. "Vegetable oil as engine fuels—prospect and retrospect". *Proceedings on Recent Trends in Automotive Fuels*, Nagpur, India, 2002.

45. Czerwinski J. "Performance of D.I. Diesel engine with addition of ethanol and rapeseed oil", SAE 940545, 1994.
46. Knothe G., 2005. "Dependence of biodiesel fuel properties on the structure of fatty acid alkyl esters". *Fuel Proc. Technol.*, 86, 1062, 1059-1070.
47. Michael S. Graboski, Robert L. McCormick, 1998. "Combustion of fat and vegetable oil derived fuels in diesel engines". *Prog. Energy Combust. Sci.*, 24, 125-164.
48. Kinast J.A., 2003. "Production of Biodiesels from Multiple Feed stocks and Properties of Biodiesels and Biodiesel/ Diesel Blends". Final Report. National Renewable Energy Laboratory. 1617 Cole Boulevard Golden, CO, USA.
49. McCormick R., Graboski M., Alleman T., Herring A., and Shainetyson K., 2001. Impact of biodiesel source material and chemical structure on emissions of criteria pollutants from a heavy-duty engine. *Environ. Sci. Technol.*, 35, 1742-1747.
50. Reece D.L and Peterson C.L., 1993. A report on the Idaho onroad vehicle test with RME and neat rapeseed oil as an alternative to diesel fuel. ASAE Paper No. 93-5018.
51. Rakopoulos C.D., Antonopoulos K.A., Rakopoulos D.C., Hountalas D.T., and Giakoumis E.G., 2006. "Comparative performance and emissions study of a direct injection Diesel engine using blends of diesel fuel with vegetable oils or bio-diesels of various origins". *Energy Conversion and Manag.*

52. Arkoudeas, P., Kalligeros, S., Zannikos, F., Anastopoulos, G., Karonis, D., Korres, D. and Lois, E. (2003) 'Study of using JP-8 aviation fuel and biodiesel in CI engines', *Energy Conv. Manag.*, Vol. 44, pp.1013–1025.
53. Knothe G., Bagby M.O., and Ryan T.W., 1997. "Cetane numbers of fatty compounds: influence of compound structure and of various potential cetane improvers". Soc. Aut. Eng. Techn. Paper No. 971681.
54. Kalligeros S., Zannikos F., Stournas S., Lois E., Anastopoulos G., Teas Ch., and Sakellaropoulos F., 2003. An investigation of using biodiesel/marine diesel blends on the performance of a stationary diesel engine. *Biomass and Bioenergy*, 24, 141-149.
55. Choudhury S, Bose P.K., 'Empirical approach for the prediction of cetane number from the FAME composition', *Int. J. Renewable Energy Technology*, Vol. – 2, No. – 2, 2011, pp 143 – 154.
56. Ghormade TK, Deshpande NV. Soyabean oil as an alternative fuels for I. C. engines, *Proceedings of Recent Trends in Automotive Fuels*, Nagpur, India, 2002.
57. Van Gerpen J.A., 1996. Cetane number testing of biodiesel. *Proc. 3rd Conf. ASAE Liquid Fuel*, September 15-17, Nashville, TN, USA.
58. Liang Y.E., May C.Y., Foon C.S., Ngan M.A., Hock C.C., and Basiron Y., 2006. The effect of natural and synthetic antioxidants on the oxidative stability of palm diesel. *Fuel*, 85, 867- 870.

59. Van Gerpen J., Shanks B., Pruszko R., Clements D., and Knothe G., 2004. Biodiesel Analytical Methods. NREL/SR-510-36240.
60. Vellguth G., 1983. Performance of Vegetable Oils and their Monoesters as Fuels for Diesel Engines. SAE Paper No. 831358/30.
61. Ayhan Demirbas, Relationships derived from physical properties of vegetable oil and biodiesel fuels, Fuel 87 (2008) 1743–1748.
62. Demirbas Ayhan. Fuel properties and calculation of higher heating values of vegetable oils, Fuel 1998;77(9/10):1117–20.
63. N. Kapilan N ,R. P. Reddy, Evaluation of Methyl Esters of Mahua Oil (*Madhuca Indica*) as Diesel Fuel, J Am Oil Chem Soc (2008) 85:185–188.
64. S.M. Sadrameli, Wayne Seames, Mike Mann, Prediction of higher heating values for saturated fatty acids from their physical properties, Fuel 87 (2008) 1776–1780.
65. Senthil Kumar M, Ramesh A, Nagalingam B, An experimental comparison of methods to use methonal and Jatropha oil in a compression ignition engine, Biomass and Bioenergy 2003;25:309–18.
66. Mitra S., Bose P.K., Choudhury S., 'Mathematical Modeling for the prediction of Fuel Properties of Biodiesel from their FAME Composition', Key Engineering Materials Vol. 450 (2011) pp 157-160

LIST OF PUBLICATIONS

International Conference:

- i. Choudhury S., Bose P.K., 'Karanja or Jatropha – a better option for an Alternative Fuel in CI Engine', Proceedings of the INTERNATIONAL CONFERENCE & XX NATIONAL CONFERENCE On I.C. ENGINES AND COMBUSTION (ICONICE – 2007), pp 321 – 326.
- ii. Choudhury S., Bose P.K., 'Jatropha Derived Biodiesel – its suitability as CI engine fuel', Proceedings of the SAE INDIA International Mobility Conference **SIIM C 2008** (SAE Number 2008 – 28 – 0040).

International Journal:

- i. Mitra S., Bose P.K., Choudhury S., 'Production of bio-diesel from jatropha curcas and performance along with emission characteristics of an agricultural diesel engine using bio-diesel', 2ND International Conference On Energy and Sustainability, Energy 2009, Italy, Energy and Sustainability II, Vol. – 121, pp. 367 – 376.
- ii. Choudhury S, Bose P.K., 'Empirical approach for the prediction of cetane number from the FAME composition', Int. J. Renewable Energy Technology, Vol. – 2, No. – 2, 2011, pp 143 – 154.
- iii. Mitra S., Bose P.K., Choudhury S., 'Mathematical Modeling for the prediction of Fuel Properties of Biodiesel from their FAME Composition', Key Engineering Materials Vol. 450 (2011) pp 157-160

- iv. Choudhury S., Mitra S., Bose P.K., 'Mathematical Modeling of Brake Thermal Efficiency of Vegetable Oils by Using Buckingham's π (Pi) Theorem', International Journal of Emerging Technology and Advanced Engineering, Vol. – 5, Issue – 10(October 2015) pp 124 – 131.
- v. Choudhury S., Mitra S., Bose P.K., 'Effect of Temperature and Unsaturation of Fatty Acid Methyl Ester) on Viscosity Prediction for Biodiesel', International Journal of Emerging Technology and Advanced Engineering, Vol. – 5, Issue – 10(October 2015) pp 174 – 178.

National Journal:

- i. Choudhury S., Bose P.K., 'Karanja oil – its potential and suitability as biodiesel', The Bulletin of Engineering and Science, Vol. – 3, No. – 2, BES/3/2/2008, pp20 – 27.

Appendix 1

SPECIFICATIONS AND ACCURACY OF THE INSTRUMENT USED FOR MEASURING FUEL PROPERTIES.

A. BOMB CALORIMETER:

Specifications:

- Complete with Stainless Steel bomb with Stainless Steel crucible (18/8 quality)
- 3000 cc capacity jacket
- Calorimeter vessel
- Motorised stirrer
- Briquette press for making sample specimen for testing
- Firing unit with control. Electric 220/230 v A.C. with digital Beckman thermometer (i.e. digital differential thermometer)
- Oxygen pressure gauge with pipe fittings & fine adjustment cock
- Head support, Lifting Hook, Bomb connecting wire Nichrome wire 40 swg
- Cotton reel
- Valve opening key

B. CLOUD AND POUR POINT APPARATUS:

Specifications: as per IP-15, 216, ASTM D 2500 & IS: 1448 (P-10) (without thermometer)

- Single Test apparatus with insulated body with Refrigeration System. Temp. Up to (--) 30°C
- CONTROL SYSTEM: Digital Temperature Indicator – Cum – Controller

- Complete with Glass jar, Metal Jacket & Cork Sheet
- Thermometers for Cloud & Pour Point apparatus :
 - a) IP.1C (-38/50°C X 1°C)
 - b) IP.2C (-80/20°C X 1°C)

C. FLASH AND FIRE POINT APPARATUS:

Specifications: Cleveland FLASH & FIRE POINT APPARATUS, CLEVELAND OPEN CUP, AS PER IS 1448 (P- 69), ASTM D 92 & IP 36 A

Electrically Heated Model with Energy Regulator Control, with Oil Jet gas flame.

Thermometers: For Cleveland Flash & Fire Point Apparatus: IP.28C (-6 / 400°C X 2°C)

D. REDWOOD VISCOMETER:

Model: Electrically heated with Digital temperature controller-cum-indicator as per IP- 70

Specifications:

- Stainless steel bath with electrical heating arrangement suitable to operate at 220 Volts AC Mains with water/ oil overflow & drain system, hole for pouring heating media
- Oil cup with precision stainless steel jet,
- Cup cover,
- Ball valve,
- Thermometer – clip,
- Stirrer (motorized) fitted in the bath with self-illuminated on/off switch for operating stirrer

- M.S. Sheet strong stand with powder coated paint finish with levelling screws.
- Digital temperature indicator and controller.
- Also fitted lower side of bath white illumination system (operated by self-illuminated on/off switch) for better visibility of redwood flask during test sample collection & arrangement to keep flask on exact position quickly without any error by provided support.
- Thermometers for Redwood Viscometer:
 - a) IP 8C (0/45C X 0.2C)
 - b) IP 9C (40/85C X 0.2C)
 - c) IP10C (76/122C X 0.2C)
 - d) Spare Redwood flask of glass

E. ANILINE POINT APPARATUS:

Specifications: AS PER IP-2, 1977 METHOD ' D' , BY 'U' TUBE METHOD.

- A Borosilicate Glass Tube With A Metal Shield
- A Lamp Attached Assembled On Insulating Cover
- A 600 ml Beaker Used As Water Or Oil Bath.
- The Auger Shaped Glass Rod Producing A Down Current In The U Tube Is Driven By A Variable Speed Electric Motor Mounted With Adjustable Clamps On A Stand. Electrically Heated With Energy Control And Digital Temp. Indicator. a) Spare 'U' tube
- THERMOMETER

- a. IP 20C RANGE : - 38⁰C TO 42⁰C X 0.2⁰C
- b. IP 21C RANGE : 25⁰C TO 105⁰C X 0.2⁰C
- c. IP 59C RANGE : 90⁰C TO 170⁰C X 0.2⁰C

Appendix 2

Engine Technical specification

Name of the engine manufacturer	:	Kirloskar
Type of engine	:	Vertical, 4 stroke, single cylinder, direct injected, compression ignition diesel engine
Engine model	:	AV1
Rated Power	:	5HP
Rated Speed	:	1500 r.p.m
Compression Ratio	:	16.5:1
Bore x Stroke	:	80 x 110 mm
Cubic capacity	:	0.553
Governor type	:	Mechanical Centrifugal
Muffler type	:	Peeper pot
Weight of engine	:	160 Kg
Method of cooling	:	Water cooled
Lubricating oil	:	HD- Type 3
Connecting rod length	:	241 mm
Filter type	:	Dry
Injector Opening pressure	:	200 bar
Inlet valve opening ⁽⁰⁾	:	4.5 ⁰ before TDC
Inlet valve closing ⁽⁰⁾	:	35.5 ⁰ after BDC
Exhaust valve opening ⁽⁰⁾	:	35.5 ⁰ before BDC
Exhaust valve closing ⁽⁰⁾	:	4.5 ⁰ after TDC
Injection Timing	:	26 ⁰ before TDC

Appendix 3

Eddy current Dynamometer specifications

Make	:	Dynaspede
Model	:	WED – 20K – 0
Rating	:	50 kgm
Power	:	110 kW
Method of cooling	:	Water cooled
Rated speed	:	2200 r.p.m
Attachments	:	Universal brake controller 5 Nos. of cables PC software Electronic controller EC 80 – 24 Controller card Power ON/OFF switch AUTO/MAN switch without meter.

Appendix 4

Technical Data of AVL DiGas Gas Analyzer (Model 444)

Measuring principle	CO, HC, CO ₂	Infrared measurement
Measuring principle	O ₂ , NO _x	Electrochemical measurement
Operating temperature	+5.....+45°C	Keeping measurement
accuracy	+1.....+50°C	Ready for measurement with
	+5.....+35°C	integral NO sensor
		(peaks of: +40°C)
Storage temperature	-20.....+60°C	
	-20.....+50°C	With integrated O ₂ sensor
	-10.....+45°C	With integrated NO sensor
	0.....+50°C	With water in filter and/or pump
Air humidity	90% max., non-condensing	
Power drawn	150VA	
Dimension	470x431x230mm	
weight	17.7 kg	

Measurement parameters:

	Measurement range	Resolution	DiGas
CO	0.....10% by vol.	0.01% by vol.	•
CO ₂	0.....20% by vol.	0.1% by vol.	•
HC	0.....20000 ppm vol.	1 ppm vol.	•
O ₂	0.....4% by vol.	0.01% by vol.	•
	0.....22% by vol.	0.1% by vol.	
NO _x	0.....4000ppm	1 ppm vol.	•

Appendix 5

Performance and emission data for diesel

Engine performance						Engine emission			
Fuel	% load	Torque N-m	BSFC Kg/Kw-hr	BSEC Kj/Kw-hr	$\eta_{B.Th}$	NO _x (ppm)	CO (%vol)	HC (ppm)	Exhaust Temp (°C)
Diesel	0	0	0.0000	0.00	0.00	76	0.040	65	110
	25	5.89	0.4089	17785.8	20.24	184	0.035	54	192
	50	11.78	0.2638	11474.7	31.37	310	0.029	42	237
	75	17.67	0.2478	10779.3	33.40	431	0.027	35	276
	100	23.55	0.2405	10462.2	34.41	557	0.024	32	312

Appendix 6

Performance and emission data for KOMÉ blend with diesel

Fuel	% load	BSFC Kg/Kw- hr	BSEC Kj/Kw- hr	$\eta_{B.Th}$	Exhaust Gas Temp (°C)	CO (%VOL)	HC (ppm)	Nox (ppm)
KB05	0	0.0000	0.0	0.00	112	0.036	49	114
	25	0.4100	17680.6	20.36	187	0.032	52	203
	50	0.2828	12193.5	29.52	252	0.028	45	347
	75	0.2603	11225.8	32.07	284	0.025	36	479
	100	0.2485	10715.5	33.60	319	0.022	30	595
KB10	0	0.0000	0.0	0.00	114	0.034	47	108
	25	0.4112	17572.5	20.49	196	0.032	50	192
	50	0.2836	12119.0	29.71	257	0.027	43	351
	75	0.2674	11429.3	31.50	292	0.024	35	495
	100	0.2570	10982.8	32.78	320	0.021	29	607
KB15	0	0.0000	0.0	0.00	114	0.033	45	101
	25	0.4229	17913.5	20.10	195	0.030	46	179
	50	0.2844	12045.3	29.89	266	0.027	41	370
	75	0.2682	11359.8	31.69	291	0.024	34	507
	100	0.2577	10916.0	32.98	319	0.020	27	619
KB20	0	0.0000	0.0	0.00	114	0.031	44	99
	25	0.4352	18269.2	19.71	195	0.027	45	167
	50	0.2953	12397.0	29.04	278	0.023	40	392
	75	0.2756	11570.5	31.11	295	0.021	32	515
	100	0.2668	11197.3	32.15	327	0.019	26	625
KB25	0	0.0000	0.0	0.00	114	0.028	42	85
	25	0.4365	18154.9	19.83	195	0.025	43	165
	50	0.3071	12775.6	28.18	278	0.022	39	395
	75	0.2764	11498.1	31.31	295	0.019	30	522
	100	0.2764	11498.1	31.31	327	0.017	24	631
KB100	0	0.0000	0.0	0.00	125	0.024	40	219
	25	0.5758	20660.7	17.42	207	0.023	42	297
	50	0.4113	14757.6	24.39	259	0.020	38	409
	75	0.3715	13329.5	27.01	289	0.018	21	536
	100	0.3599	12912.9	27.88	318	0.016	23	627

Appendix 7

Performance and emission data for JOME blend with diesel

Fuel	% load	BSFC Kg/Kw- hr	BSEC Kj/Kw- hr	$\eta_{B.Th}$	Exhaust Gas Temp ($^{\circ}C$)	CO (%VOL)	HC (ppm)	Nox (ppm)
JB10	0	0.0	0.0	0.0	116	0.033	47	130
	25	0.4214	18138.9	19.85	200	0.030	51	211
	50	0.2834	12196.8	29.52	245	0.027	44	349
	75	0.2490	10718.4	33.59	284	0.023	35	515
	100	0.2568	11053.4	32.57	325	0.020	29	607
JB20	0	0.0	0.0	0.0	123	0.031	46	122
	25	0.4346	18508.7	19.45	211	0.028	50	205
	50	0.2949	12559.4	28.66	255	0.025	43	371
	75	0.2561	10904.3	33.01	287	0.022	33	529
	100	0.2664	11344.0	31.73	339	0.019	28	622
JB30	0	0.0	0.0	0.0	137	0.031	45	120
	25	0.4426	18644.5	19.31	215	0.027	49	199
	50	0.3073	12947.6	27.80	261	0.024	42	385
	75	0.2634	11097.9	32.44	298	0.020	31	531
	100	0.2766	11652.8	30.89	367	0.018	27	634
JB40	0	0.0	0.0	0.0	151	0.027	44	117
	25	0.4507	18782.0	19.17	217	0.025	47	195
	50	0.3207	13364.1	26.94	269	0.023	41	379
	75	0.2712	11299.7	31.86	310	0.021	30	552
	100	0.2779	11582.2	31.08	398	0.018	26	651
JB50	0	0.0	0.0	0.0	160	0.025	43	112
	25	0.4529	18665.6	19.29	223	0.023	46	193
	50	0.3286	13541.7	26.58	275	0.019	40	387
	75	0.2725	11229.7	32.06	402	0.018	29	569
	100	0.2793	11510.4	31.28	426	0.016	25	674
JB60	0	0.0	0.0	0.0	163	0.024	42	110
	25	0.4613	18801.2	19.15	227	0.020	44	190
	50	0.3367	13724.9	26.23	284	0.018	39	396
	75	0.2806	11437.4	31.48	417	0.017	28	584
	100	0.2806	11437.4	31.48	445	0.015	24	692

Fuel	% load	BSFC Kg/Kw- hr	BSEC Kj/Kw- hr	$\eta_{B.Th}$	Exhaust Gas Temp ($^{\circ}C$)	CO (%VOL)	HC (ppm)	Nox (ppm)
JB70	0	0.0	0.0	0.0	165	0.023	41	140
	25	0.4699	18938.6	19.01	231	0.021	43	235
	50	0.3452	13914.1	25.87	291	0.019	37	405
	75	0.2892	11654.5	30.89	427	0.017	26	599
	100	0.2819	11363.2	31.68	476	0.015	23	707
JB80	0	0.0	0.0	0.0	171	0.022	40	159
	25	0.4788	19077.8	18.87	237	0.020	41	277
	50	0.3469	13821.7	26.05	303	0.017	35	449
	75	0.2982	11881.8	30.30	439	0.016	24	628
	100	0.2931	11676.9	30.83	493	0.014	21	721
JB90	0	0.0	0.0	0.0	185	0.021	38	166
	25	0.4879	19218.9	18.73	252	0.019	39	285
	50	0.3558	14013.8	25.69	321	0.016	32	466
	75	0.3162	12456.7	28.90	452	0.015	21	641
	100	0.3050	12011.8	29.97	526	0.013	18	739
JB100	0	0.0	0.0	0.0	195	0.020	36	170
	25	0.5046	19646.7	18.32	259	0.019	37	292
	50	0.3730	14521.4	24.79	332	0.017	29	488
	75	0.3466	13494.7	26.68	465	0.015	20	651
	100	0.3300	12845.9	28.02	547	0.013	16	772